NUMERICAL ANALYSIS ON EFFECT OF FIN SHAPE ON DOUBLE PIPE HEAT EXCHANGERS

2024
MASTER THESIS
MECHANICAL ENGINEERING

Ali Mahmood Mohamed MOHAMED

Thesis Advisor
Prof. Dr. Kamil ARSLAN

NUMERICAL ANALYSIS ON EFFECT OF FIN SHAPE ON DOUBLE PIPE HEAT EXCHANGERS

Ali Mahmood Mohamed MOHAMED

Thesis Advisor
Prof. Dr. Kamil ARSLAN

T.C.
Karabuk University
Institute of Graduate Programs
Department of Mechanical Engineering
Prepared as
Master Thesis

KARABÜK
May 2024

I certify that in my opinion the thesis submitted by Ali Mahmood Mohamed MOHAMED titled “NUMERICAL ANALYSIS ON EFFECT OF FIN SHAPE ON DOUBLE PIPE HEAT EXCHANGERS” is fully adequate in scope and in quality as a thesis for the degree of Master of Science.

Prof. Dr. Kamil ARSLAN .....
Thesis Advisor, Department of Mechanical Engineering

This thesis is accepted by the examining committee with a unanimous vote in the Department of Mechanical Engineering as a Master of Science thesis. 29.05.2024

Examining Committee Members (Institutions)	Signature
Chairman : Prof. Dr. Mustafa YAŞAR (KBU)	.....
Member : Prof. Dr. Veli ÇELİK (AYBU)	.....
Member : Prof. Dr. Kamil ARSLAN (KBU)	.....

The degree of Master of Science by the thesis submitted is approved by the Administrative Board of the Institute of Graduate Programs, Karabük University.

Assoc. Prof. Dr. Zeynep ÖZCAN .....
Director of the Institute of Graduate Programs

I declare that all the information within this thesis has been gathered and presented in accordance with academic regulations and ethical principles, and I have, according to the requirements of these regulations and principles, cited all those that do not originate in this work as well.

Ali Mahmood Mohamed MOHAMED

ABSTRACT

M. Sc. Thesis

NUMERICAL ANALYSIS ON EFFECT OF FIN SHAPE ON DOUBLE PIPE HEAT EXCHANGERS

Ali Mahmood Mohamed MOHAMED

Karabük University
Institute of Graduate Programs
Department of Mechanical Engineering

Thesis Advisor:
Prof. Dr. Kamil ARSLAN
May 2024, 87 pages

Heat exchangers are crucial components of thermal engineering equipment, including power plants, chemical industries, air conditioning systems, and cooling of electronic instruments. Researchers have developed various methods to improve the thermal efficiency of heat exchangers. One of such methods is the use of expanded surfaces. In this context, various surface geometries were examined to enhance the heat transfer efficiency of the heat exchanger. This study evaluated the performance of different heat exchangers using helical-annular finned tube, half-annular finned tube and annular finned tube, as well as the standard double-tube heat exchanger as a reference. A numerical comparison was conducted on four concentric tube double pipe heat exchangers with the same materials and dimensions. The inner tube has length of 1.8 meters, diameter of 20 mm, wall thickness of 2 mm and it is positioned inside a tube with diameter of 50 mm and the same length.

The objective of the study is to investigate how different fin shapes affect the thermal and hydraulic properties of two-tube heat exchangers. The study has been made use of numerical simulations carried out with ANSYS Fluent Software 2022 R2. The simulation model was developed using incoming hot and cold-water temperatures set at 65°C and 20°C, respectively. The simulation was performed under four different hot water conditions, with flow rates ranging from 1 to 4 liters per minute, and corresponding cold water flow rates from 1 to 4 liters per minute. Hot water flows through the tube, while cold water flows in the opposite direction through the annular space.

According to the simulation findings, the use of fins is highly effective in improving the thermal efficiency of heat exchangers compared to heat exchangers with smooth pipes. Among the different types of fins, the helical-annular finned pipe heat exchanger showed the highest convective heat transfer rate increments. The increment of convective heat transfer of helical-annular finned pipe heat exchanger was better than smooth, annular, and half-annular finned pipes by 59.2%, 28.2%, and 31.6%, respectively. The heat transfer rate of all heat exchangers was also found inversely proportional to the resistance. Compared to finned pipe heat exchangers, smooth pipe heat exchangers had lower friction factor magnitudes. The friction factor of smooth pipe heat exchanger was 18.58% , 8.66%, and 29.04% lower than that of annular, half-annular, and helical-annular pipe heat exchangers. Smooth pipe heat exchangers generally had lower effectiveness than finned pipe heat exchangers, except when the value of C is 0.99, at which point their effectiveness surpasses that of annular and half-annular finned pipe heat exchangers. Helical-annular finned pipe heat exchangers exhibited superior performance in terms of C values compared to other heat exchangers. The helical-annular finned tube heat exchange worked more effectively than the smooth, annular-finned, and half-annular tube heat exchangers by 49.9%, 20.3%, and 21.8%, respectively. Furthermore, the numerical simulation results gave a high level of agreement between the experimental investigation data in literature, with an error rate not exceeding 10.32%, thereby validating their accuracy.

Key Words : Double-Pipe Heat Exchanger, Finned Pipe, Numerical Simulation, Heat Exchanger Efficiency.

Science Code **:**91411

ÖZET

Yüksek Lisans Tezi

ÇİFT BORULU ISI DEĞİŞTİRİCİSİNDE KANATÇIK ŞEKLİNİN VERİM ÜZERİNDEKİ ETKİSİNİN SAYISAL ANALİZİ

Ali Mahmood Mohamed MOHAMED

Karabük Üniversitesi
Lisansüstü Eğitim Enstitüsü
Makine Mühendisliği Anabilim Dalı

Tez Danışmanı:
Prof. Dr. Kamil ARSLAN
Mayıs 2024, 87 sayfa

Isı değiştiricileri, enerji santralleri, kimya endüstrileri, iklimlendirme sistemleri ve elektronik cihazların soğutulması dahil olmak üzere termal mühendislik ekipmanlarının önemli bileşenleridir. Araştırmacılar ısı değiştiricilerin ısıl verimliliğini artırmak için çeşitli yöntemler geliştirmişlerdir. Bu yöntemlerden biri genişletilmiş yüzeylerin kullanılmasıdır. Bu bağlamda, ısı değiştiricinin ısı transfer verimliliğini arttırmak için çeşitli yüzey geometrileri incelenmiştir. Bu çalışma, referans olarak standart çift borulu ısı değiştiricinin yanı sıra sarmal-halkalı, yarım-dairesel ve dairesel kanatçıklı borular kullanan farklı ısı değiştiricilerin performansını değerlendirmiştir. Aynı malzeme ve boyutlara sahip dört adet eşmerkezli borulu çift borulu ısı değiştirici üzerinde sayısal bir karşılaştırma yapılmıştır. İç borunun uzunluğu 1,8 metre, çapı 20 mm ve et kalınlığı 2 mm'dir ve çapı 50 mm ve aynı uzunlukta olan bir borunun içerisine yerleştirilmiştir.

Çalışmanın amacı, farklı kanatçık şekillerinin iki borulu ısı değiştiricilerin ısıl ve hidrolik özelliklerini nasıl etkilediğini araştırmaktır. Çalışmada ANSYS Fluent Software 2022 R2 ile gerçekleştirilen sayısal analizlerden yararlanılmıştır. Sayısal analiz modeli, sırasıyla sisteme 65°C ve 20°C'de giren sıcak ve soğuk su sıcaklıkları kullanılarak geliştirilmiştir. Analizler, sıcak su akış hızlarının dakikada 1 ila 4 litre arasında olduğu ve buna karşılık gelen soğuk su akış hızlarının ise dakikada 1 ila 4 litre olduğu dört farklı sıcak su koşulu altında gerçekleştirilmiştir. Sıcak su borunun içinden akarken, soğuk su halka şeklindeki boşluktan ters yönde akmaktadır.

Sayısal çalışmaların bulgularına göre kanatçık kullanımının, kanatçıksız ısı değiştiricilere kıyasla ısı değiştiricilerinin ısıl verimliliğini arttırmada oldukça etkili olduğu görülmüştür. Farklı kanatçık türleri arasında, helisel-halka şekilli kanatçıklı borulu ısı değiştirici, en yüksek konvektif ısı transfer hızı artışını göstermiştir. Helisel-halka kanatçıklı borulu ısı değiştiricinin konvektif ısı transferindeki artış, kanatçıksız, dairesel ve yarım-daireli kanatçıklı borulara göre sırasıyla %59.2, %28.2 ve %31.6 oranında daha iyi gerçekleşmiştir. Tüm ısı değiştiricilerin ısı transfer hızı da dirençle ters orantılı bulunmuştur. Kanatçıklı borulu ısı değiştiricilerle karşılaştırıldığında kanatçıksız ısı değiştiricilerin sürtünme faktörü büyüklükleri daha düşük çıkmıştır. Kanatçıksız ısı değiştiricinin sürtünme faktörü, dairesel, yarı dairesel ve helisel-halkalı kanatçıklı borulu ısı değiştiricilere göre %18,58, %8,66 ve %29,04 daha düşük gerçekleşmiştir. Kanatçıksız borulu ısı değiştiricileri, C değerinin 0,99 olduğu durumlar hariç, genellikle kanatçıklı borulu ısı değiştiricilerinden daha düşük verimliliğe sahiptir; bu noktada etkinlikleri, dairesel ve yarım daire kanatçıklı borulu ısı değiştiricilerinkini aşmaktadır. Helisel-halkalı kanatçıklı borulu ısı değiştiriciler diğer ısı değiştiricilere göre C değerleri açısından üstün performans sergilemiştir. Helisel-halka şeklindeki kanatçığa sahip ısı değiştiricisinin verimi, kanatçıksız, dairesel kanatçıklı ve yarım-dairesel kanatçıklı ısı değiştiricilerden sırasıyla, %49,9, %20,3 ve %21,8 oranlarında yüksek olduğu elde edilmiştir. Ayrıca, sayısal analiz sonuçları ile literatürdeki deneysel araştırma verileri arasında %10,32'yi aşmayan bir hata oranıyla yüksek düzeyde bir uyum sağlamış ve sayısal çalışmaların doğruluğu kanıtlanmıştır.

Anahtar Kelimeler : Çift Borulu Isı Değiştiricisi, Kanatçıklı Boru, Sayısal Analiz, Isı Değiştiricisi Verimi.

Bilim Kodu :91411

ACKNOWLEDGMENT

My profound gratitude to my advisor, Prof. Dr. Kamil ARSLAN, for his invaluable guidance and unwavering support throughout the entire process of preparing this thesis. I am sincerely thankful for his enduring interest and assistance. I also extend my thanks and appreciation to my teacher, Prof. Dr. Ehsan Fadhil Abbas from Kirkuk Engineering Technical College/Northern Technical University, for his efforts and assistance in completing this study.

Above all, I want to express my gratitude to my family for their prayers and support, especially my wife, sister, and brothers. They gave me a lot, but most especially, they gave me the strength to go on. Thank you very much.

CONTENTS

Page

Page

Page

LIST OF FIGURES

Page

Page

Page

Page

LIST OF TABLES

Page

INDEX OF SYMBOLS AND ABBREVIATIONS

A : Area, m^2

C : Heat capacity rare ratio

C_p : Specific heat, J/kg.^oC

D : The diameter of the outer pipe, m

d : The diameter of the inner pipe, m

i : Enthalpy, J/kg

k : Thermal conductivity, W/m.^oC

$\dot{m}$: Mass flow rate, kg/s

NTU : Number of transfer units

Nu : Nusselt number

Pr : Prandtl number

q : Heat transfer rate, W

Re : Reynolds number

T : Temperature, ^oC

$\overline{T}$: Average temperature, ^oC

U : Overall heat transfer coefficient, W/m^2.^oC

V : Volume, m^3

SUBSCRIBE SYMBOLS

b : Bulk

c : Cold

e : Effective

f : Fluid

H : Hydraulic

h : Hot

i : Inlet

lm : Log mean

I : Inside

o : Outlet

GREEK SYMBOLS

ε	: Effectiveness
μ	: Dynamic viscosity, kg/m.s
ρ	: Density, kg/m^3

PART 1

INTRODUCTION

Heat exchangers transfer heat between two fluids at different temperatures while maintaining strict separation. These devices are widely used in various industries, including thermal power plants, refrigeration and air conditioning systems, chemical processing plants, nuclear power plants, and dairy factories. Heat is transferred in heat exchangers through convective heat transfer within the fluid and conductive heat transfer through the wall that separates the two fluids. Heat exchangers can be classified into various types, as shown in Figure 1.1.

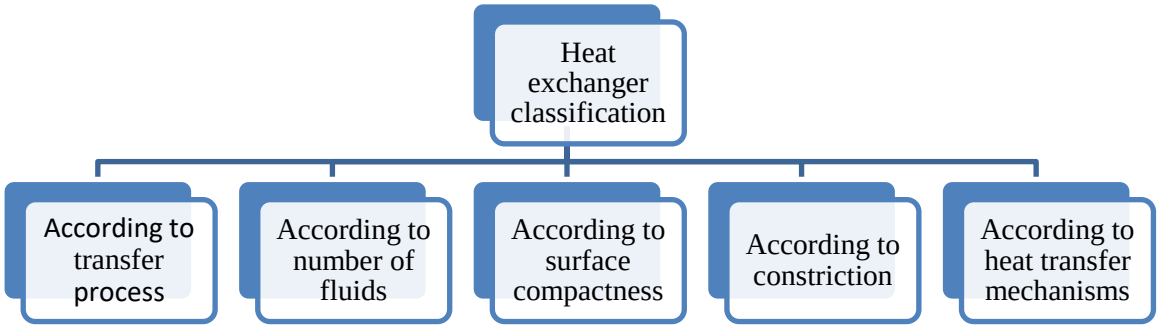

Figure 1.1. Heat exchangers classification [1]

1.1. DOUBLE-PIPE HEAT EXCHANGER

A typical exchanger comprises two pipes, one inside the other. The inner tube can either be plain or finned. For optimal outcomes, the fluids should flow in a counter flow direction, with one in the annulus between the pipes and the other in the inner tube. However, parallel flow can be used to maintain a consistent wall temperature. This heat exchanger is easy to disassemble and clean, making it ideal

for high-pressure applications. When there is high pressure, double-pipe heat exchangers are frequently used because it is less expensive to contain fluids in small-diameter pipelines rather than large-diameter shells. These heat exchangers are commonly employed in small-capacity applications with a 50 m2 or less surface area. Some industrial applications also utilize stacks of double-pipe or multitube heat exchangers with radial or longitudinal fins. Heat exchangers are critical components of many industrial processes. One of the most basic types of heat exchangers is the double-pipe exchanger, which comprises of two concentric pipes with either plain or finned inner pipes. A standard configuration is illustrated in Figure 1.2. In the inner tube, the fluid requiring heating is circulating, whereas the heat source traverses the annulus between the two pipelines. Counter flow, or the movement of fluids in contrary directions, is required for optimal performance. Nevertheless, parallel flow of the fluids is possible when an almost constant wall temperature is necessary [2, 3]. When dealing with pipelines that have a diameter of 150 mm or greater, hairpin or jacketed U-tube exchangers are utilized. It comprises a shell encasing a collection of U-shaped cylinders and employs segmental baffles [2, 3].

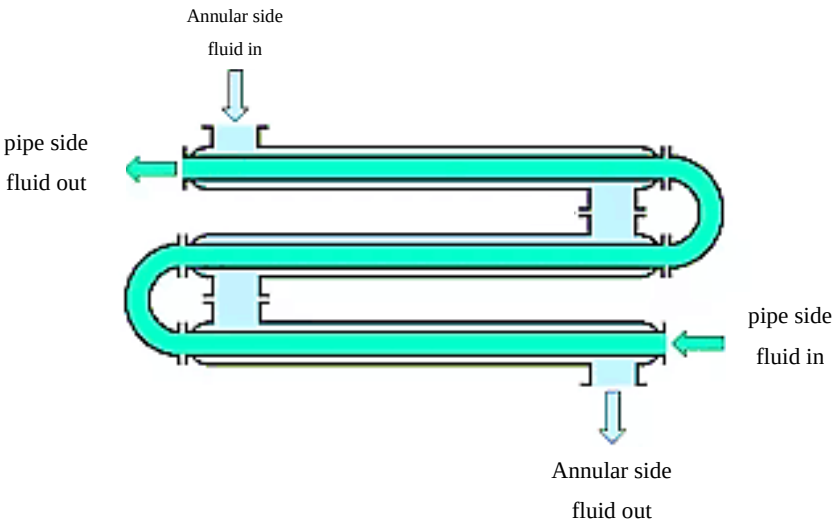

Figure 1.2. Double-pipe heat exchanger

1.2. ADVANTAGES AND DISADVANTAGES OF DOUBLE PIPE HEAT EXCHANGER

1.2.1. Advantages

This heat exchanger is still widely used in many industrial fields, including petrochemicals, because of its many advantages.

- The structure is simple, and the heat transfer area is adjustable. Installation requires no extra processing because it uses standard components.
- The higher fluid velocity and heat transfer coefficient on both sides greatly enhance this heat exchanger's efficiency. Fluids with low heat transfer coefficient, low flow rates, high pressure, and good heat exchange are also successful .
- This simple and flexible structure allows for easy adjustments to the surface area and fluid flow velocity, improving the heat transfer coefficient. Fins, a scraping film, and a perturbation device can be added to the outer surface of the inner tube to enhance heat transfer and facilitate high-viscosity fluid flow.
- The form of the object can be adjusted according to the installation position, making the installation process more manageable.

1.2.2. Disadvantages

Double-pipe heat exchangers used five times more metal per heat transfer surface than shell-and-tube heat exchangers. Multiple pipe joints result in both leakage and increased flow resistance.

- It is difficult to perform maintenance due to the potential leaks at detachable connections during overhaul, cleaning, and disassembly.
- Production constraints restrict the range of materials that can be used. Welding the inner tube in pipe-in-tube heat exchangers is prohibited since it can cause thermal expansion and breaking. Double-pipe heat exchangers are commonly formed into a serpentine shape by bending and coiling, which necessitates using specialist materials that are resistant to corrosion.

- Recuperative heat exchangers are less expensive compared to non-recuperative heat exchangers.
- The main issue is leakage, which means having a perfect seal is necessary.

1.3. FLUID FLOW ARRANGEMENTS

There are two prevalent configurations of flow routes in a heat exchanger: counter flow and parallel. A counter flow heat exchanger involves the flow of two fluids in opposite directions. On the other hand, a parallel flow heat exchanger enables the simultaneous flow of both liquids in the same direction [5]. Figure 1.3 illustrates the direction of fluid flow in parallel and counter flow heat exchangers.

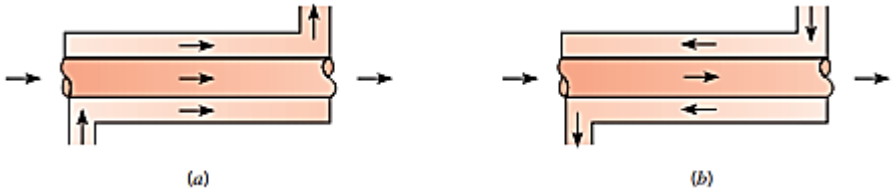

Figure 1.3. Shows two types of double-pipe heat exchangers: (a) parallel-flow, and (b) counter-flow [5]

1.4. PARAMETERS FOR ENHANCING A HEAT EXCHANGER

When designing and operating exchangers, various thermal parameters must be considered as they directly impact performance. Some of these parameters are mentioned below [6]:

i. Fluid mass flow rate
ii. Fluid specific heat
iii. Thermal conductance factor
iv. Coefficient of convection heat transfer
v. Heat exchange area
vi. The temperatures of hot and cold fluids at the inlet and exit

1.5. HEAT TRANSFER IMPROVEMENT METHODS IN HEAT EXCHANGERS

Active and passive heat exchangers are two broad categories for the various methods used to improve heat transfer. Active methods such as electrohydrodynamic, jet, spray, mechanical aid, fluid, and surface vibration necessitate external power sources. In contrast, passive techniques incorporate specific structures or chemicals into fluids to increase heat transfer without the need for external power sources [7].

1.5.1. Active techniques

- *Electrohydrodynamic technique:* A low-current, high-voltage joint is utilized for improved active heat transfer**.** The principal aim of this methodology is to transform electrical energy into kinetic energy, thereby generating motion and propelling the fluid.
- *Jet technique:* In this method, a single-phase fluid is propelled toward the surface of the tube using one or multiple jets. This technique also enhances heat transfer by using a plane between the liquid flows.
- *Spray technique:* The spray is made up of liquid droplets, created by air or pressure-assisted showers. A thin layer of liquid or an evaporated layer forms as these droplets spread across the surface. When it comes into contact with a hot surface, this increases heat transfer.
- *Mechanical aid technique:* A rotary heat exchanger tube manages equipment in commercial practice. Mechanically sweeping or rotating the liquid is involved in this process. Chemical process industries can apply mechanical surface abrasives to gas tubes and viscous fluids.
- *Fluid vibration technique*: Heat exchangers typically exhibit vibrations ranging from low-frequency pulses of approximately 1 Hz to high-frequency ultrasonic, making it a viable approach for experimental vibration augmentation. These vibrations are utilized in diverse manners to isolate liquids. Electrostatic fields can be manipulated to enhance fluid mixing close to the thermal transfer surface.

- *Surface vibration technique:* Surface vibration can be of low or high frequency and is primarily used to enhance monovalent heat transfer. using piezoelectric devices, the surface is shaken, and a few drops are sprayed on the hot surface to promote "cooking spray".
- Three main methods of enhancing heat transfer are as follows: a synthetic jet that drives flow from a membrane movement connecting the vacuum; dynamic deformation of high-capacity solid material, and periodic motion of a solid wall using sound waves from high-frequency membrane oscillations.

1.5.2. Passive Techniques

In a heat exchanger, passive methods such as inserts or modifications to the surface or geometry enhance heat transfer. These inserts enhance the heat transfer coefficients, leading to improved heat transfer. There are several passive techniques available for this purpose [7]

- *Surface roughness technique:* The technique of coating surfaces with metallic or non-metallic materials is passive coating. This coating makes the surface non-wetting or hydrophilic. The surface roughness can be attained by either reconfiguring the underlying surface by machining or by introducing a neighboring roughness. Figures 1.4 [8] and Figure 1.5 [9] display illustrations of surfaces that have been coated.

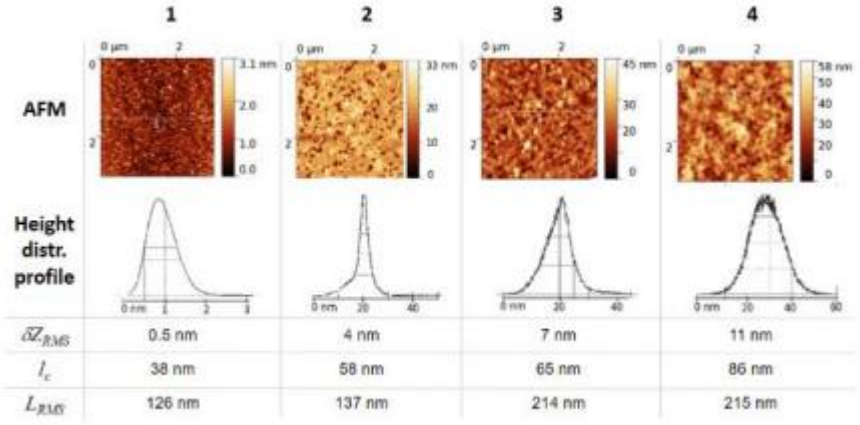

Figure 1.4. Photo of surface roughness [8]

Figure 1.5. Rough pipes in the inner and outer surfaces [9].

- *Extended surface technique:* Extended surfaces in multi-fluid or multi-fluid heat exchangers are equipped with fins connected to the main component on one side. Fins of various geometric configurations, flat, wavy, or serrated, may be affixed to cylindrical, flat, elliptical, or segmented panels from either the interior, exterior, or both sides. Fins enhance the overall heat transfer rate by increasing surface area, particularly in cases where the liquid side's heat transfer coefficient is relatively low. In addition, the heat transfer coefficient is higher with improved fin geometry than with a standard fin. Figure 1.6 demonstrates exterior finned tubes on an individual basis, while Figure 1.7 depicts longitudinal fins on a variety of tubes. Lastly, Figure 1.8 showcases various twisted taps employed as fins within tubes [1, 2, 9, 10].

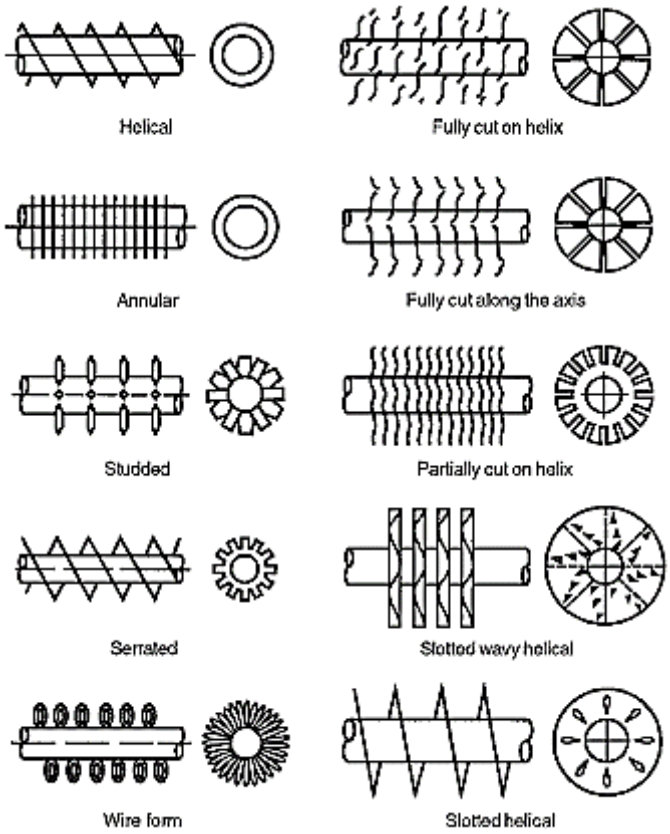

Figure 1.6. Finned tube with individual fins [1]

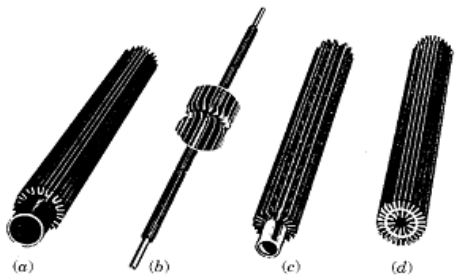

Figure 1.7. Longitudinal fins on individual tubes, (a) continuous plain, (b) cut and twisted, (c) perforated, (d) internal and external longitudinal fins [2]

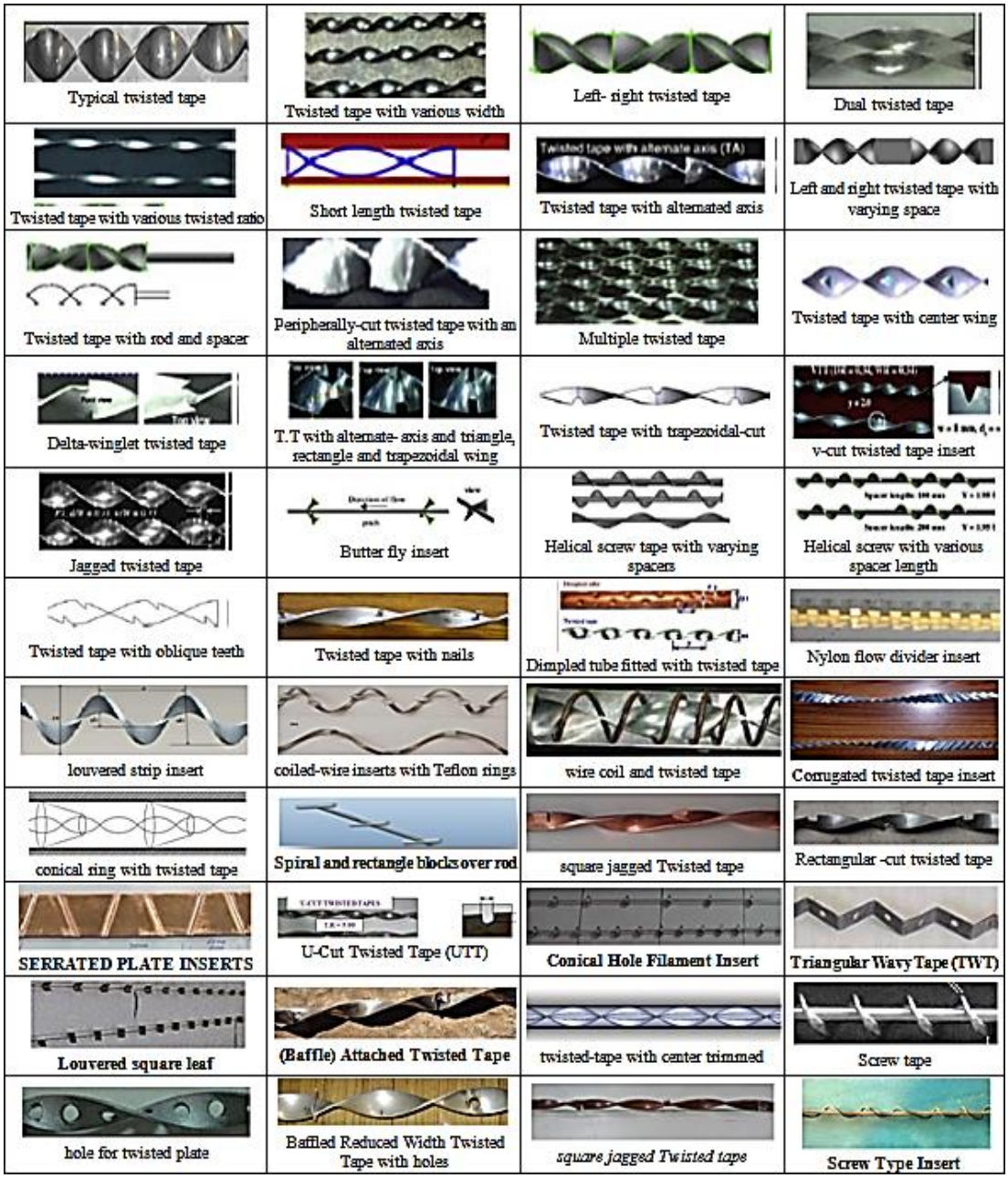

Figure 1.8: Photographs depicting various varieties of twist taps utilized in heat exchangers [9]

- *Nanofluid solutions technique:*

The advancement of technology presents a significant challenge for high-tech industries: improving heat transfer. To tackle this difficulty, nanofluids have been introduced as supplementary substances to augment the heat transfer coefficient. Solid nanofluids have a much higher thermal conductivity than liquid nanofluids. The following types of nanofluids are used to improve heat exchanger performance [11].

a. Al_2O_3/H_2O nanofluid
b. CuO/H_2O nanofluid
c. Carbon nanotube/H_2O nanofluid
d. TiO_2/H_2O nanofluid
e. ZrO_2/H_2O nanofluid

- *Porous media technique:*

A porous medium is a material that contains a network of solids and empty spaces. The solid material cannot be considered a porous medium without this network. The empty spaces between the solid mesh allow fluids to flow through the material, but the pathway is intricate and irregular. Because holes are small and comparable, studying the material's microscopic structure is impossible. Figure 1.9 shows open-cell foam, a lightweight, cellular material with oval-shaped voids surrounded by a solid 3D grid. This lightweight material is strong and stiff, making it perfect for many applications. A variety of methods, including casting, electrophoresis replication, infiltration, and molding, can be used to produce open-cell foam from aluminum, copper, steel, nickel, and ceramics like Al_2O_3, Mullite, SiC, and OBSiC [12, 13].

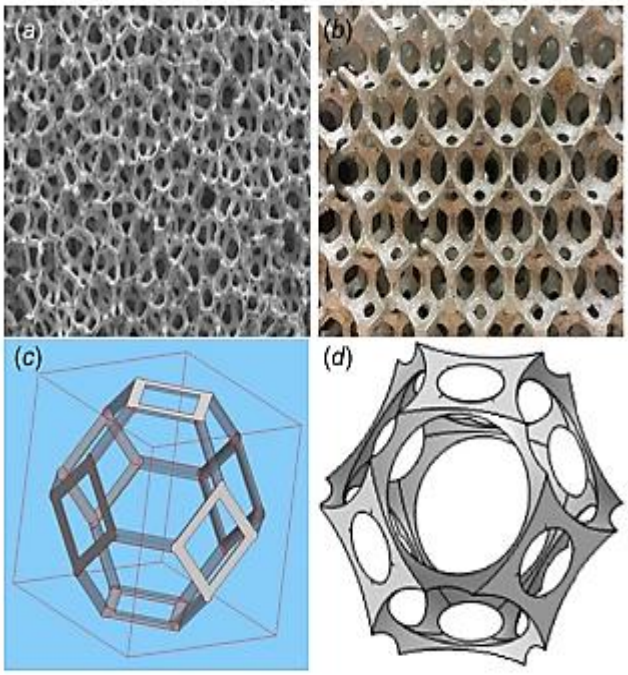

Figure 1.9. Open-cell foam examples include (a) a sample produced using a commercial replication method, (b) a sample cast in sand, and (c, d) two instances of isotropic idealized Kelvin-like unit cells [12]

1.6. OBJECTIVE OF THE STUDY

Heat exchangers are essential in both industrial and domestic settings. Improving their performance is crucial, and many inventions have been proposed. One such proposed approach is the extended surface technique, which has successfully enhanced heat transfer in the area. This study used a numerical method to select three fins, helical-annular, half-annular and annular finned tube, to assess their thermal efficiency compared to without finned heat exchangers operating under similar working conditions. This comparative analysis will assist in ascertaining the most optimal approach to augment heat transfer in heat exchangers to achieve peak performance.

PART 2

LITERATURE REVIEW

Heat exchangers are essential elements that are required in the majority of industrial facilities. A multitude of inquiries have been conducted in an effort to evaluate the thermal efficacy of this apparatus. This chapter extensively examines research methodologies and developments in thermal performance that have been pursued by numerous countries worldwide. There exist multiple techniques for augmenting the heat exchanger's surface area. This study focuses primarily on research made on the surface improvement method.

Eiamsa-ard et al. [14] improved heat transfer and reduced pressure drop in a double-tube heat exchanger. The heat conduction through the 19.6-mm inner tube was improved. The study examined the pressure drop and heat transfer coefficient in turbulent flow throughout the Re number range of 6000 to 42000. Metal strips with inclined fins at angles of 15˚, 25˚, and 30˚ were used in the annular gap. A cold fluid traversed the annular gap while the heated fluid remained within the inner tube. The presence of fins in the annular gap enhances tube heat transfer by inducing turbulent flow. Fins increased the Nu number and f factor in the flow direction by 263% and 233%, respectively, and in the other direction by 284% and 413%, respectively. The surface was improved by 9–24% when tapes were placed in the direction of flow.

Sahiti et al. [15] conducted a study to investigate the effect of pin fins on heat transfer in double-tube heat exchangers. Two identical heat exchangers were put to the test; one had screw fins on the inner tube and the other did not. Air passed through the annular gap and heated water went through the inner tube. Within the range of 7000 to 35000 Reynolds numbers, counterflow and turbulent flow conditions were used for the experiments. The coefficient, Nusselt number, and rate

of heat transfer were all computed by the researchers. Compared to exchangers without fins, they discovered that applying pin fins increased heat transfer by a factor of 70.

Wang et al. [16] used ANSYS software to simulate the impact of helical fins on the inner tube of a double-pipe heat exchanger. The simulation investigated how helix angle α affects Nu number and friction coefficient for Re numbers in the range f 2362 to 16860. This work assessed PEC values and heat transfer performance at various helix angles (α). The approach was suitable with an average inaccuracy of 7.1% for Nu and 1.3% for f. Results indicate that Nu and f decrease with α. In particular, f significantly rose below α=35°. Applications with a PEC of 1.26-1.62 work best with a 35° helix angle. Oblique helical fins reduce f by 12.5%-14.5% and increase Nu for heat transfer. Oblique helical fins (α=35°, β=10°) had a significantly higher Nu value than double-pipe heat exchangers with standard fins. The field synergy principle verified these findings.

Rao and Kumar [17] conducted a theoretical and experimental heat transfer analysis in a double-pipe heat exchanger. The outside surface of the inner tube was equipped with a copper spiral strip plate, which had three different torsional ratios (4.167, 5.556, and 6.944) and a pitch of 0.5 mm. The working conditions were 300 K cold and 353 K hot fluid inlets. Twisted tapes were compared to a standard heat exchanger. The heat transfer was increased by 3.54% and the friction coefficient by 7.532% at Re number 9072.782 when the tape was twisted with a twist ratio of 4.167. Compared to the usual exchanger at Re number (12073.779), numerical findings for the identical tape indicated heat transfer coefficient rose to 3.364 times and friction coefficient to 10.39 times. AT the Re number of 20135, tape twisted with a ratio of 6.944% improved friction coefficient by 4.723 times and heat transfer rate by 1.450 times.

Kailash et al. [18] examined how the hydrothermal performance of a double-pipe heat exchanger is affected by enlarging the outer surface of its inner tube. Two similar double-pipe heat exchangers were used in the study. One heat exchanger had 18 half-circular fins 1.6mm thick, 10mm high, and 50mm apart, whereas the other was ordinary. Re numbers ranged from 6407 to 15957 for hot fluid and 5984 to 17161 for cool fluid. At the most incredible flow range with a Re number of 17161, the finned

exchanger had a 220% poorer total heat transfer coefficient at 0.3832 kg/s on the cold-water side. The hot water heat transfer coefficient rose by 125%. While both exchangers had identical hot-water friction coefficients, the one with the larger heat transfer surface had a 140% cold-water increase. Finally, the fin-equipped exchanger lowered pressure by 450% more than usual.

Dong et al. [19] suggested using oblique helical fins to decrease the frictional resistance coefficient, f, in a double-pipe heat exchanger that has been improved with helical fins. Oblique helical fins reduce f by 1.7%-3.3%, 12.5%-14.5%, and 6.3%-7.8% when β grows to 5°, 10°, and 15°, respectively. Oblique helical fins exhibit greater PEC values than conventional helical fins. When β reaches 10°, PEC rises to 1.38-1.71 from 1.26-1.62. Oblique helical fins have lower entrance dissipation rates than typical helical fins. The lowest rate occurs when β equals 10°, consistent with the same pump power.

Hatami et al. [20] numerically modeled three diesel engine exhaust heat exchangers (HEXs) to optimize exergy recovery. The study involved modeling primary heat exchangers (HEXs) with both longitudinal and circular fins to investigate their effectiveness in recovering waste heat. Circular and longitudinal fins with the same surface area were compared for exhaust exergy recovery and pressure drop. Circular fins capture gases and lower pressure more than longitudinal fins, reducing exergy recovery. The most critical longitudinal fin characteristics for this heat exchanger's optimal design were identified using an L16 Taguchi array. A multi-objective optimization was conducted using the central composite design to find the best HEX size at different engine loads.

Zhang et al. [21] found that adding helical fins and triangle-winglet-pair vortex generators to the shell side of a double-pipe heat exchanger made it better at moving heat. The centerline of the VG will have a rectangular cross-section helical channel installed. Triangle-winglet-pair vortex generators (VGs) were analyzed to determine the optimal design, considering factors like pressure drop, heat transfer efficiency, shape, and angle of attack. Between 680 and 16,000 Reynolds air was the range in which they worked. Heat exchange efficiency on the shell side is increased by 16.6%

when vortex generators (VG) are used. The substantial rise was ascribed to VG vortices and instability in the flow. The most advantageous angle of attack, which outperformed 45° and 60°, was 30° when similar pressure drop conditions were applied. Equivalent mass flow rate, pressure drop, and power would improve the maximum volumetric growth (VG) size. This study shows that three pairs of VG in a single pitch are ideal for shell sides. Furthermore, a right triangle with an isosceles angle showed more improvement than one with a triangle with a 30° acute angle.

Salem et al. [22] examined convection heat transfer and the contraction of the annulus side of horizontal double-pipe heat exchangers. We built 12 counter-flow heat exchangers, some with single-segmental perforated baffles (SSPBs) and some without. It included parameters such as the spacing between holes, the presence of voids, cuts, pitch ratios, and the degree of inclination. During the tests, Reynolds numbers varied between 1380 and 5700 on the annulus side, and Prandtl numbers varied between 5.82 and 7.86 on the inclination side. The findings showed that the average Nu number (Nu_{avg}) and the fan friction factor in the annulus improved as the cut and pitch ratios went down and the inclination angle, the spacing between SSPB holes, and the void ratios went up. The researchers performed a comparative analysis of perforated baffled double-pipe heat exchangers and unbaffled ones utilizing the thermal performance index (TPI). It was discovered that by raising the SSPB hole spacing ratio and inclination angle and decreasing the void ratio, cut ratio, and pitch ratio, there was an observed increase in the thermal performance index.

Rao and Gollamudi [23] worked on computational fluid dynamics (CFD) to investigate the shapes of longitudinal fins on double-pipe heat exchangers. Two longitudinal strips, one in a round form and the other in a square form, were employed to test the Nu number, pressure drop, and heat transfer coefficient. The Fluent CFD software was used to construct and simulate meshed grills in heat exchangers by placing longitudinal circular and square strips at different Reynolds numbers. The validated model established the objective and parameters for thermal energy transfer in double-pipe heat exchangers. After numerical modeling, the pressure effect and heat transfer coefficient were evaluated for longitudinal circular and square strips of varied sizes and flow rates under turbulent flow. The study found that the longitudinal circular strip

improves heat transfer compared to the square strip. However, the square strip side has a more significant pressure drop.

In a study conducted by Sivalakshmi et al. [24], experiments were carried out to investigate the impact of helical fins on the performance of double-pipe heat exchangers. A heat exchanger with a simple inner pipe was compared to one with helical fins above the inner tube to see which had the best average heat transfer rate, coefficient, and effectiveness. The experiment involved adjusting the flow rate of hot fluid between 0.01 and 0.05 kg/s while keeping the intake temperature constant at 80°C. The results showed that fins improved the heat transfer coefficients. The heat exchanger's average heat transfer rate and efficiency rose to 35% and 38.46%, respectively, at higher flow rates.

Amin et al. [25] studied how the fins' arrangement affects the solidification and melting processes in a double-pipe latent heat storage system with vertical fins. An evaluation was conducted on the fins' positioning, width, and size. Water flows within an inner tube, while the phase change material (PCM) is confined within the outer tube. A fixed number of fins surround the internal pipe and PCM region. Fins reduce the time it takes for melting by 23.9% in the finest arrangement of fins and by 41.4% in the uniform arrangement of fins, compared to the scenario without fins. The presence of fins in a homogenous fin array reduces solidification time by 9.7% compared to the lack of fins. An evenly distributed arrangement of fins is the most effective for solidification, as it leads to an 11.4% improvement in the amount of heat that can be recovered. The study also revealed that fins with a reduced thickness have a more rapid melting process. However, once the diameter exceeds a certain threshold, it inhibits natural convection.

Abdul Wahhab et al. [26] conducted a study to improve the performance of a double-pipe heat exchanger using passive heat transfer techniques. They used various methods and equipment to enhance the heat transfer in the inner pipe of the heat exchanger. One of the techniques they used was corrugated tape with dimpled inner and outer lines. The study used hot water at 50°C and cold water at 25 °C, with Reynolds numbers ranging from 6000 to 15000. They tested five heat exchangers, including a smooth pipe, two pipes with tiny indentations at 0.95, and two tapes with wavy patterns

at 0.5 and 1. To evaluate the heat transfer and pressure loss of nine pipe types, including dimpled, corrugated, and twisted tapes, they employed ANSYS design modular and fluent R1-2019 software. The inwardly staggered dimple pipes with a pitch ratio of x/do = 0.95 increased the average Nusselt number by 54.5% and the friction factor by 136%. Comparing the perforated tape to a plain tube, the friction factor increased by 14.62 times, and the Nusselt number increased by 195.8% with a pitch ratio of (x/w=0.5). The corrugated tape variants had an average Nusselt number of 347.10% and 42 times the friction of plain pipes.

Farhan et al. [27] examined heat exchangers with MF between pipes. The study employed copper MF with a plate number of 1 and a porosity of 0.95 on an inner pipe's outer surface in a counter-flow double-pipe heat exchanger. The crew assessed hydraulic and thermal capacities. Two copper and polyvinyl chloride concentric pipes comprised the test segment. The hot and cold sides utilized air, with cold air flow rates from 3 to 36 m3/h (2811<Re<31,335) evaluated. Hot air circulated at three cubic meters per hour. The input hot and cold air differed by 20°C, 30°C, 40°C, and 50°C. Research showed that the MF heat exchanger had a higher Nu number and performed better thermally than the smooth one. The Nu number peaked at 50°C ΔT. Cases 1 and 8 had the highest and lowest friction values, 1.033 and 0.0833. Case 7 had 2800 Re and the highest PEC (1.62).

Albayat and Khalifa [28] studied the effects of active and passive procedures on heat transfer using different positions of the U-shaped heat exchanger (U and Inverse U shape) connected in parallel with the tube liquid in series. They measured flow and temperature with an appropriate heat exchanger and flow meters and thermocouples. The study discovered that tube bending and angle of curvature generate vortex flow, which boosts heat transfer and performance. The study uses a circular fin for passive and a small compressor to inject air bubbles through a novel air diffuser for active methods. The results show that the inverse U shape (∩) performed best, enhancing active approaches by 19.1% and passive techniques by 11.1%. Combining both methods increased 30.272%. The study provides new insights for future research.

Ishaq et al. [29] developed a computer model of a heat exchanger with two pipes, one of which has longitudinal fins formed like diamonds on the inner tube. We looked at Hussein and Hameed (30) analyzed the efficiency of heat transfer in an air-water double-pipe heat exchanger. The annular side of the heat exchanger was lined with segmental baffles that had semi-circular holes and fins. While the annulus operated on air, the inner tube was filled with water. The study analyzed three different semi-circular perforations: 30 mm, 25 mm, and 20 mm, with seven air Reynolds values ranging from 2700 to 4000 and 34,159 for water. The study did not calculate the number of units, heat transfer coefficient, friction factor, or thermal performance factor. The study compared heat exchangers with baffled and unbaffled pipes. It was found that heat exchangers with baffled pipes performed better. Perforated baffles with 30-, 25-, and 20-mm holes improved the average heat transfer coefficient by 29.7%, 62%, and 80.6%, respectively. All heat exchanger perforated baffles had thermal performance factors (TPFs) more significant than one, with 20 mm baffles performing the best.

Albayat and Khalifa [31] used active air injection on the shell side of a U-shaped heat exchanger. The researchers used a double-pipe heat exchanger with a transition from higher U to lower ∩ positions. The vortex that the curved shell and tube created improved exchanger performance, according to tools for monitoring flow rates and parameters. Injection of air bubbles on the shell side of the exchanger showed that an inverted U-shaped diffuser performed best. This design improved the exchanger by 24.4%. Exchanger efficiency was highest in an inverted (∩) design. This dynamic approach increased fluid and airflow agitation and turbulence to improve heat transfer and exchanger performance.

Mohammed et al. [32] conducted a quantitative analysis to investigate the impact of applying "Alumina nanofluid" on the external surface of the inner tube in a double-pipe heat exchanger, with the aim of enhancing heat transfer. During the investigation, water with varying mass flow rates ranging from 0.03 to 0.07 kg/s and hot de-ionized water with variable Reynolds numbers ranging from 250 to 2500 were passed through the annuli and inner tube. The simulations employed Al2O3 nanoparticles with 1%, 3%, and 5% volume concentrations. The numerical study employed CFD software,

while modeling was done using Solid Works. The governing equations were resolved using the semi-implicit method for pressure equations and discretized through finite volume. The finned tube heat exchanger enhanced the ratio between (2.3) and (3.1). The convective heat transfer coefficient increased proportionally with the Reynolds number and volume concentration. When the volume concentration is at 5%, both the heat transfer coefficient and thermal conductivity see a 20% and 4.7% rise, respectively.

Lafta and Mohammed (33) examined vibration and inclination angle to determine a dual heat pipe exchanger's hydrothermal quality. Vibration frequencies from sub-resonance to over-resonance were tested on inclined angles of 0, 10, 20, and 30 degrees. The compound technique across the whole temperature and flow rate range of the working fluid enhanced heat transfer coefficients. The resonance frequency and 30° inclination angle caused the most significant increases in the overall heat transfer coefficient. The double-pipe heat exchanger's efficiency increased with temperature, inclination angles, and vibration amplitude. However, increasing the hot working flow rate reduced efficacy. The synergistic use of vibration frequencies and inclination angles increased heat transport more than other methods. The improvements were 191%, 164.4%, and 183.4% for the heat transfer coefficient, efficacy, and enhancement, respectively. These resonance frequency readings were acquired at an angle of 30° inclination.

Haya and Basim [34] examined how fin designs affect double-pipe heat exchanger efficiency. Researchers tested longitudinal, split longitudinal, in-line, staggered, and semi-helical fins. The fins were tested at 90̊, 180̊, and 270̊ angles, with a constant heat flux of 8000 W/m2 to the inner tube surface. The numerical investigation used ANSYS Fluent 2022 R1 for all models. The study measured Nu number, pressure drop, and heat resistance. The standard and optimal models (Model D) were created to validate the numerical results, and they matched well. The study found that fin type significantly affects DPHE efficiency. With its semi-helical eight-finned design and 90′ angle, the Model D outperformed other fin types investigated. It improved total performance by 1.47% and Nu number by 66.76%. This study accurately evaluates DPHE performance.

Hassan et al. [35] examined the performance of two heat exchangers that employed aluminum fins and copper foam as a porous material. The investigation encompassed a variety of air intake velocities, spanning from 0.9 to 9.3 m/s, and water inlet temperatures, ranging from 10°C to 18°C. They performed trials using various water flow rates. The thermal resistance, efficiency, Colburn factor, Nusselt number, friction factor, and area goodness factor were computed to compare the two heat exchangers. Both heat exchangers showed almost comparable heat transfer coefficients when the air velocities were low. Copper foam demonstrates an increased heat transfer coefficient at high air velocities. The heat exchanger, fitted with copper foam, had a higher Colburn factor of 0.1959, in contrast to 0.1186. However, fins exhibited better thermal conductivity than copper foam heat exchangers.

This study stands out for its originality in presenting comprehensive studies, encompassing practical approaches aimed at improving heat transfer in heat exchangers. These studies have demonstrated that while increasing the heat exchange surface area improves heat transfer, the presence of inhibitors causes a pressure drop. The thermal and hydraulic characteristics of three distinct kinds of annular fins in a double pipe heat exchanger were examined in this work using ANSYS software and numerical analysis. Fin forms of annular, half-annular, and helical-annular are present in the fins. In earlier studies, these fins' pressure drop and thermal performance were not compared to those of conventional exchangers or to one another.

PART 3

RESEARCH METHODOLOGY

Heat exchangers can be developed using two methods: the first involves applying the principle of energy equilibrium as dictated by the first law of thermodynamics, while the second method consists in utilizing the heat transfer rate equation [1]. These techniques are employed to examine the thermal energy transfer in the heat exchangers. This chapter provides the equations utilized for the computation of significant parameters in heat transfer, including the log mean temperature difference (LMTD), the overall heat transfer coefficient (UA), effectiveness (ε), number of transfer units (NTU), and the Nusselt number (Nu). A series of assumptions are employed to determine the heat transfer problem in the heat exchangers. The following assumptions are listed: [1, 36].

a. The heat exchanger works in steady-state conditions.
b. The heat exchanger gains or loses negligible heat from its surroundings.
c. no energy source supplies power to the heat exchanger wall or the fluids.
d. The longitudinal thermal resistance of the fluids and the wall can be considered insignificant.
e. Individual and overall heat transfer coefficients remain constant regardless of position, time, or temperature.
f. Throughout the heat exchanger, the specific heat of each fluid remains constant.
g. The velocity and temperature of the fluid are consistent throughout the cross-section at the intake of the heat exchanger.
h. There are negligible variations in the potential and kinetic energy.

3.1. PROBLEM FORMULATION

3.1.1. Heat Transfer Rate

The heat transfer analysis in a heat exchanger entails the application of the energy balance equation between the heated and cold water. This necessitates considering the simplifications for both the energy balance and heat transfer equations. By employing this method, the heat transfer equation may be written with precision [1-3].

$$q = \dot{m}_h\left(i_{h,i} - i_{h,o}\right) \tag{3.1}$$

and

$$q = \dot{m}_c\left(i_{c,o} - i_{c,i}\right) \tag{3.2}$$

Assuming that the fluid does not undergo a phase change and that its specific heat, Eq. (3.1) and Eq. (3.2) are replaced with [5]:

$$q = \dot{m}_h\, Cp_h\left(T_{h,i} - T_{h,o}\right) \tag{3.3}$$

and

$$q = \dot{m}_c\, Cp_c\left(T_{c,o} - T_{c,i}\right) \tag{3.4}$$

Another helpful expression relates the total heat transfer rate to the temperature difference (ΔT) between hot and cold fluids.

$$\Delta T = T_h - T_c \tag{3.5}$$

The heat transfer rate can be expressed using the overall heat transfer coefficient (U) as follows:

$$q = U\, A\, \Delta T_m \tag{3.6}$$

The mathematical expression of ΔT_m can be determined based on the arrangement of the flow.

3.1.2. The long mean temperature difference (LMTD)

Figure 3.1 illustrates the phenomenon of heat transfer between hot and cold fluids in a counter-flow double-pipe heat exchanger. One can obtain variables associated with its thermal efficiency by utilizing the energy balance equation on a differential element (dA × dx) present in both fluids. This calculation relies on the premise that the quantity

of heat transferred from the hot fluid is equivalent to the amount of heat transferred to the cold fluid [36].

$$dq = -\dot{m}_h \, Cp_h \, dT_h = -C_h dT_h \tag{3.7}$$

and

$$dq = -\dot{m}_c \, Cp_c \, dT_c = -C_c dT_c \tag{3.8}$$

where $C_h$and C_c are denoted as the hot and cold heat capacity rates, respectively. Heat transfer can also be represented [2].

$$dq = U(T_h - T_c) \, dA \tag{3.9}$$

Using the Eq. (3.7) and Eq. (3.8), it is determined both as;

$dT_h = -\frac{dq}{C_h}$ and $dT_c = -\frac{dq}{C_c}$

Thus,

$$d(T_h - T_c) = -dq\left(\frac{1}{C_h} - \frac{1}{C_c}\right) \tag{3.10}$$

and can be integrated between conditions 1 and 2 as shown in Figure 3.1 [2]

$$\int_1^2 \frac{d(T_h - T_c)}{T_h - T_c} = -U\left(\frac{1}{C_h} - \frac{1}{C_c}\right)\int_0^A dA \tag{3.11}$$

it yields

$$\ln\frac{(T_{h,o} - T_{c,i})}{(T_{h,i} - T_{c,o})} = -U\left(\frac{1}{C_h} - \frac{1}{C_c}\right)A \tag{3.12}$$

Returning to Eq (3.3) and Eq. (3.4), the products C_h and C_c can be stated in terms of the q and overall temperature differences $(T_{h,i} - T_{h,o})$ and $(T_{c,o} - T_{c,i})$. Thus,

$$C_h = \frac{q}{(T_{h,i} - T_{h,o})} \tag{3.13a}$$

and

$$C_c = \frac{q}{(T_{c,o} - T_{c,i})} \tag{3.13b}$$

By substituting Eq. (3.12) into Eq. (3.11) and rearranging, we can obtain the expression [2, 3]:

$$q = UA \, \frac{(T_{h,o} - T_{c,i}) - (T_{h,i} - T_{c,o})}{\ln\left[\frac{(T_{h,o} - T_{c,i})}{(T_{h,i} - T_{c,o})}\right]} \tag{3.14}$$

Upon comparing Equation 3-14 with Equation 3-6, we can see that the grouping of terms in the brackets represents the mean temperature difference.

$$\Delta T_m = \frac{(T_{h,o} - T_{c,i}) - (T_{h,i} - T_{c,o})}{\ln\left[\frac{(T_{h,o} - T_{c,i})}{(T_{h,i} - T_{c,o})}\right]} \tag{3.15}$$

3.1.3. Overall heat transfer coefficient (U)

The overall heat transfer coefficient includes convection and conduction. This can be stated using Figure 3.1's concentric pipe heat exchanger equation [2, 3, 5]:

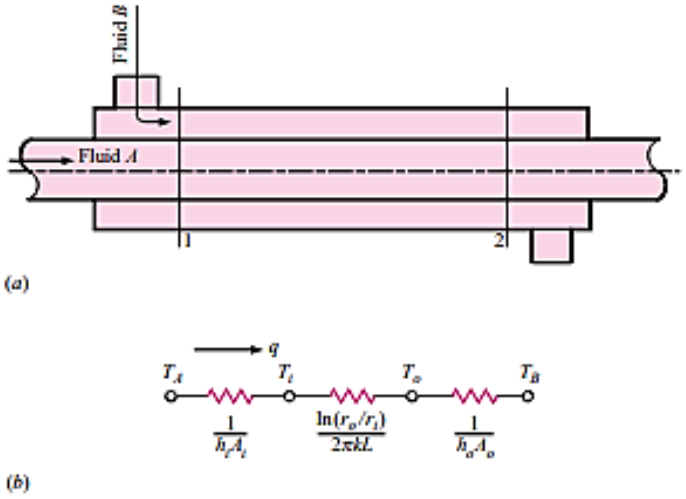

Figure 3.1. Double-pipe heat exchanger, (a) sketch diagram, (b) thermal resistance network [2]

$$q = \frac{\Delta T_m}{\frac{1}{h_i A_i} + \frac{\ln\frac{r_o}{r_i}}{2\pi kL} + \frac{1}{h_c A_o}} \tag{3.16}$$

By comparing Eq. (3.16) with Eq. (3.14) and Eq. (3.15), it can be observed that the denominator of Eq. (3.16) represents the total thermal conductance, UA. The designer can choose whether to base UA on the inside or outside area of the tube. Accordingly.

$$U_i = \frac{1}{\frac{1}{h_i} + \frac{A_i \ln\frac{r_o}{r_i}}{2\pi kL} + \frac{A_i}{A_o}\frac{1}{h_c}} \tag{3.17}$$

$$U_o = \frac{1}{\frac{A_o}{A_i}\frac{1}{h_i} + \frac{A_o \ln\frac{r_o}{r_i}}{2\pi kL} + \frac{1}{h_c}} \quad (3.18)$$

3.1.4. Convection Heat Transfer Coefficient

The Nusselt number (Nu) is a dimensionless parameter that quantifies the convective heat transfer coefficient. In mathematics, the term "ratio" refers to the relationship between the convective heat transfer coefficient and the conductance. This definition is supported by [37].

$$Nu = \frac{h\, d_H}{k} \quad (3.19)$$

The following expression can be used to compute pressure drop [2]:

$$\Delta P = f\frac{4L}{D_h}\frac{G^2}{2\rho} \quad (3.20)$$

where

$$G = \frac{\dot{m}}{A} \quad (3.21)$$

3.1.5. Effectiveness and NTU Method

The Log Mean Temperature Difference (LMTD) approach is utilized for the analysis of heat exchangers, assuming that the intake and outlet temperatures of the hot and cold fluids are known. The heat transfer surface area can be calculated using the values of T_m, mass flow rates, and the overall heat transfer coefficient. In 1955, Kays and London developed the effectiveness-NTU approach as a means to streamline heat exchanger study by eliminating the requirement for several iterative phases. The concept relies on a dimensionless parameter known as heat transfer efficacy [3]:

$$\varepsilon = \frac{Acual\ heat\ transfer\ rate\ (q)}{Maximum\ possible\ heat\ transfer\ rate\ (q_{max})}$$

where

$$q = C_h\left(T_{h,i} - T_{h,o}\right) \quad (3.26a)$$

or

$$q = C_c\left(T_{c,o} - T_{c,i}\right) \quad (3.26b)$$

and

$$q_{max} = C_{min}\left(T_{h,i} - T_{c,i}\right) \tag{3.26a}$$

$C_h = \dot{m}_h Cp_h$ and $C_c = \dot{m}_c Cp_c$

$$C_{min} = \begin{cases} C_h & if\ C_h < C_c \\ C_c & if\ C_c < C_h \end{cases} \tag{3.27}$$

The grouping of terms *UA/C_min* represents the number of transfer units (NTU), which is the size of the heat exchanger. This has a mathematical expression.

$$NTU = \frac{UA}{C_{min}} \tag{3.28}$$

PART 4

NUMERICAL MODELING AND SIMULATION

4.1. MATHEMATICAL MODEL DESCRIPTION

This study aimed to analyze the thermal performance and pressure drop of a counter-flow concentric pipe heat exchanger with an extended inner tube outer surface. The study compared the results with those of an ordinary concentric heat exchanger. The numerical simulation model based on the technical specifications of an experimental concentric heat exchanger, as detailed in the work of Abbas et al. [39] has been used. Table 4.1 presents the technical requirements of the utilized heat exchange extended surfaces, which are shown in Figure 4.1.

Table 4.1. Description of the heat exchanger's technical specifications and the fin types used.

Components name	Descriptions
Inner tube	Copper tube with a 20 mm inner diameter, 22 mm outer diameter, and 1.8 m length.
Outer pipe	Galvanize, inner diameter, outer diameter, and length are 50 mm, 58 mm, and 1.8 m, respectively
Circular fins	Galvanize, inner diameter, outer diameter, and thick are 22 mm, 40 mm, and 3 mm, the number of the fins is 58, and the fin pitch is 30 mm.
Half-circle fin	Galvanize, inner diameter, outer diameter, and thick are 22 mm, 40 mm, and 3 mm, the number of the fins is 58 pairs, and the fin pitch is 30 mm.
Helical fin	Galvanize, inner diameter, outer diameter, and thick are 22 mm, 40 mm, and 3 mm, number of fin is 58, and the fin pitch is 30 mm. 5 mm gap

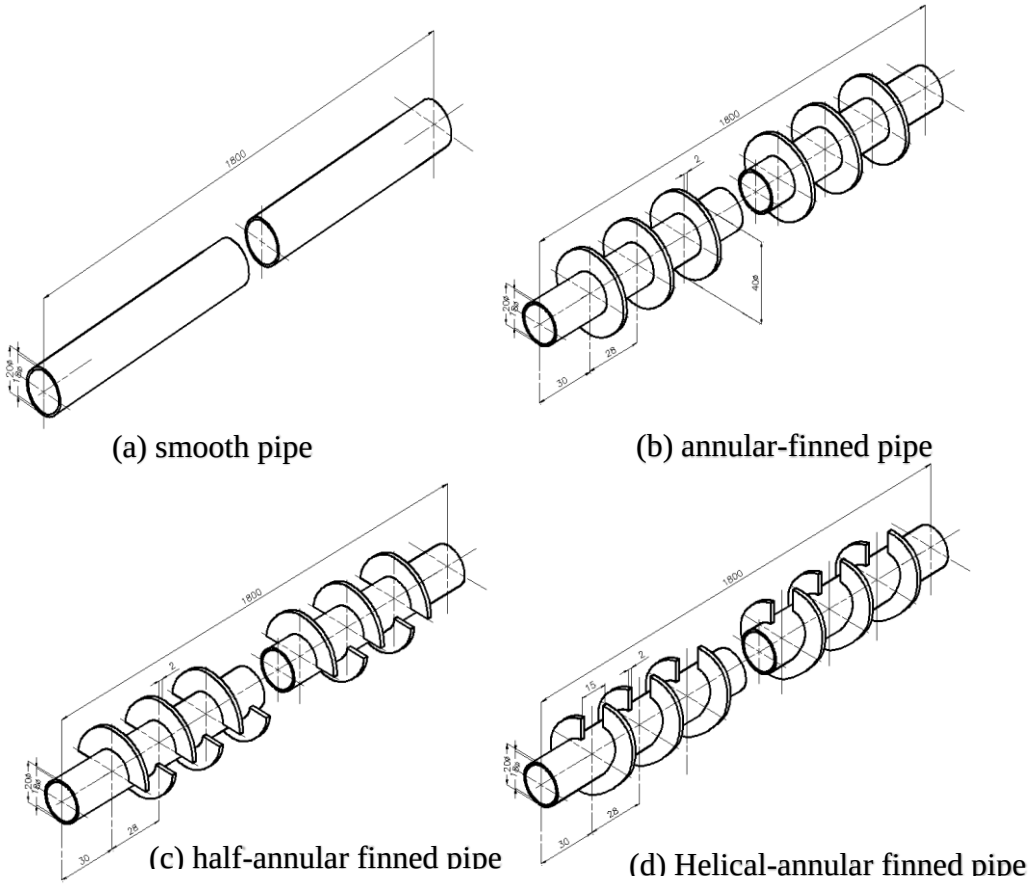

Figure 4.1. Sketch of smooth and finned pipes used in the present study[39]

To construct solutions to engineering problems using Finite Volume Method (FVM), one can either develop a computer program based on the FVM formulation or use a commercially available general-purpose FVM program like ANSYS Fluent. ANSYS is a versatile and powerful analysis tool that can be employed in numerous engineering disciplines. The ANSYS program is perfectly suited for the studies involved in this project. It offers comprehensive and specialized analyses for every field, with a wide range of possibilities. Many companies in the aeronautical industry rely on this program to conduct the necessary tests.

4.1.1. Ansys Software That Processes Data

This software tool executes The model generation process, encompassing defining materials, creating solid models, and, ultimately, establishing bonds between

components. The essential responsibilities surrounded by this processor include [40, 41]:

- Specify the type of element
- Define real constants
- Specify material qualities
- Create the geometry for the model
- Produce the mesh

Although boundary conditions can be given in this processor, they are normally specified in the Solution Processor.

4.1.2. Description of the Numerical Model

This study investigates the effects of adding a surface to the inner tube of a double-pipe heat exchanger on its hydrothermal properties under counterflow using ANSYS Fluent 2022 R2. Numerical models have been developed for four types of double-pipe heat exchangers: circular, half-circular, spiral, and smooth-finned tubes. Table 4.1 lists the material and dimensions of a double-pipe heat exchanger's inner tubes and fins, as shown in Figure 4.1.

4.1.3. Governing Equations

To determine the hydrothermal characteristics of water passing through a double-pipe heat exchanger, the current investigation has made the following assumptions:

The system is experiencing steady-state conditions with a fully developed turbulent flow that is incompressible. Heat transfer happens through forced convection, and the properties of water are considered at the bulk temperature. The inner tube is made of a homogeneous, isotropic material, and radiation heat transfer is negligible. Given these presumptions, the governing equations of fluid dynamics, which include continuity, momentum, and energy, form the foundation of computational fluid dynamics. These equations are related to the field of physics. Fluid mechanics is based on three fundamental principles expressed in different mathematical forms. These

principles serve as the foundation for all fluid dynamics [42]. The following are the governing equations in three-dimensional (3-D) form [5].

- *Continuity Equation*

$$\frac{1}{r}\frac{\partial(ru_r)}{\partial r}+\frac{1}{r}\frac{\partial u_\emptyset}{\partial \emptyset}+\frac{\partial u_z}{\partial z}=0 \tag{4.1}$$

- *Momentum Equations*

$$u_r\frac{\partial u_r}{\partial r}+\frac{u_\emptyset}{r}\frac{\partial u_r}{\partial \emptyset}-\frac{u_\emptyset^2}{r}+u_z\frac{\partial u_r}{\partial z} = \frac{\partial P}{\partial r}+\mu\left(\frac{1}{r}\frac{\partial}{\partial r}\left(r\frac{\partial u_r}{\partial r}\right)+\frac{1}{r^2}\frac{\partial^2 u_r}{\partial \emptyset^2}+\frac{\partial^2 u_r}{\partial z^2}-\frac{u_r}{r^2}-\frac{2}{r^2}\frac{\partial u_\emptyset}{\partial \emptyset}\right) \tag{4.2}$$

$$\rho\left(u_r\frac{\partial u_\emptyset}{\partial r}+\frac{u_\emptyset}{r}\frac{\partial u_r}{\partial \emptyset}+u_z\frac{\partial u_\emptyset}{\partial z}+\frac{u_r u_\emptyset}{r}\right) = -\frac{1}{r}\frac{\partial P}{\partial \emptyset}+\mu\left(\frac{1}{r}\frac{\partial}{\partial r}\left(r\frac{\partial u_\emptyset}{\partial r}\right)+\frac{1}{r^2}\frac{\partial^2 u_\emptyset}{\partial \emptyset^2}+\frac{\partial^2 u_\emptyset}{\partial z^2}-\frac{u_\emptyset}{r^2}-\frac{2}{r^2}\frac{\partial u_r}{\partial \emptyset}\right) \tag{4.3}$$

$$\rho\left(u_r\frac{\partial u_z}{\partial r}+\frac{u_\emptyset}{r}\frac{\partial u_z}{\partial \emptyset}+u_z\frac{\partial u_z}{\partial z}\right) = -\frac{\partial P}{\partial z}+\mu\left(\frac{1}{r}\frac{\partial}{\partial r}\left(r\frac{\partial u_z}{\partial r}\right)+\frac{1}{r^2}\frac{\partial^2 u_z}{\partial \emptyset^2}+\frac{\partial^2 u_z}{\partial z^2}\right) \tag{4.4}$$

- *Energy Equation*

$$\left(u_r\frac{\partial T}{\partial r}+\frac{u_\emptyset}{r}\frac{\partial T}{\partial \emptyset}+u_z\frac{\partial T}{\partial z}\right)=\alpha\left(\frac{1}{r}\frac{\partial}{\partial r}\left(r\frac{\partial T}{\partial r}\right)+\frac{1}{r^2}\frac{\partial^2 T}{\partial \emptyset^2}+\frac{\partial^2 T}{\partial z^2}\right) \tag{4.5}$$

When solving the equations that govern a physical domain, it is essential to carefully select the boundary conditions. For internal pipe and annulus surfaces, the velocity components are assumed to have no-slip conditions ($u_r=u_\emptyset=0$) [43]. In the case of the heat exchanger, cold fluid passes through the shell, while hot fluid flows through the inner tube in the opposite direction. As a result, uniform velocity and boundary conditions are applied at the inlet of the inner tube and the central annulus, the inner tube's outlet, the outer tube, and the casing gap ($P=P_{guage}$). The incoming cold fluid has a temperature of 20°C, while the hot water has a temperature of 65°C. To minimize losses, the perimeter of the outer tube has been neglected. Table 4.2 presents the

specifications of the convective heat transfer between the inner tube fluid and the jacket fluid of the heat exchanger through the separating wall.

Table 4.2. The boundary conditions

Boundaries	**Flow boundary conditions**	**Heat transfer boundary conditions**
Hot fluid inlet	Fully developed, turbulent	65°C
Cold fluid inlet	Fully developed, laminar	20°C
Both sides outlet	P_{outlet}	(0 gauge) Pa
Tube's inner surface	No slip condition	Convection mode
Tube's outer surface	No slip condition	Convection mode

4.1.4 Description of the Turbulence Model

For this particular study, the SST k-ω models were selected over other models because they provided the most accurate results. The choice of these models was due to the presence of fins, which necessitate high accuracy near the pipe wall. Menter created it to combine the robust and accurate formulation of the model in the near-wall region with the free-stream independence of the model in the far field. To achieve this, the model was converted into a formula. The SST k-ω model is given as follows [44]:

The equations of the SST k-ω model:

$$\frac{\partial}{\partial t}(\rho k) + \frac{\partial}{\partial x_i}(\rho k u_i) = \frac{\partial}{\partial x_i}\left(\Gamma_k \frac{\partial k}{\partial k_i}\right) + \widetilde{G_k} + Y_k + S_k \tag{4.6}$$

and

$$\frac{\partial}{\partial t}(\rho \omega) + \frac{\partial}{\partial x_i}(\rho \omega u_i) = \frac{\partial}{\partial x_i}\left(\Gamma_\omega \frac{\partial k}{\partial k_i}\right) + \widetilde{G_\omega} + Y_\omega + S_\omega + \ D\omega \tag{4.6}$$

Where:

$\widetilde{G_k}$:Generation of turbulence kinetic energy to mean velocity

$\widetilde{G_\omega}$:Generation of ω

Γ_k : represent the effective diffusivity of k

Γ_ω : represent the effective diffusivity of ω

Y_k :The dissipation of k

Y_ω :The dissipation of ω

$D\omega$: The cross-diffusion term

S_k :User defined source term of k

S_ω :User defined source term of ω

4.1.5. Mesh Independence Test

The mesh study aims to determine the appropriate number of elements required to obtain accurate output data. The study methodology involves starting with any number of elements and progressively increasing the number until a point is reached where the output data no longer changes significantly. It is important to note that the number of elements is the only variable being altered in the study. The results obtained at each step are analyzed to determine the optimal number of elements needed to generate reliable output data.

Comparing them with relevant experimental data is crucial for accurate results from numerical simulations. To evaluate mesh quality, this study selected a similar experiment [39], which analyzed the exit temperature on the cold and hot sides of four types of double-pipe heat exchangers. The independence of mesh size was investigated for each type separately, and the results are presented below:

4.1.5.1. Smooth Pipe Heat Exchanger

The present analysis evaluated mesh quality using five different mesh quantities ranging from one to five million. The results for the outlet temperature of the hot and cold fluids are presented in Table 4.3. The findings indicated that the optimal number of meshes is one million, which resulted in a minimum error rate of approximately , as shown in the table below.

Table 4.3. Comparing numerical simulation and smooth tube experimental data for smooth tube

Mesh number	Hot fluid			Cold fluid		
	$T_{exp.}$	$T_{num.}$	Error%	$T_{exp.}$	T_{num}	Error%
1000000	42	40.550	-	25	27.770	-
2000000	42	40.355	- 0.48	25	28.087	1.14
3000000	42	40.356	0.002	25	27.770	-1.12
4000000	42	40.324	-0.08	25	28.352	2.09
5000000	42	40.704	0.94	25	28.540	0.66

4.1.5.2. Annular Finned Pipe Heat Exchanger

The mesh independence of circular finned tubes and two additional types of fins was investigated using the same technique as in investigating mesh independence for a smooth tube. The task was completed using this approach, employing an equal amount of mesh. The outcome is displayed in Table 4.4. The analysis showed that using a mesh number of one million produced the most accurate results when comparing the outlet temperature of both fluids with the experimental data at a hot flow rate of 3 LPM and a cold flow rate of 4 LPM. This resulted in a minimal error rate, as shown in the table below.

Table 4.4. Comparing numerical simulation and smooth tube experimental data for the circular finned tube.

Mesh number	Hot fluid			Cold fluid		
	$T_{exp.}$	$T_{num.}$	Error%	$T_{exp.}$	T_{num}	Error%
1000000	42	43.686	-	25	26.406	-
2000000	42	43.761	0.17	25	26.298	-0.4
3000000	42	43.759	-0.4	25	26.494	0.7
4000000	42	43.779	0.04	25	27.539	3.9
5000000	42	43.812	0.07	25	27.021	-1.88

4.1.5.3. Half-Annular Finned Pipe Heat Exchanger

The study tested a numerical model of a half-circle finned tube heat exchanger and found that the best mesh independence was achieved with a mesh number of one million. This resulted in a minimum error rate of approximately 3 LPM for hot fluid and 4 LPM for cold fluid, as shown in Table 4.5.

Table 4.5. Comparing numerical simulation and smooth tube experimental data for the half-circular finned tube.

Mesh number	**Hot fluid**			**Cold fluid**		
	$T_{exp.}$	$T_{num.}$	Error%	$T_{exp.}$	T_{num}	Error%
1000000	52.3	51.9	-	34.8	37.16	-
2000000	52.3	51.82	-0.15	34.8	36.91	-0.67
3000000	52.3	51.72	-0.19	34.8	37.59	1.84
4000000	52.3	51.68	-0.07	34.8	37.64	0.13
5000000	52.3	51.65	-0.05	34.8	37.72	0.21

4.1.4.6. Helical-Annular Finned Pipe Heat Exchanger

After testing the same mesh range mentioned earlier, it was determined that the optimal mesh number for a helical-annular finned pipe heat exchanger is 5 million. The resulting error rate was minimized to approximately the level shown in Table 4.6. This was compared against experimental work at hot and cold fluid flow rates of 3 LPM and 4 LPM for the cold fluid.

Table 4.6. Comparing numerical simulation and smooth tube experimental data for the helical finned tube.

Mesh number	Hot fluid			Cold fluid		
	$T_{exp.}$	$T_{num.}$	Error%	$T_{exp.}$	T_{num}	Error%
1000000	48	50.219	-	31.8	30.346	-
2000000	48	49.995	-0.44	31.8	30.553	0.68
3000000	48	49.862	-0.26	31.8	30.5	-0.17
4000000	48	49.862	0	31.8	30.5	0
5000000	48	49.613	-0.49	31.8	30.772	0.89

4.1.5. Validation of numerical simulation

According to the results shown in Fig. 4.2, the numerical results of a heat exchanger with hot water flowing through a smooth pipe were confirmed by data from experiments done by Abbas et al. [39]. Validation was performed with hot water flow in smooth pipe heat exchangers. The study concluded that the numerical results agreed with the experimental data, with a maximum difference of 10.32%, considered acceptable in scientific research.

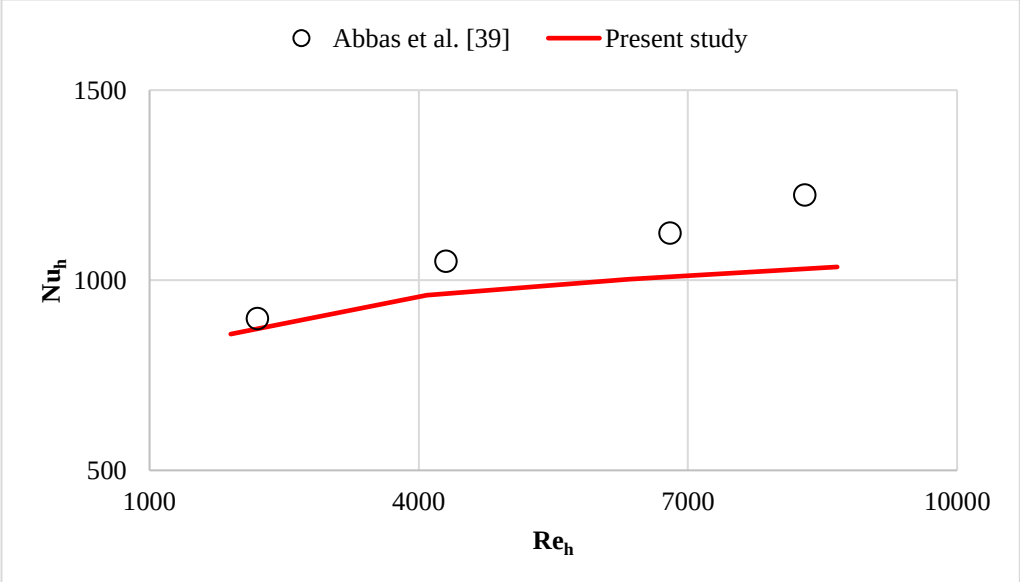

Figure 4.2 Comparing numerical results with experimental data.

4.1.6. Executing Numerical Model Simulation

ANSYS Fluent 2022 R2 software, one must adhere to a series of sequential procedures to simulate a thermal problem utilizing the ANSYS Fluent 2022 R2 software . In this section, it was classified as a seamless tube double-pipe heat exchanger.. For this type of heat exchanger to be simulated, the subsequent procedures must be executed [40]:

- ✓ Geometry

A 3D heat exchanger model is created by selecting pipe materials and working fluid based on the specifications, as shown in Fig. 4.3.

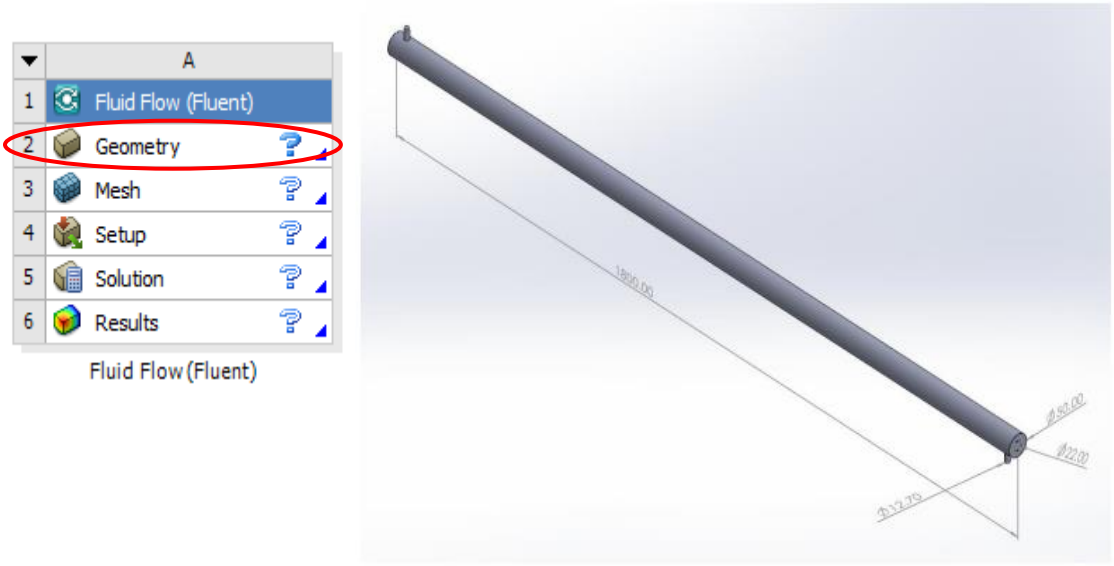

Figure 4.3. Smooth-tube heat exchanger schematic

- ✓ Meshing

When analyzing a system, dividing it into smaller domains or meshes is crucial. The type of element that should be used to separate the plan depends on the nature of each part, as shown in Fig. 4.4. In this study, a multizone mesh was used for the inner tube, while a tetrahedron mesh type was used for the other parts.

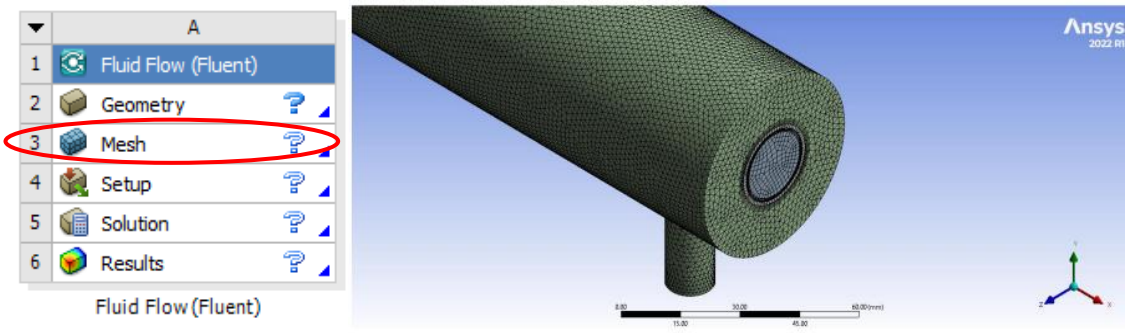

Figure 4.4. Sketch of meshing of smooth tube

✓ Labeling

This step aims to determine and pinpoint the exact locations, as illustrated in Figure 4.5.

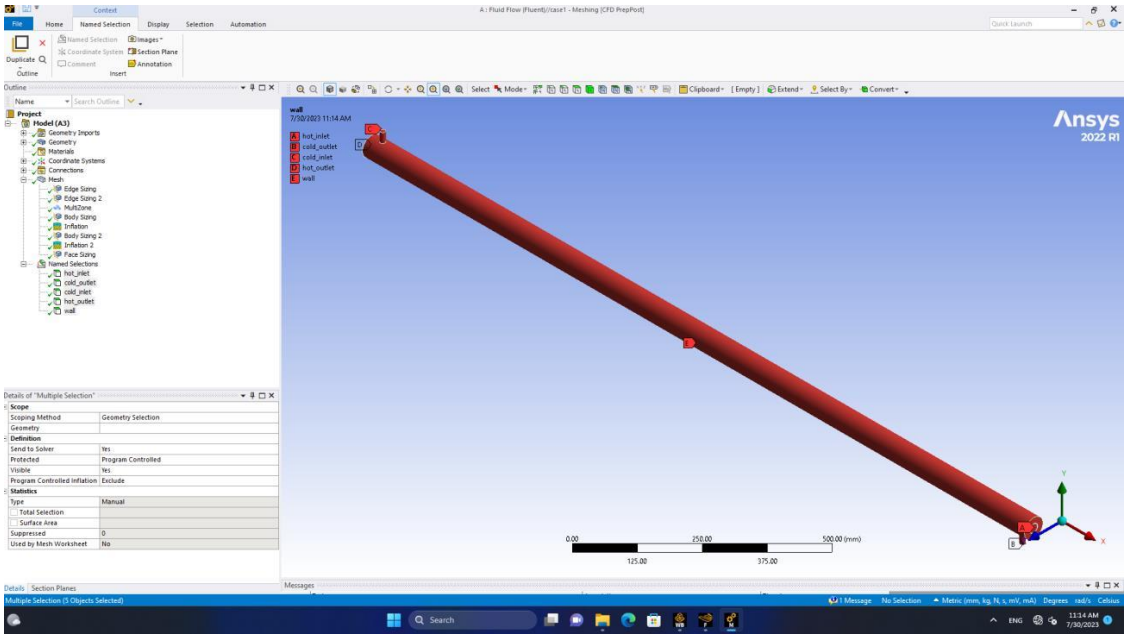

Figure 4.5. Photo of the labeling process

✓ Setup

This section defines the entry and exit points, location, and boundary conditions for each fluid. The procedure consists of the following steps:

➢ General

To begin, applying a steady state and gravity force in the downward direction (negative Y-axis) is recommended, as shown in Fig. 4.6.

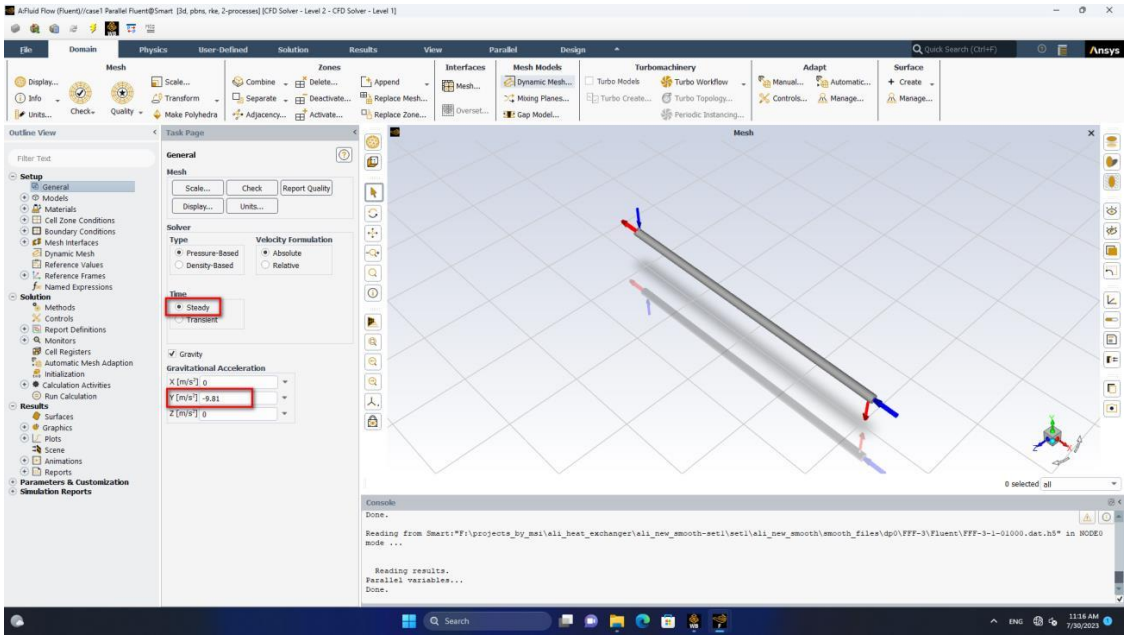

Figure 4.6. Photo of the general process

✓ Models

The energy equation is enabled by a reliable sub-model for faster processing. Enhanced wall treatment captures accurate near-wall results, as shown in Fig. 4.7.

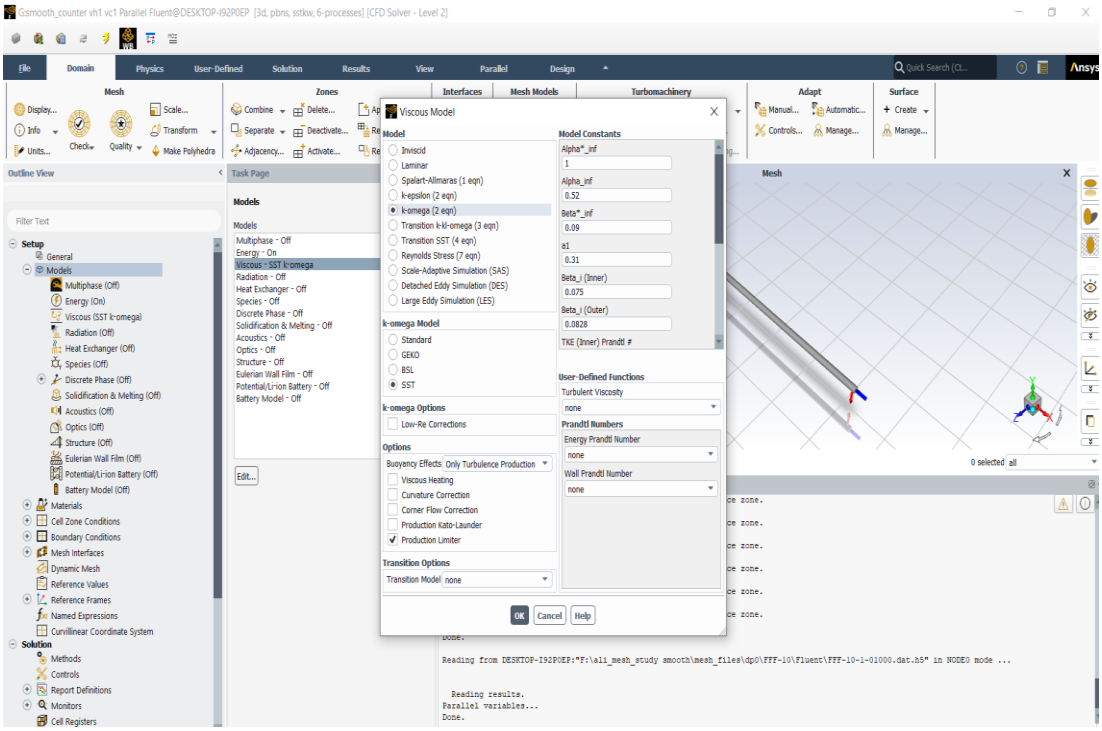

Figure 4.7. Photo of the modeling process page

✓ Identification of materials

In this step, copper is chosen as the pipe material and water is selected as the working fluid, as shown in Fig. 4.8.

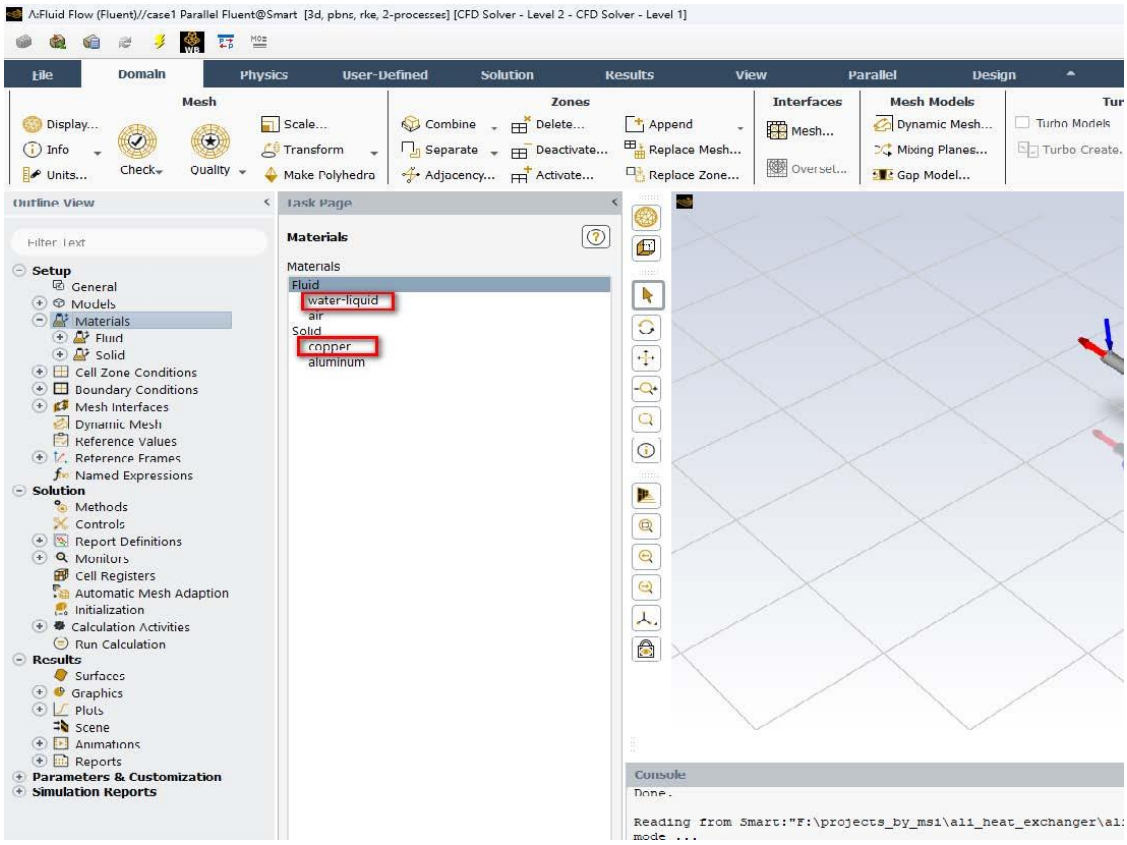

Figure 4.8. Photo of choosing materials

✓ Boundary conditions

In this stage, the thermal and hydraulic boundary conditions at the inlet ports for both hot and cold water are established as presented in Table 4.1. The technique of adding boundary conditions is illustrated in Figures 4.9 through 4.12.

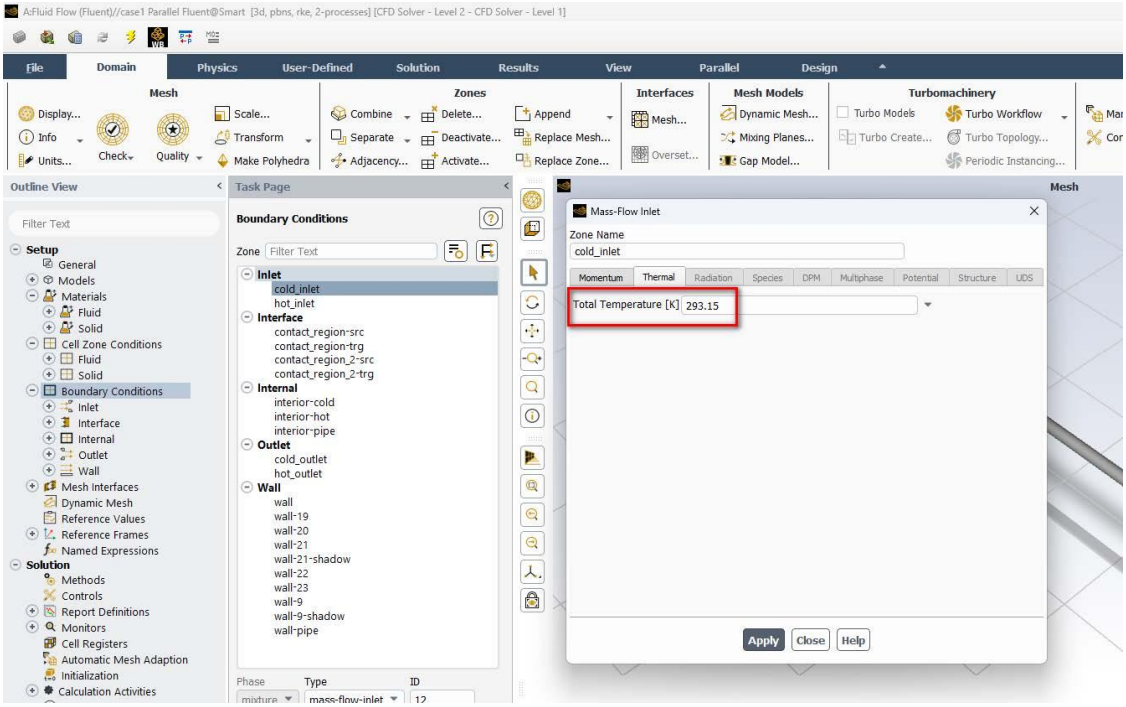

Figure 4.9. Specified cold water temperature

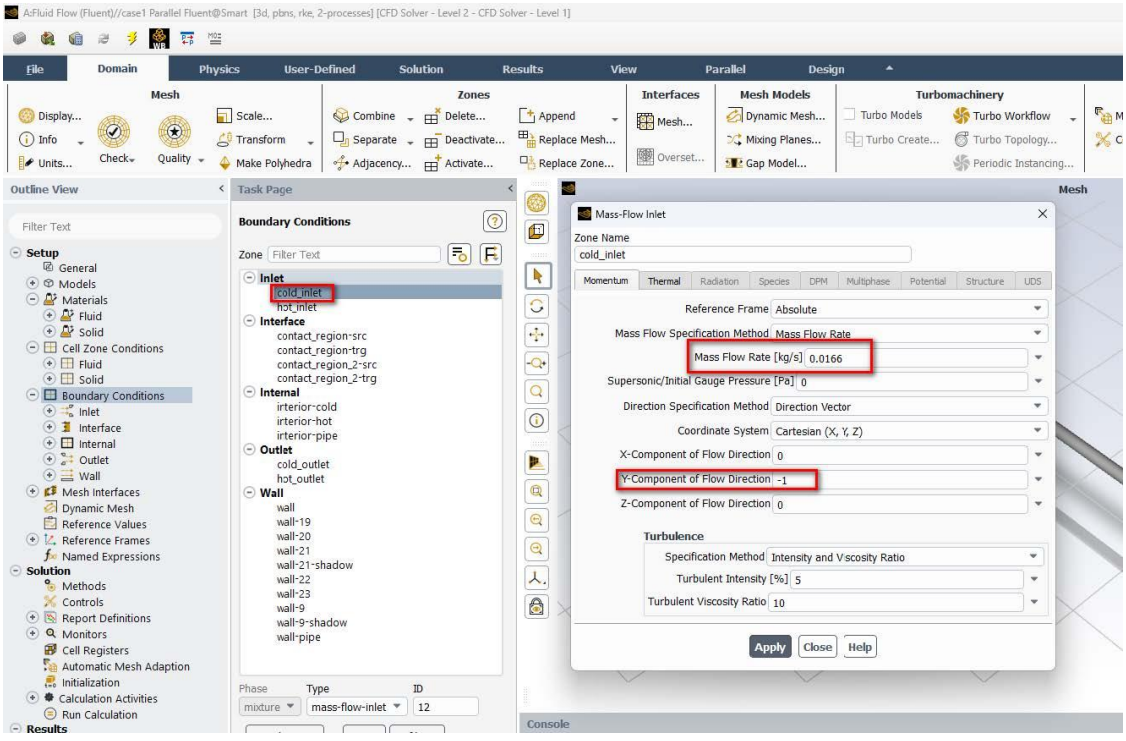

Figure 4.10. Specified cold water flow rate

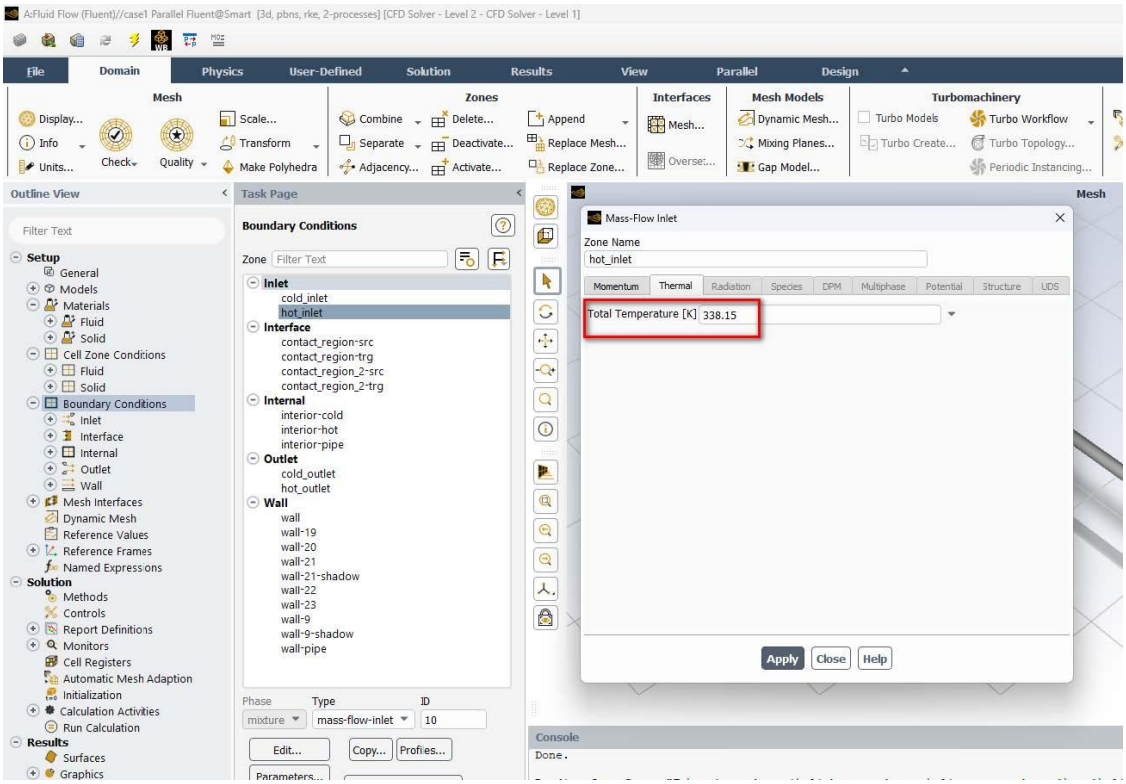

Figure 4.11. Specified hot water temperature

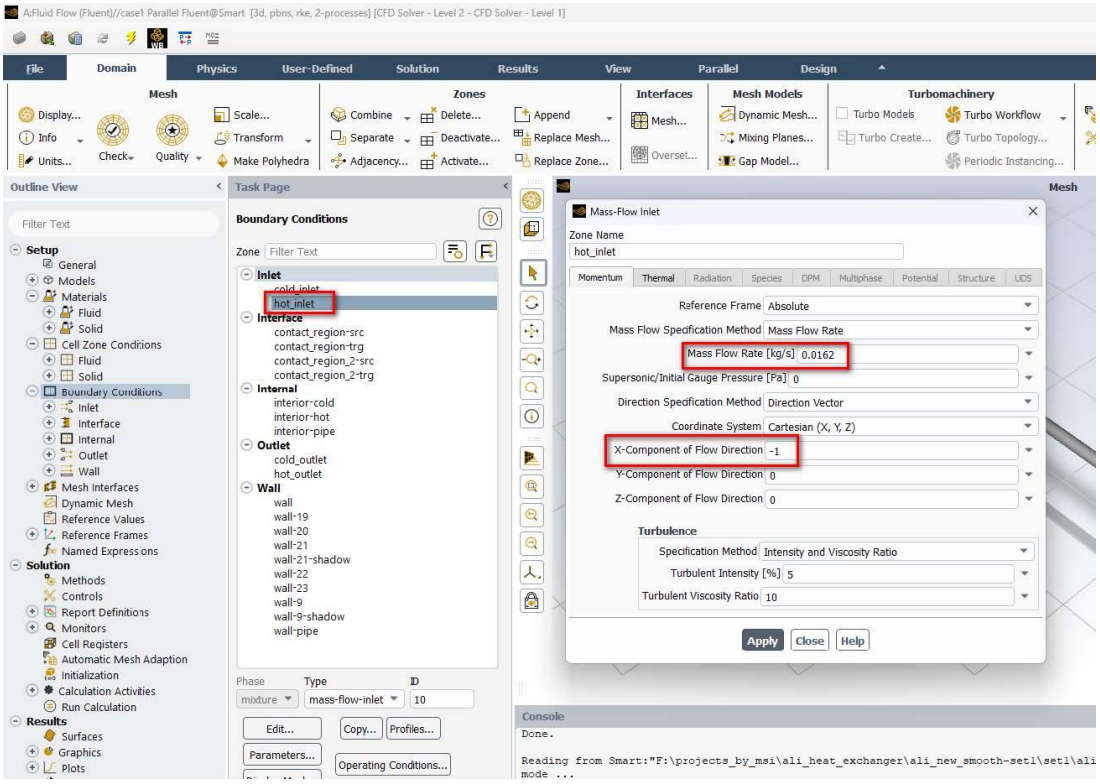

Figure 4.12. Specified hot water flow rate

✓ Solution

After creating the numerical simulation model, it was solved using second-order discretization for increased accuracy. Fig. 4.13 illustrates the process.

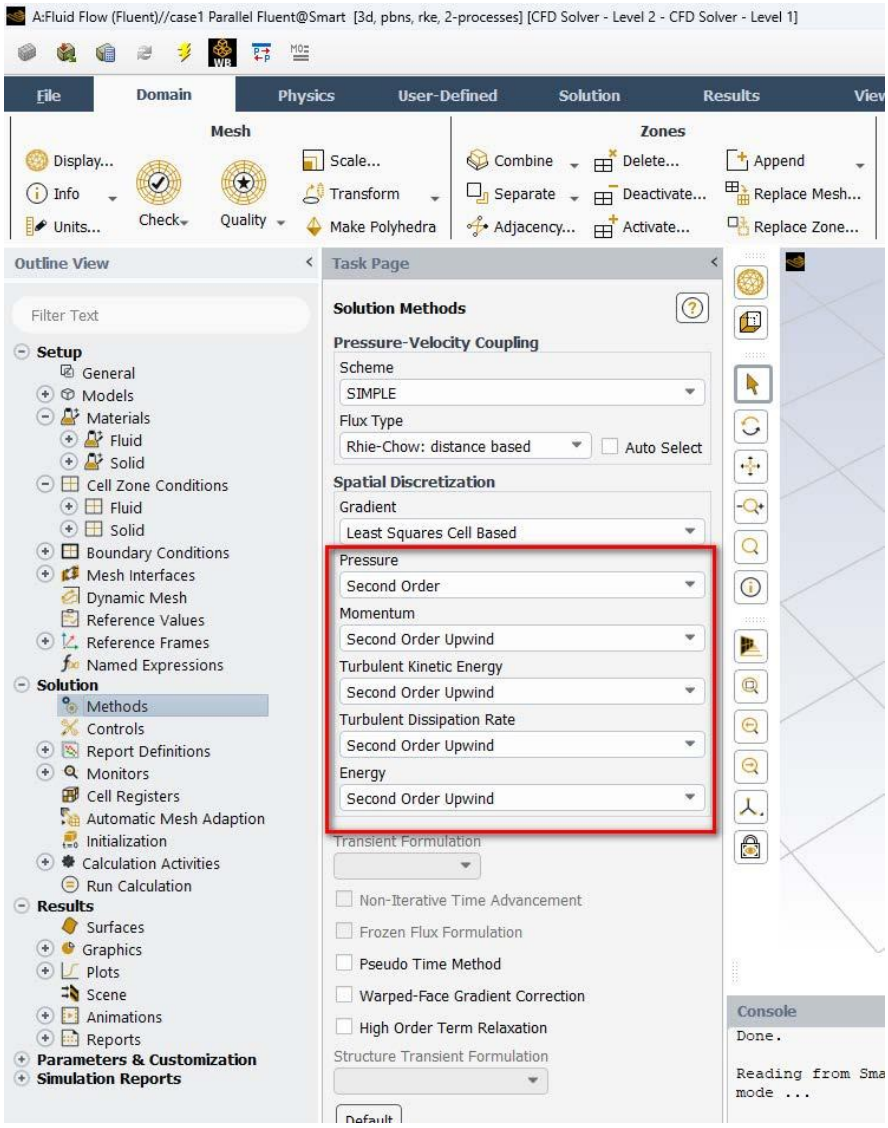

Figure 4.13. Photo of a sample of the setup process

✓ Residuals

Convergence criteria of 1×10^{-6} is used for all equations as stated in the ANSYS Fluent manual, as shown in Fig. 4.14.

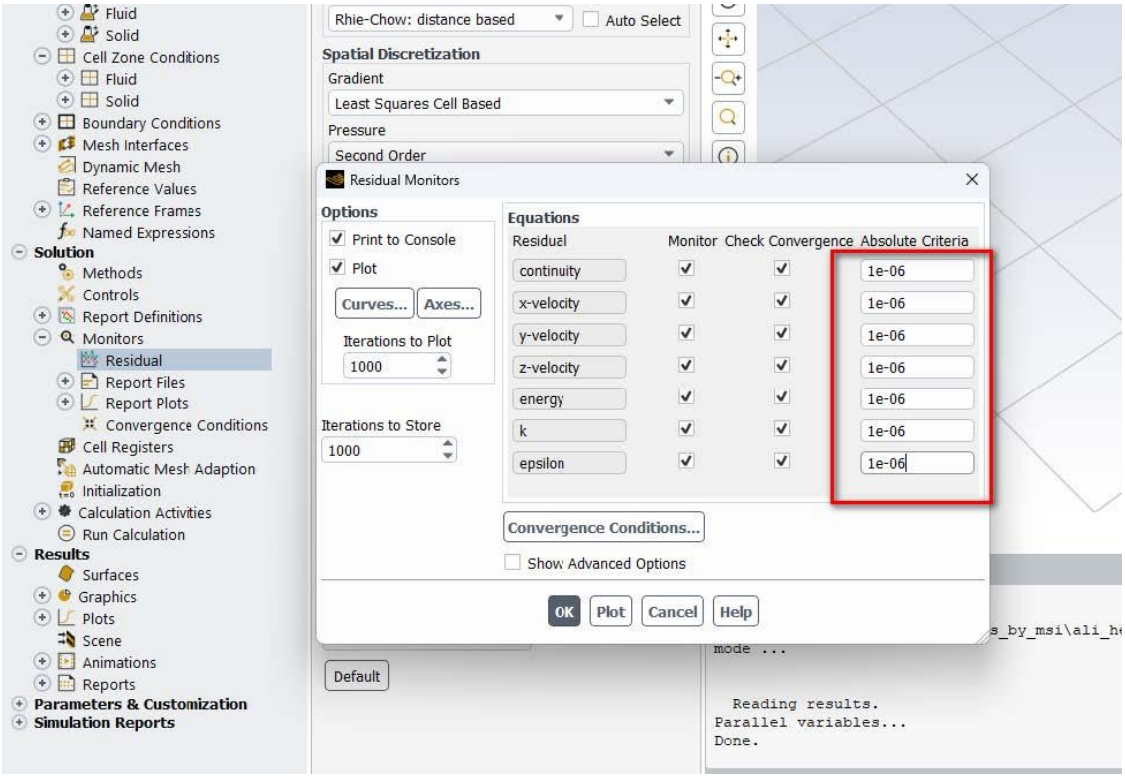

Figure 4.14. Photo of the residual step

✓ Initialization

Hybrid initialization is recommended when dealing with multiple inlet cases, as shown in Fig. 4.15.

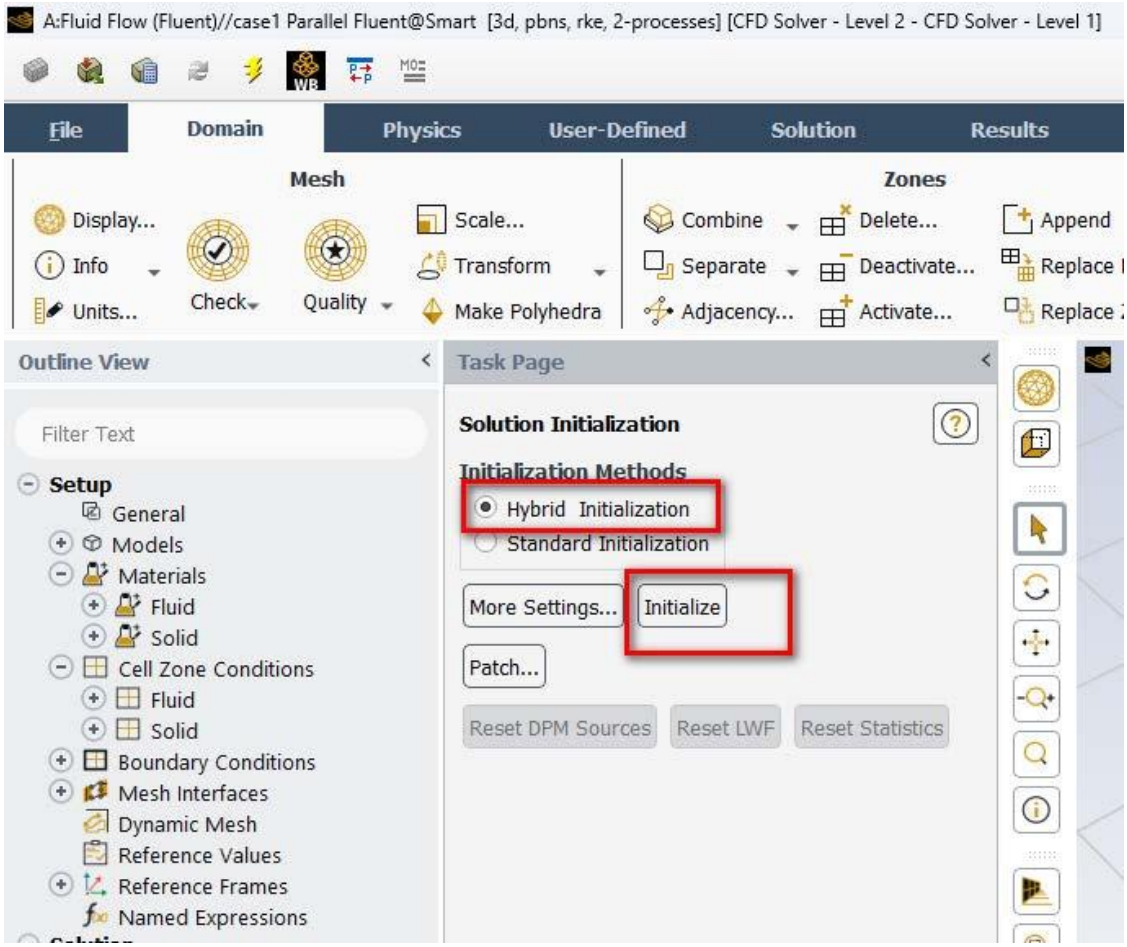

Figure 4.15. Photo of solution initialization step

- ✓ Run calculation

A 1000 iteration is used. At this value, the residual curves become flat, indicating that this is the closest the equations will get to convergence. Fig. 4.16 illustrates a running simulation process.

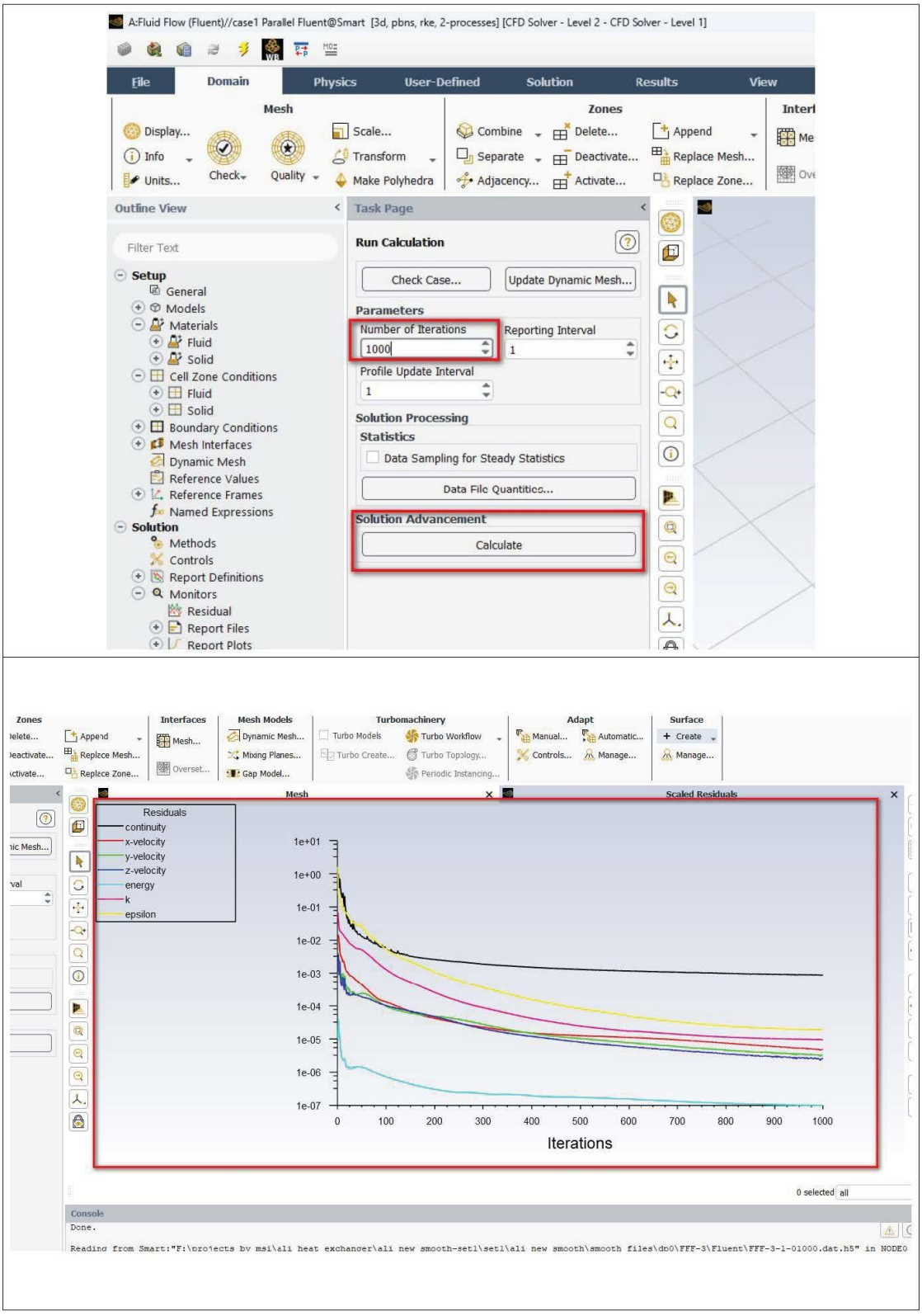

Figure 4.16. Photo of running process

✓ Results

Upon the completion of the solution procedure, the result section presents essential data encompassing temperature distribution, pressure values for each fluid, wall temperature, velocity profile, and other pertinent information.

The solution step of the smooth case is used and applied for other cases of the helical-annular finned tube, half-annular finned tube, half-annular finned tube and annular finned pipe heat exchangers.

4.1.5.1. Mesh Models

Fig. 4.17 to Fig. 4.27 illustrate mesh models for helical-annular finned tube, half-annular finned tube and annular finned pipe heat exchangers.

Annular finned pipe heat exchanger

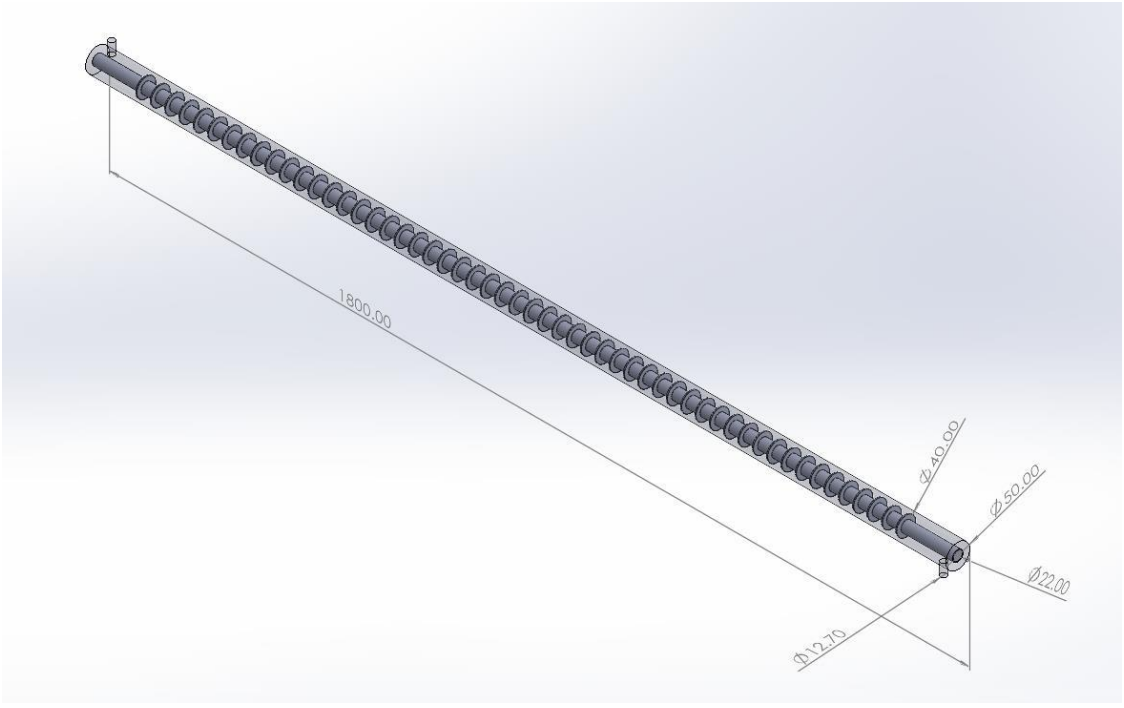

Figure 4.17. A sketch of a pipe with annular fins

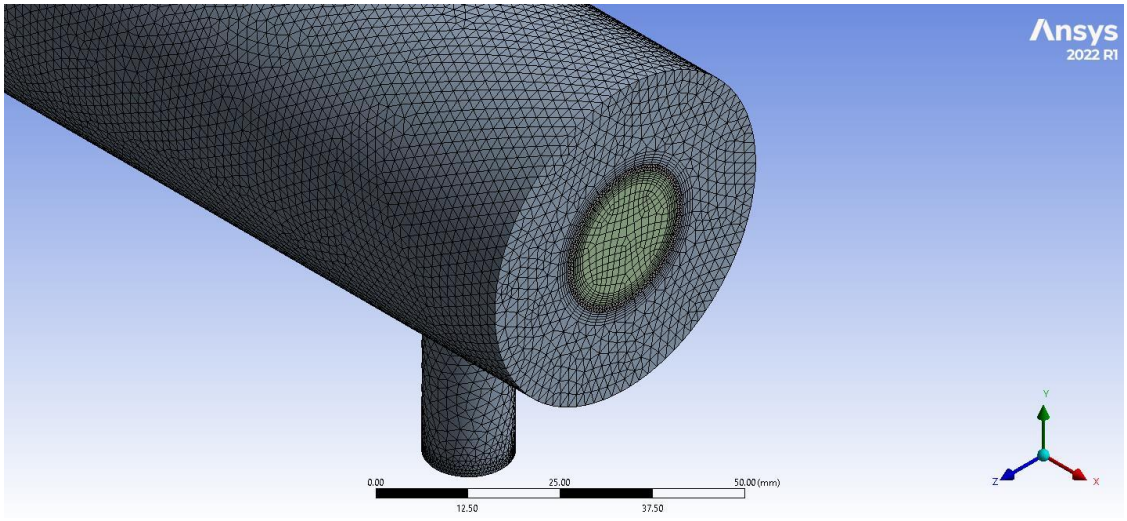

Figure 4.18. Mesh process to the heat exchanger

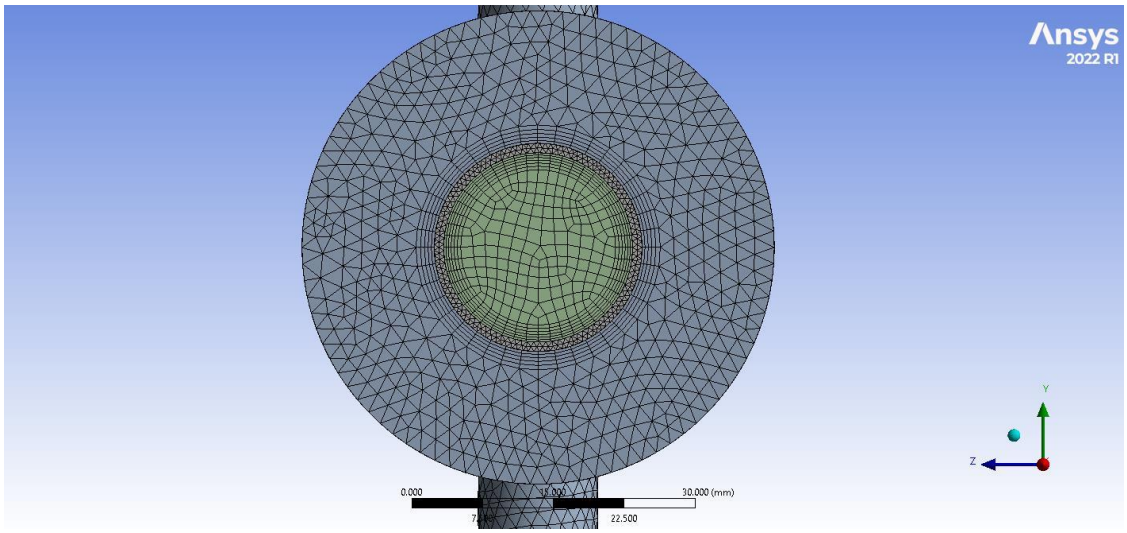

Figure 4.19. Side view of the heat exchanger

Half annular finned pipe heat exchanger

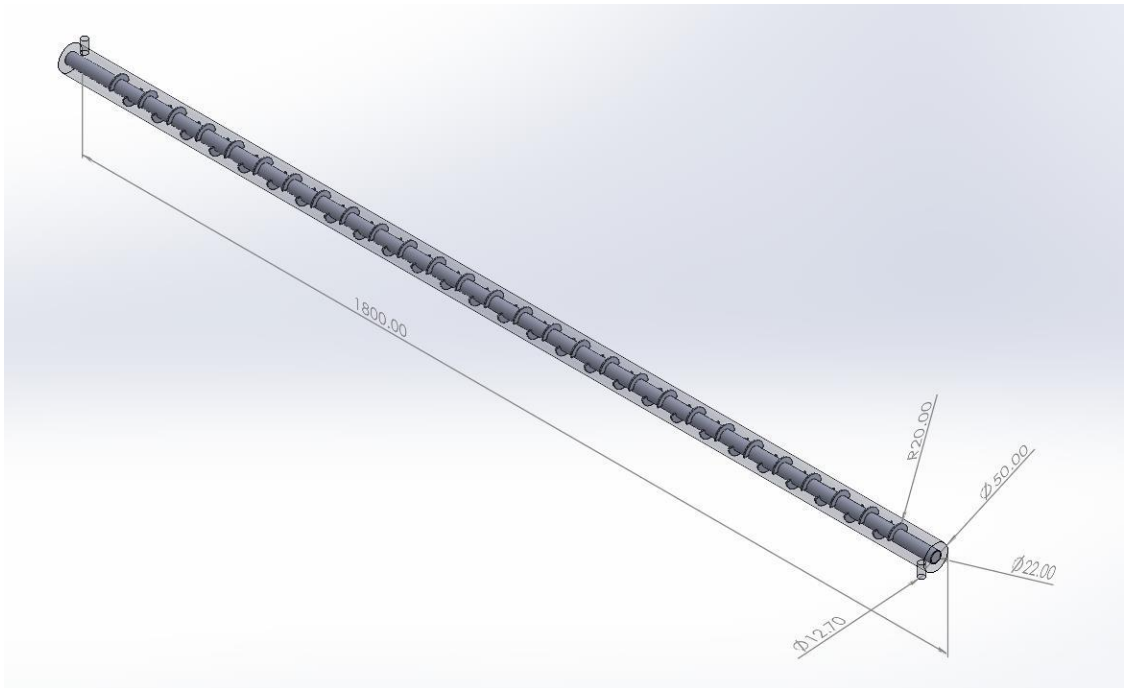

Figure 4.20. A sketch of a pipe with half-annular fins

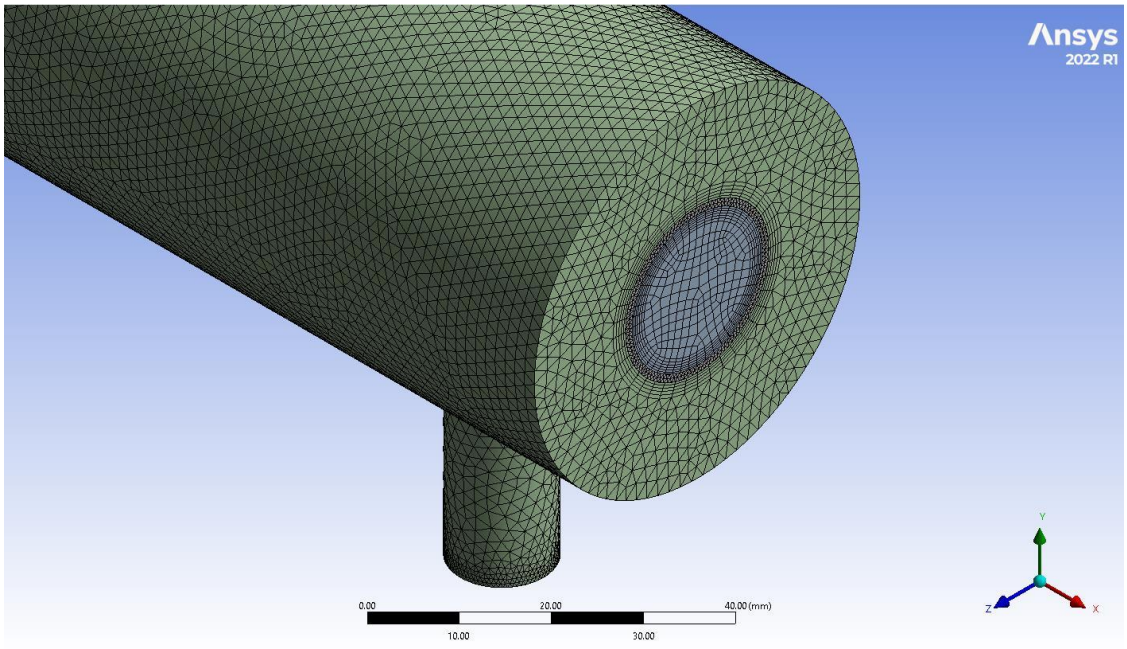

Figure 4.21. Mesh process to the half-annular finned pipe heat exchanger

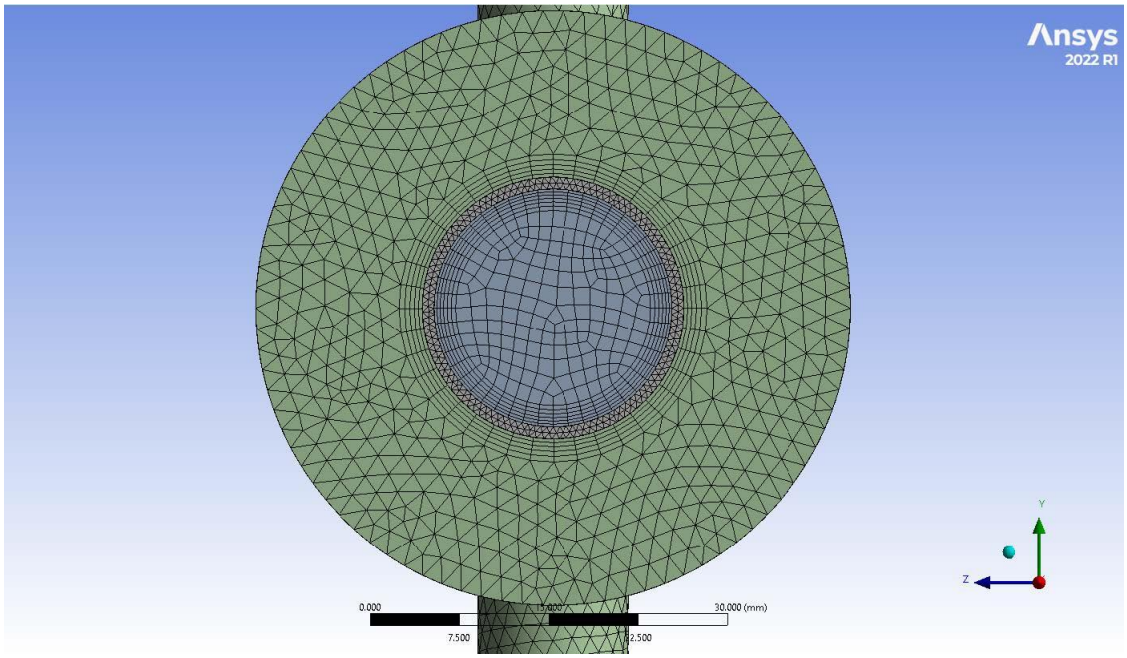

Figure 4.22. Side view of the half-annular finned pipe heat exchanger

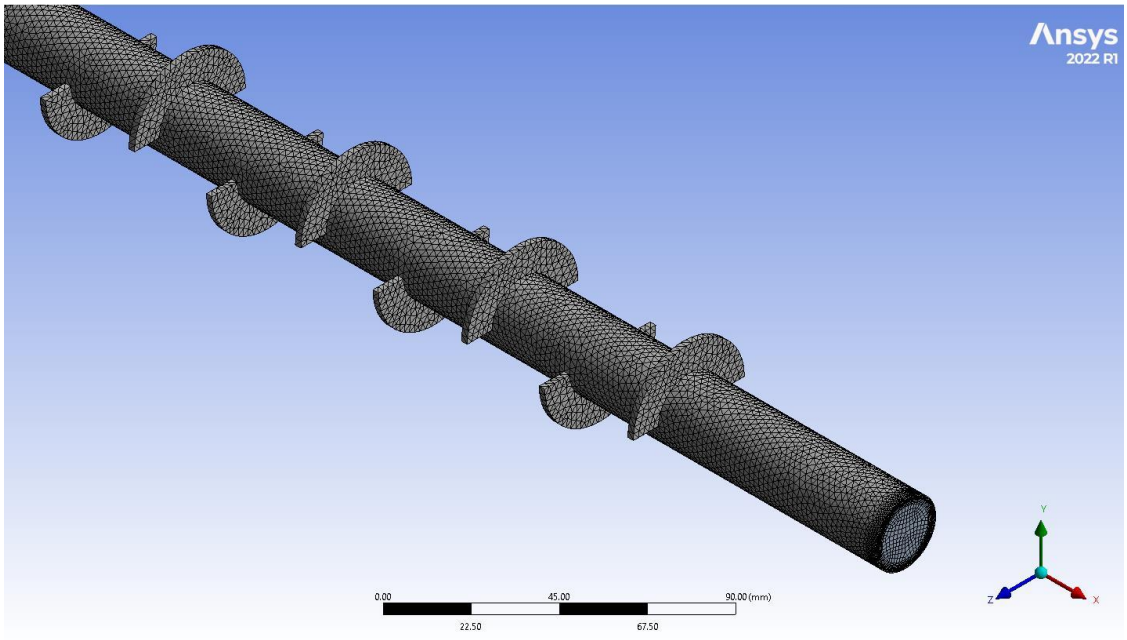

Figure 4.23. The half-annular finned pipe is created through meshing

Helical-annular finned pipe heat exchanger

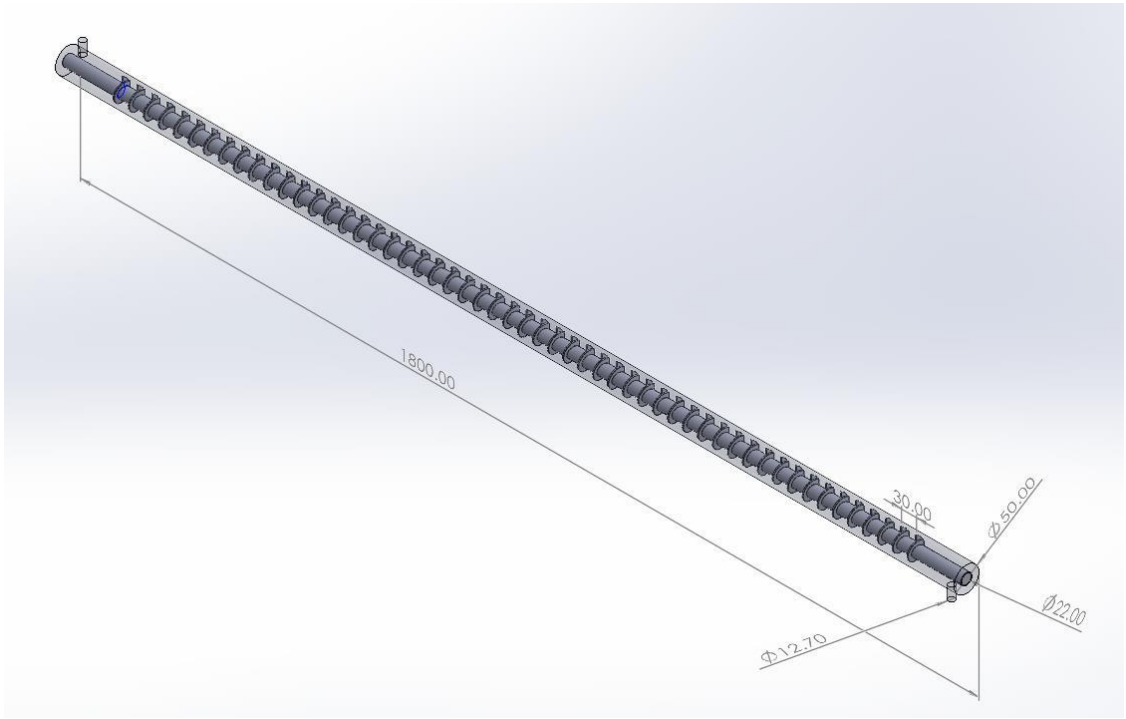

Figure 4.24. A sketch of a pipe with half-annular fins

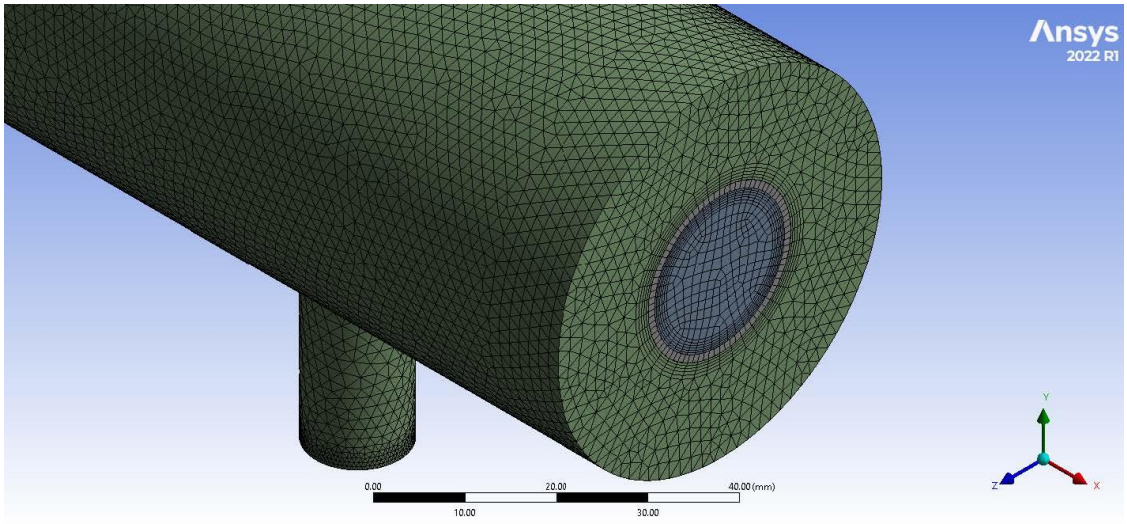

Figure 4.25. Mesh process to the helical-annular finned pipe heat exchanger

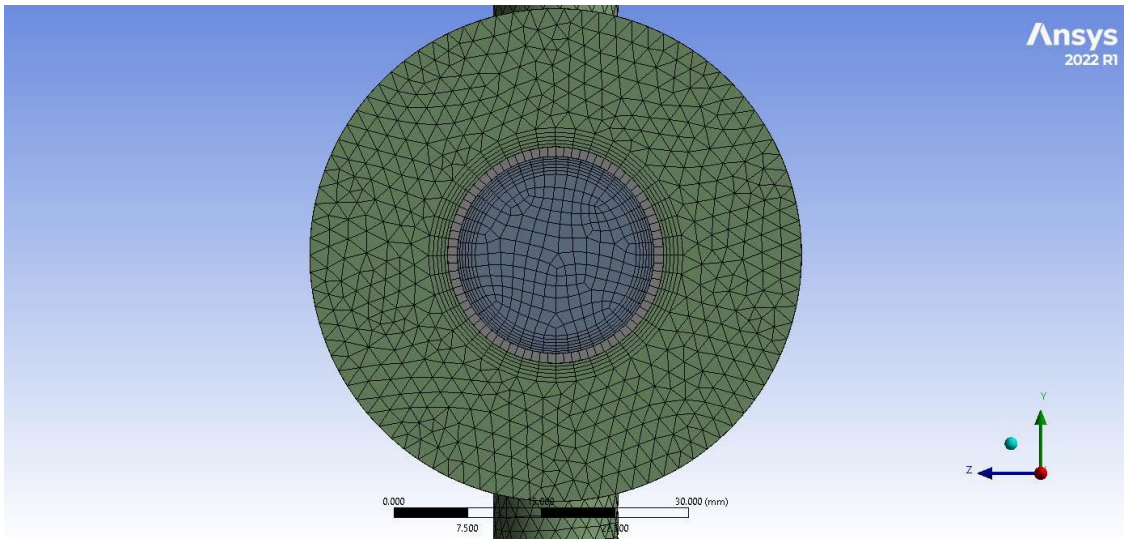

Figure 4.26. Side view of the helical -annular finned pipe heat exchanger

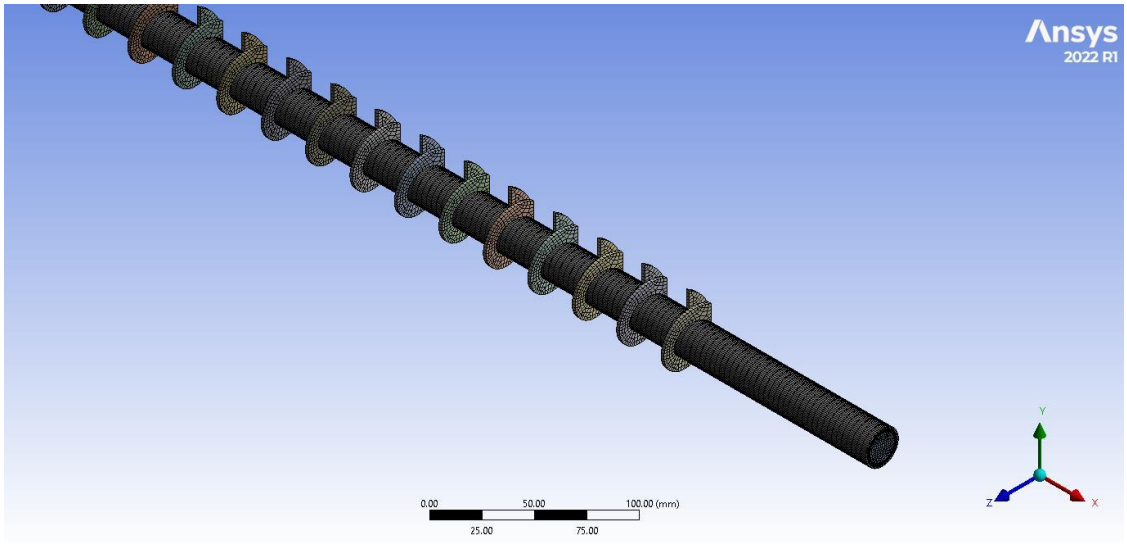

Figure 4.27. The helical-annular finned pipe is created through meshing

PART 5

RESULTS AND DISCUSSION

5.1. BACKGROUND

The numerical simulations were carried out for four different cases: smooth pipe, annular finned, half circular finned, and helical finned. The simulations were conducted with volumetric flow rates ranging from 1 to 4 LPM in four steps on both sides of the heat exchanger. Inlet temperatures of 20°C and 65°C were used, respectively, as described in Chapter 4 . The study investigated the Nu number, Re number, friction factor, NTU, and Ɛ, and their findings are displayed in the figures, which will be discussed later.

5.1.1. The Relationship Between the Nu_c and Re_c Numbers on the Cold Side

Figures 5.1 to 5.4 illustrate the variation of the Nu_c number with the Re_C number on the cool side for different types of pipes. These consist of four different types of pipes: smooth, half-annular, annular, and helical annular finned. According to the findings, the Nu_c number increased in tandem with an increase in the Re_C number. During our numerical simulation, we observed that the Nu_c number increased as the flow rate of hot water increased. The highest Nu number was observed when the hot water flow rate was 4 LPM in all heat exchanger cases, as shown in Figs. 5.1 to 5.4. Fig. 5.2 shows that increasing the Re_c number up to roughly 500 had no influence on the Nu_c number in the annular finned pipe, owing to water stagnation between fins due to low water velocity. The maximum Nu_c number of annular, half-annular, and helical annular finned from 21.48%, 37.97% , and 69.82%, respectively, increased compared with the smooth pipe.

The same phenomenon was observed in a half-annular finned pipe, as shown in Fig. 5.3, although the Nu_c number can be more significant than in an annular finned pipe, which is due to the water not stagnating entirely between fins. In this type of finned pipe, the Nu number increased by 13.6% compared to the annular finned pipe. It was observed from Fig. 5.4 that the variation of the Nu_c and Re_c numbers converged as V_h increased. A higher Nu_c value in comparison to other finned pipes resulted from an increase in water passing through the gap of a helical annular fin, which caused this convergence. Specifically, the Nu_c helical annular finned increased by 39.93% and 23.1% in this heat exchanger, respectively, in comparison to the annular and half annular finned pipes.

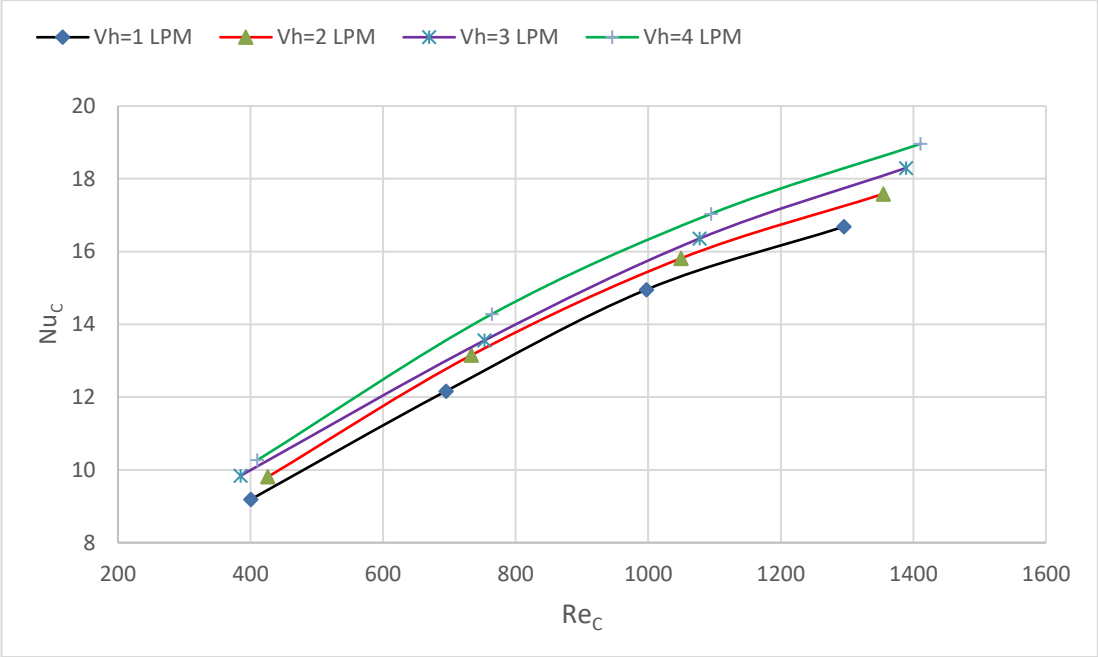

Figure 5.1. Variation of Nu with Re on the cold side for hot water flow rate from 1 to 4 LPM in a smooth pipe

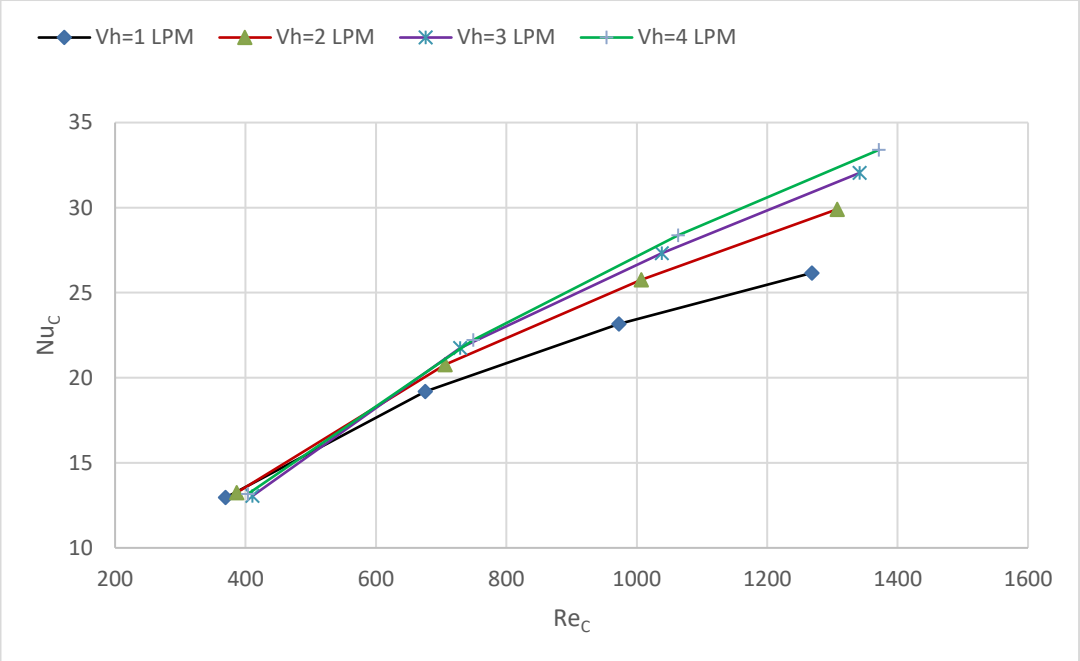

Figure 5.2. Variation of Nu with Re on the cold side for hot water flow rate from 1 to 4 LPM in an annular finned pipe

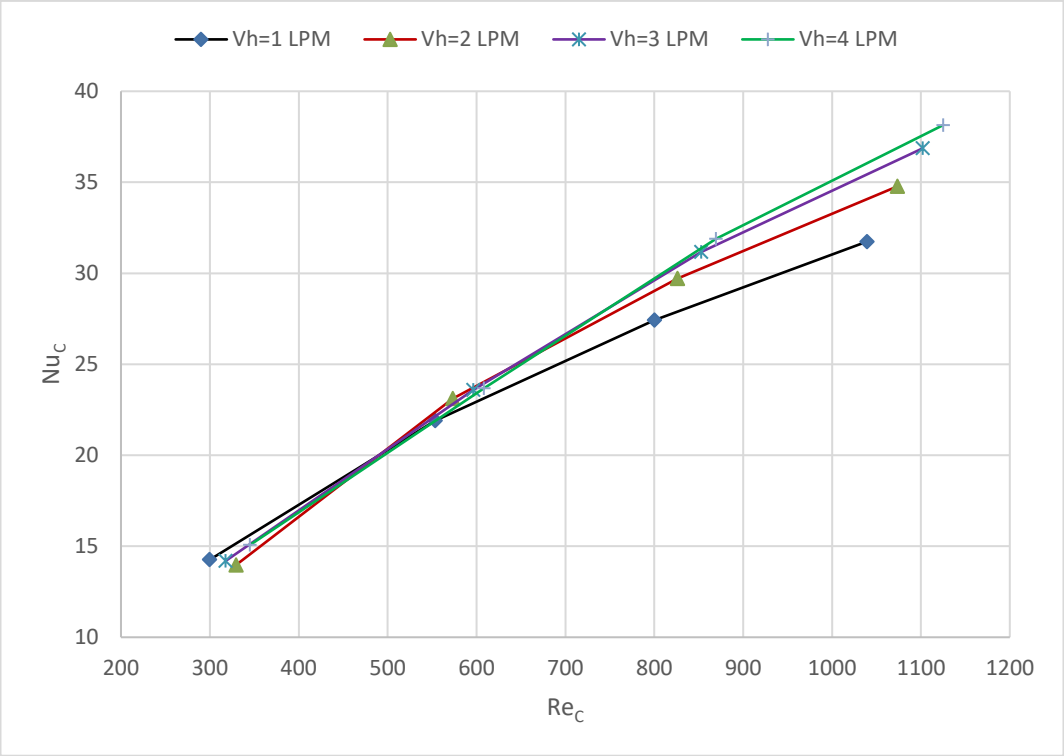

Figure 5.3. Variation of Nu with Re on the cold side for hot water flow rate from 1 to 4 LPM in a half annular finned pipe

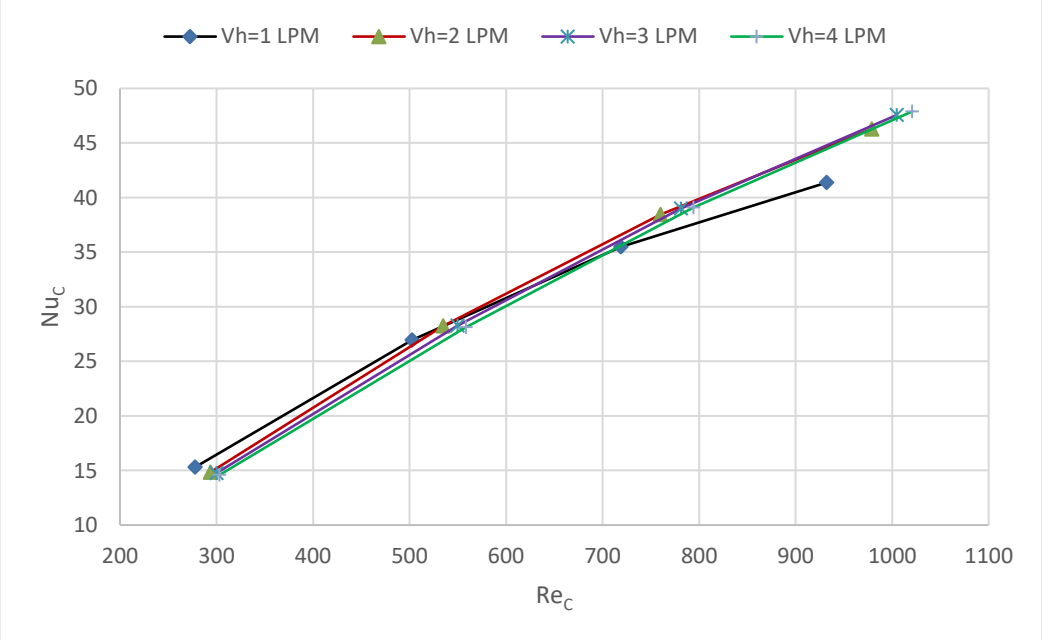

Figure 5.4. Variation of Nu with Re on the cold side for hot water flow rate from 1 to 4 LPM in a helical annular finned pipe

5.1.2. The Relationship Between the Nu_h and Re_h Numbers on the Hot Side

Figures 5.5 to 5.8 show Nu_h number variation versus Re_h number on the hot side for four different pipe types: smooth, annular finned, half annular finned, and helical annular finned. However, the numerical solution revealed that adjusting the cold water flow affected the Nu_h number. It increased their levels as the cold-water flow rate increased. The highest Nu_h number is achieved with a cold-water flow rate of 4 LPM in smooth pipe ranging from 32.68 to 39.1. In the annular-finned pipe case, the Nu_h number versus Re_h number behavior is the same as in the smooth pipe case, but at lower levels, as illustrated in Fig. 5.6. The Nu_h becomes at the highest level with a cold-water flow rate of 4 LPM, ranging from 17.62 to 22.45. In the case of a half-annular finned pipe, the relationship between the Nu_h number and the Re_h number behaves similarly to the previous cases. In this case, it is noted that the highest Nu_h number level is obtained when the cold-water flows at 1 LPM, which ranges from 6.4 to 51.85 as shown in Fig. 5.7. According to numerical simulation, the Nu_h number vs. Re_h number for cold water flow in the helical-finned pipe case behaves as a smooth pipe, as illustrated in Fig. 5.8. Based on the discussion, the study found that the half-annular finned pipe case yields the most consistent results. The maximum value of the Nu_h number occurs when cold water flows through 4 LPM, which ranges from 41.13 to 47.2.

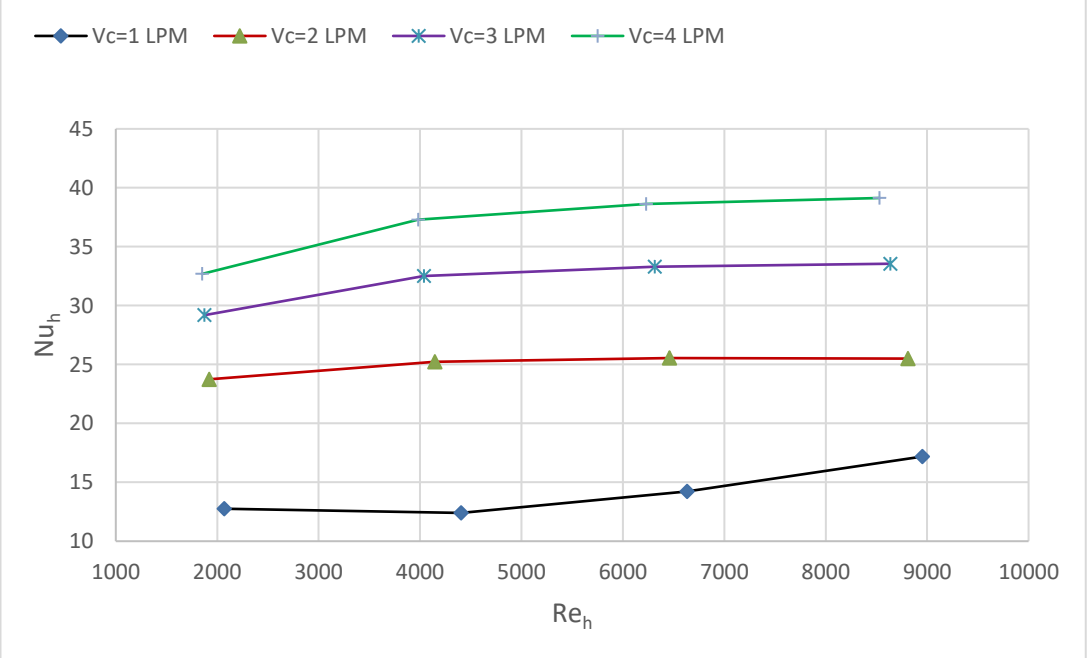

Figure 5.5. Variation of Nu vs Re number on the hot side for cold water flow from 1 to 4 LPM in a smooth pipe

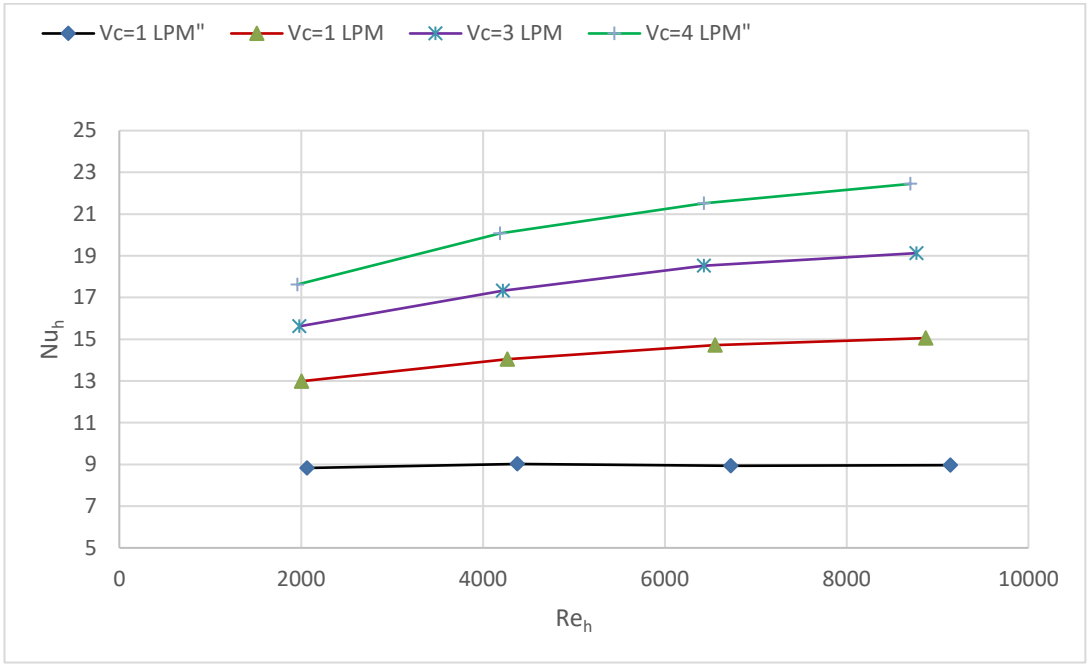

Figure 5.6. Variation of Nu vs Re number on the hot side for cold water flow from 1 to 4 LPM in an annular finned pipe

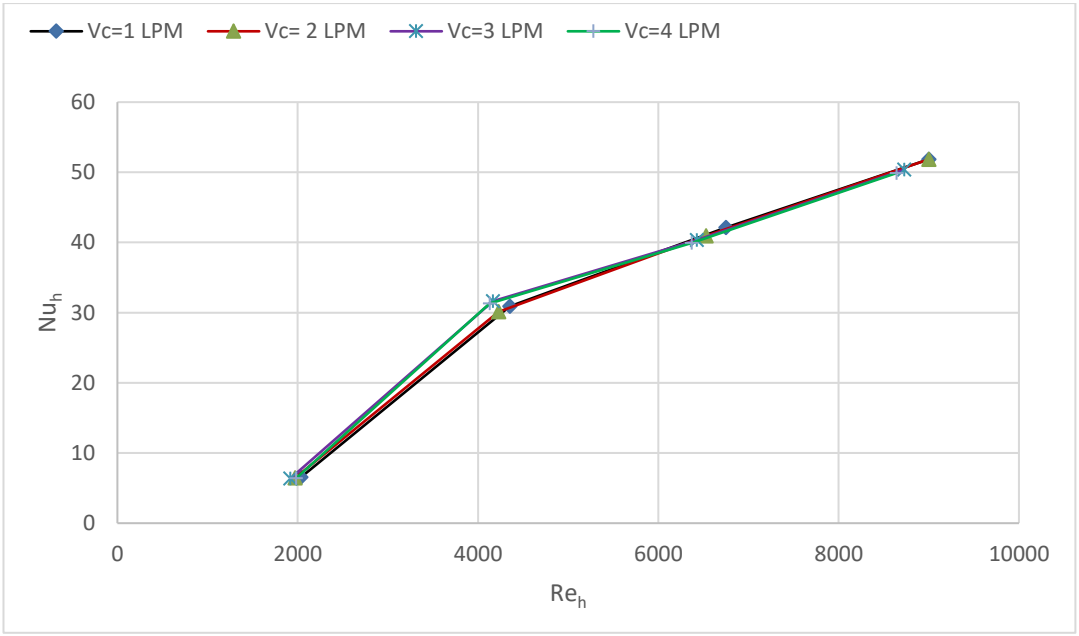

Figure 5.7. Variation of Nu vs Re number on the hot side for cold water flow from 1 to 4 LPM in a half-annular finned pipe

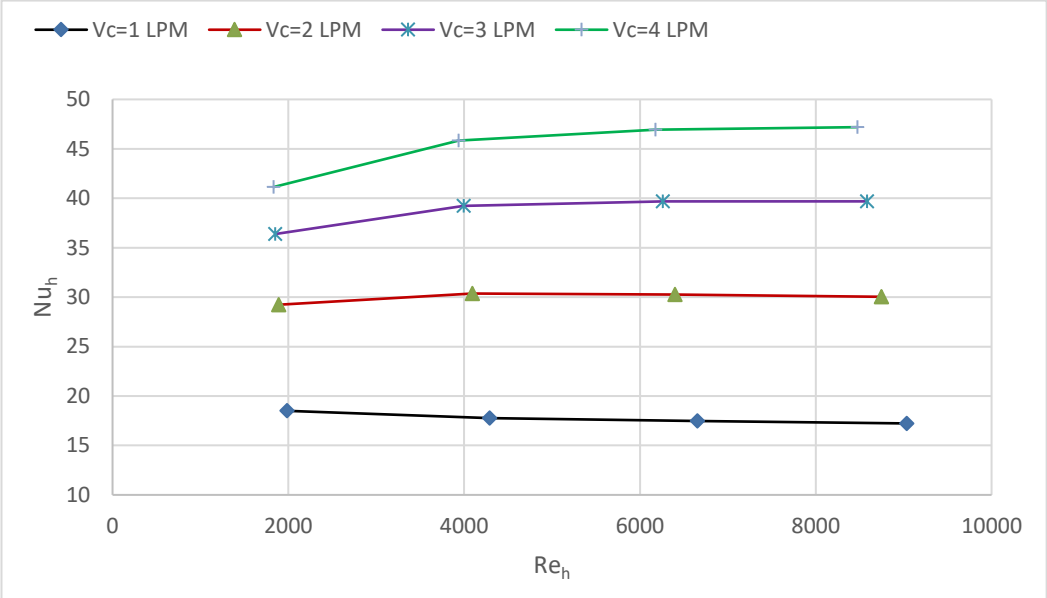

Figure 5.8. Variation of Nu vs. Re number on the hot side for cold water flow from 1 to 4 LPM in a helical annular finned pipe

5.1.3. Friction Factor on the Cold-Water Side (f_C)

Figures 5.9 to 5.12 show the friction factor on the cold-water side for four cases where both the Reynolds number and surface roughness significantly affect the friction factor. It was found that f_c is inversely proportional to the Re_C number. In Figure 5.9, the highest f_c value was obtained at a hot water flow rate of 4 LPM. The f_c factor ranged from 0.13 to 0.023, and the Re_C number varied from 410 to 1400. Conversely, the lowest f_c was obtained at 1 LPM, ranging from 0.12 to 0.0207 along Rec, from 410 to 1290. Adding fins to the heat exchanger surface increased the average f factor. An annular finned pipe varies from 0.157 to 0.0276, and the f_c factor increased by 18.58% at a hot water flow rate of 4 LPM compared to smooth pipes, as shown in Fig. 5.10. Half-annular and helical-annular finned pipes had the same effect as fins, with the annular finned pipe having the highest values, as shown in Figures 5.11 and 5.12.

Compared to smooth pipes, the f_c factors increased by 8.66% and 29.04% for half-annular and helical-annular finned pipes, respectively.

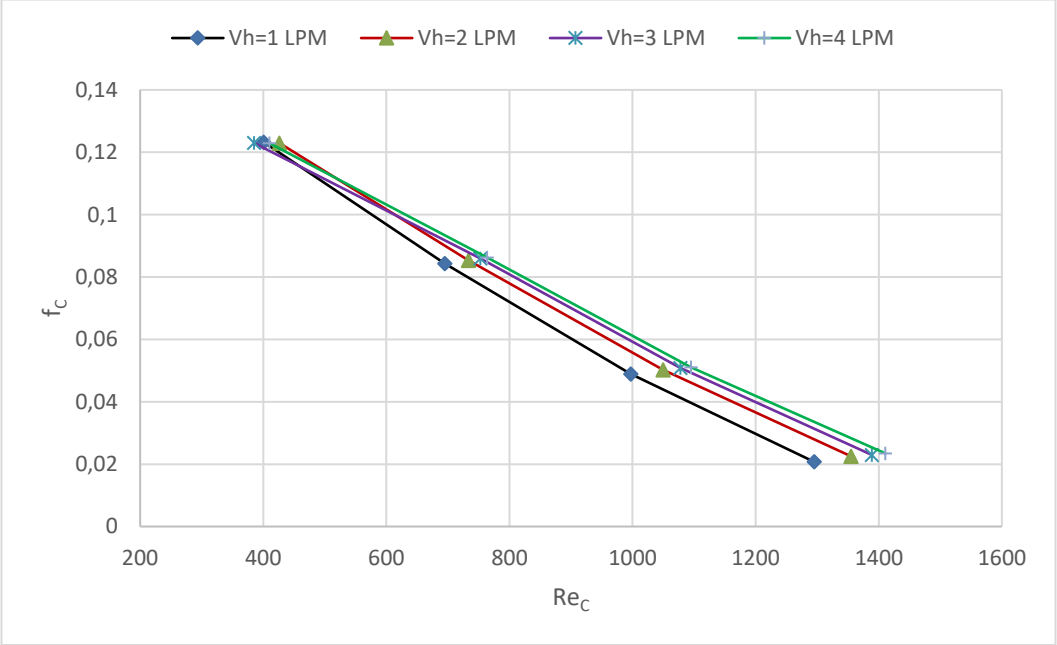

Figure 5.9. Variation of friction factor with Re number in cold water side when hot water changed from 1 to 4 LPM in smooth pipe

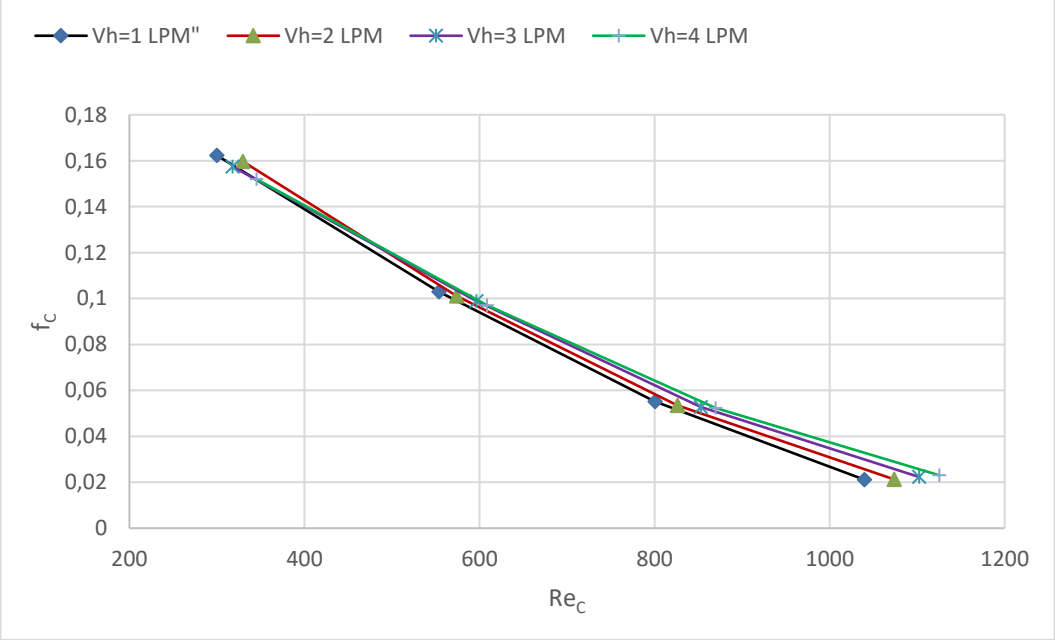

Figure 5.10. Variation of friction factor with Re number in cold water side when hot water changed from 1 to 4 LPM in an annular finned pipe

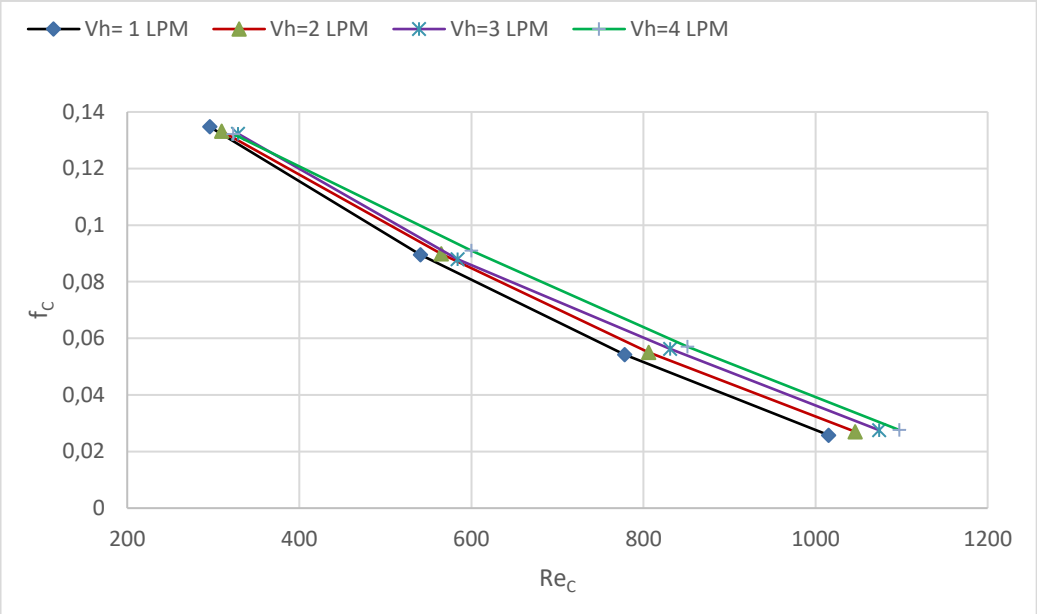

Figure 5.11. Variation of friction factor with Re number in cold water side when hot water changed from 1 to 4 LPM in a half annular finned pipe

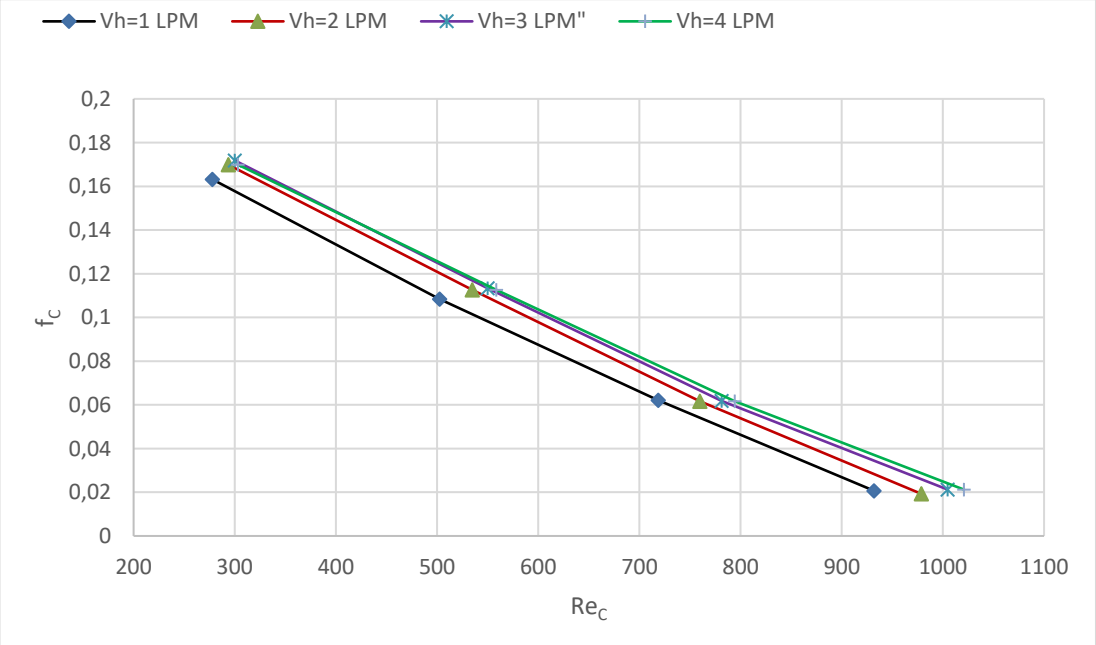

Figure 5.12. Variation of friction factor with Re number in cold water side when hot water changed from 1 to 4 LPM in a helical-annular finned pipe

5.1.4. Friction Factor on The Hot-Water Side (f_h)

The variation of f_h against Re_h for four distinct pipe configurations : smooth, annular finned, half-annular-finned, and helical-finned at various cold water flow rates, ranging from 1 to 4 LPM, is shown in Figures 5.13 to 5.16. It can be observed that the heat transfer behavior of smooth pipes and helical-annular finned heat exchangers differs from the other two finned pipe heat exchangers. There is an inverse relationship between the f_h learner and Rec. In a smooth pipe heat exchanger, there is a convergence between f_c values based on cold-water flow rates. The f_h ranges from 0.57 to 0.067 over Re_h, which ranges from 1851 to 8810, as shown in Fig. 5.13.

On the other hand, in a helical-annular finned pipe, the f_h ranged from 0.7 to 0.09 over a Re_h range from 2000 to 9000, as shown in Figure 5.16. In both annular and half-annular finned pipe heat exchangers, changes in f_h slightly decreased as Re_h was increased, as shown in Figures 5.14 and 5.15, which illustrated an approximately identical between them. According to their findings, the levels of f_h increase as the cool-water flow rate goes up. At a Vc of 4 LPM, the level of f_h ranges from 0.346 to 0.32 in the annular finned pipe, while in the half-annular finned pipe, it ranges from 0.373 to 0.337.

According to their findings, the levels of f_h decrease as the cool-water flow rate goes up. At a V_c of 4 LPM, the level of f_h ranges from 0.346 to 0.32 in the annular finned pipe, while in the half-annular finned pipe, it ranges from 0.373 to 0.337.

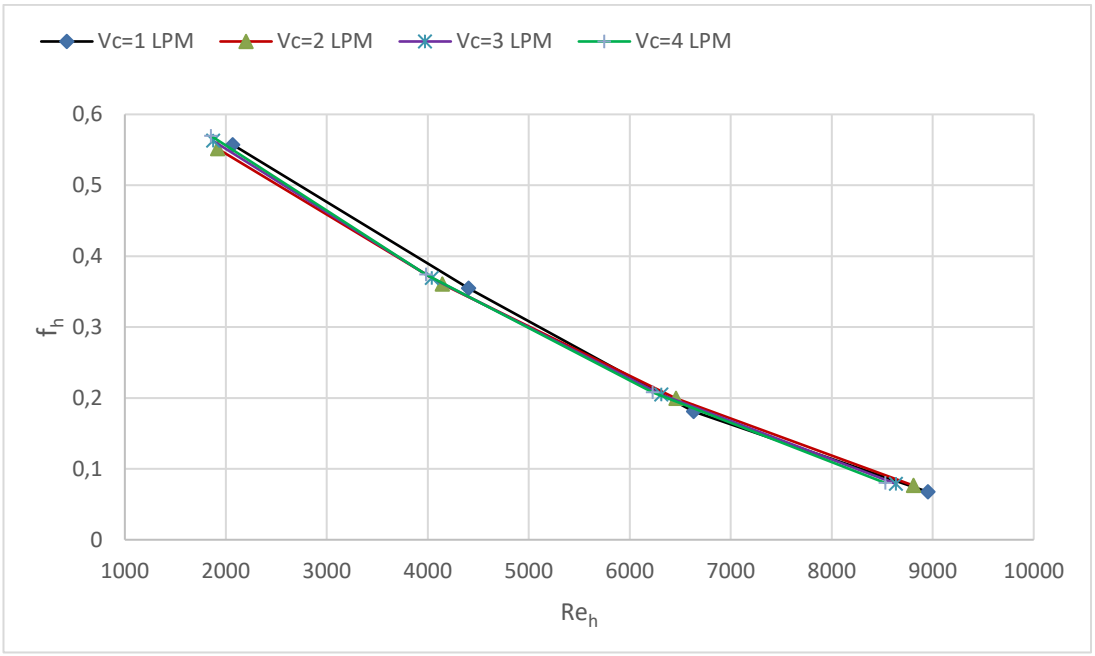

Figure 5.13. Variation of friction factor changes with Re number on hot side for the cold water varies from 1 to 4 LPM in a smooth pipe

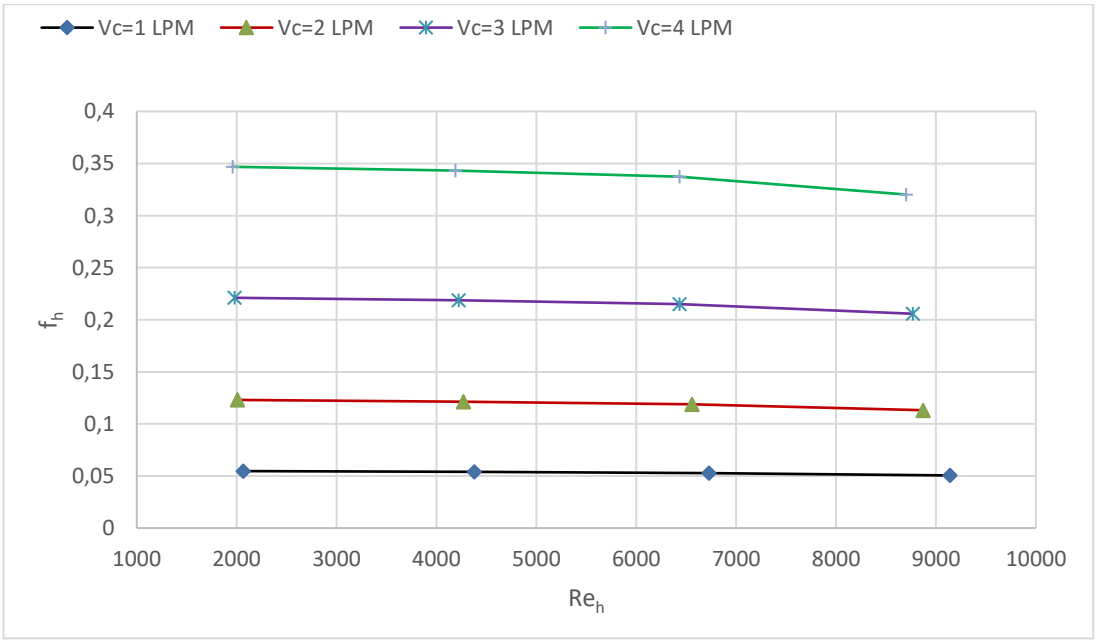

Figure 5.14. Variation of friction factor changes with Re number on the hot side for the cold water varies from 1 to 4 LPM in an annular finned pipe

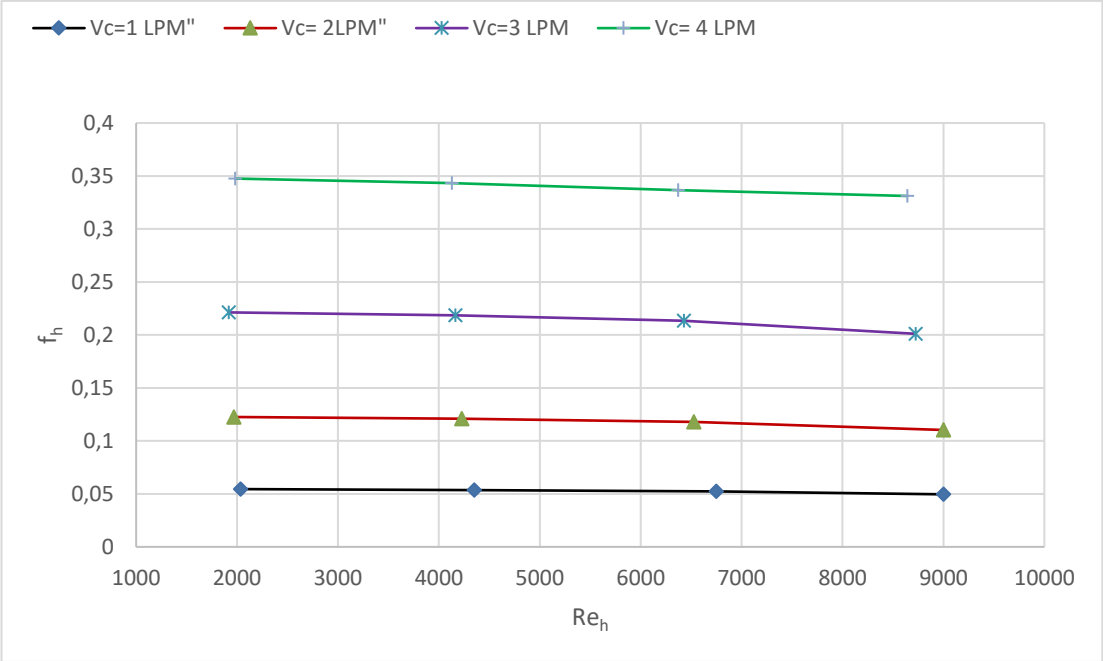

Figure 5.15. Variation of friction factor changes with Re number on the hot side for the cold water varies from 1 to 4 LPM in a half annuler finned pipe

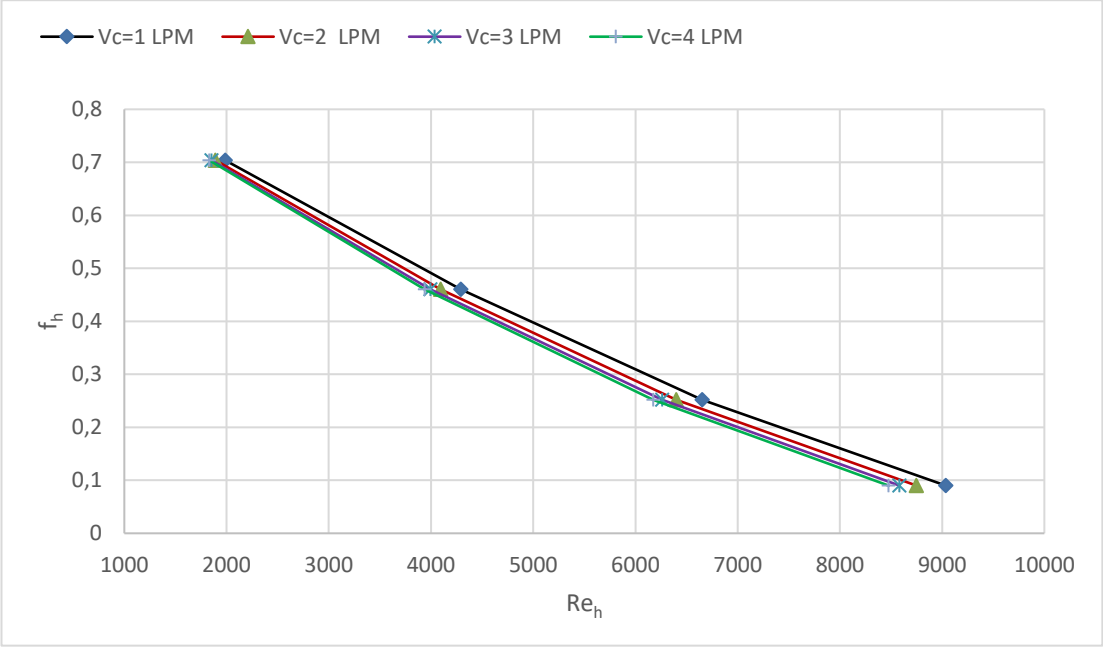

Figure 5.16. Variation of friction factor changes with Re number on the hot side for the cold water varies from 1 to 4 LPM in a helical annular finned pipe

5.1.5. Evaluation of Effectiveness

Figures 5.17 to 5.20 show the relationship between effectiveness and C for different pipe configurations, including smooth pipe, annular finned pipe, half annular finned pipe, and helical finned pipe. In the case of the smooth pipe, it was observed that the maximum effectiveness is achieved when the hot fluid flows at 1 LPM. Fig. 5.17 indicated that the efficacy decreased as C increased for hot fluid flow rates of 1 and 2 LPM but showed an inverse behavior for effectiveness with C for the other two flow rates.

The maximum effectiveness ranged from 0.772 to 0.44. Additionally, it was noted that the effectiveness for all cases may converge at a hot water flow rate of 4 LPM. Fig.5.18 shows that effectiveness decreases as C values increase in an annular finned pipe. It was observed that there is a corresponding effectiveness value for Vh ranging from 1 to 3 LPM. In general, it was noted that a flow rate of 1 LPM for hot water is the most effective. Fig. 5.19 illustrates the relationship between effectiveness and C for a half-annular finned pipe. The effectiveness of C about the hot flow is considerably similar to that of the annular finned pipe case. According to Figure (5.20), the helical annular finned pipe is the most effective among all other pipes. Additionally, the hot water flow rate of 1 LPM was found to be the most efficient compared to other flow rates.

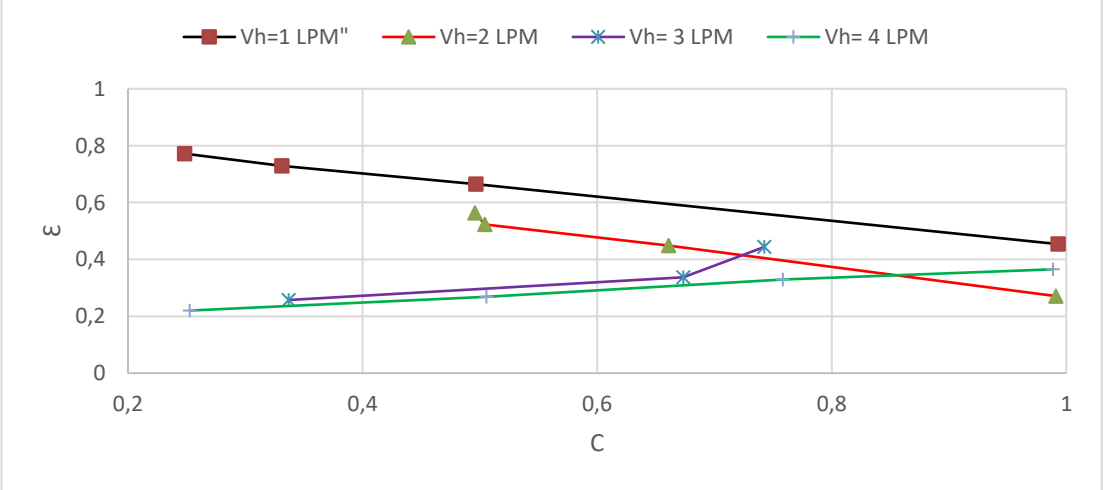

Figure 5.17. Variations of ε and C vary with cold water flow rate from 1 to 4 LPM at each hot water flow rate from 1 to 4 LPM in a smooth pipe

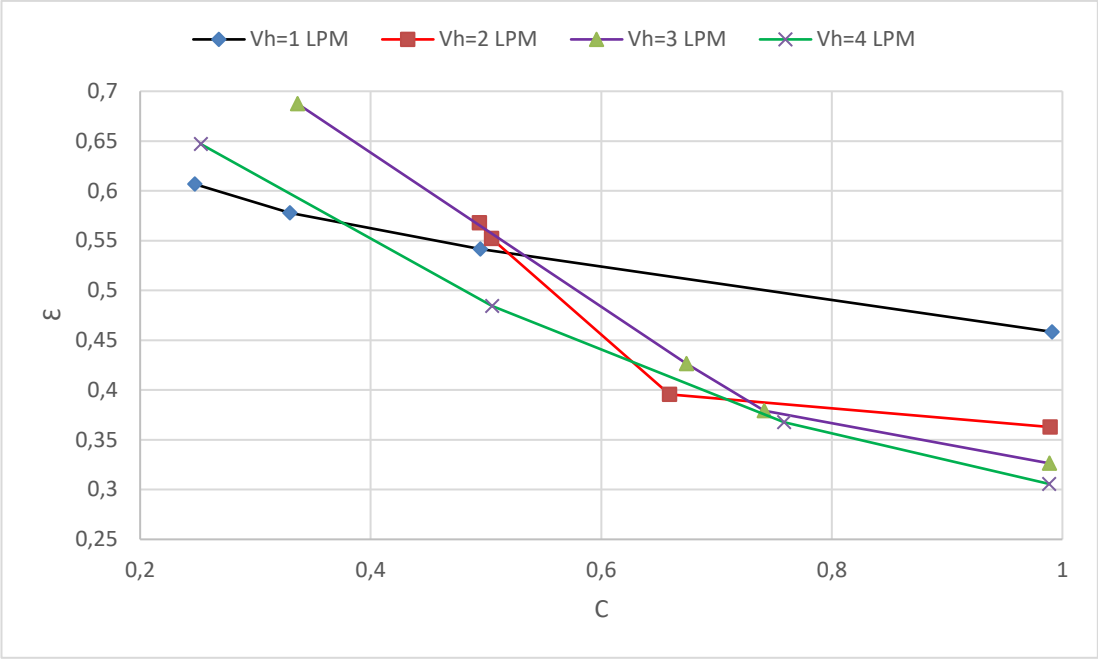

Figure 5.18. Variations of ε and C vary with cold water flow rate from 1 to 4 LPM at each hot water flow rate from 1 to 4 LPM in an annular finned pipe

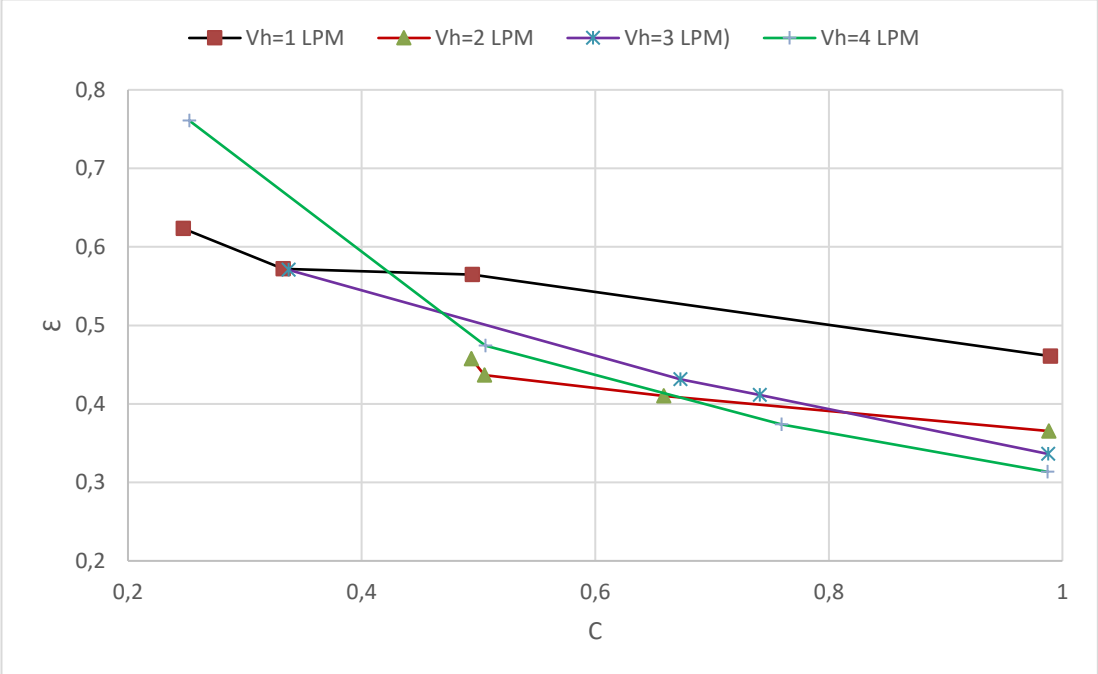

Figure 5.19. Variations of ε and C vary with cold water flow rate from 1 to 4 LPM at each hot water flow rate from 1 to 4 LPM in a half-annular finned pipe

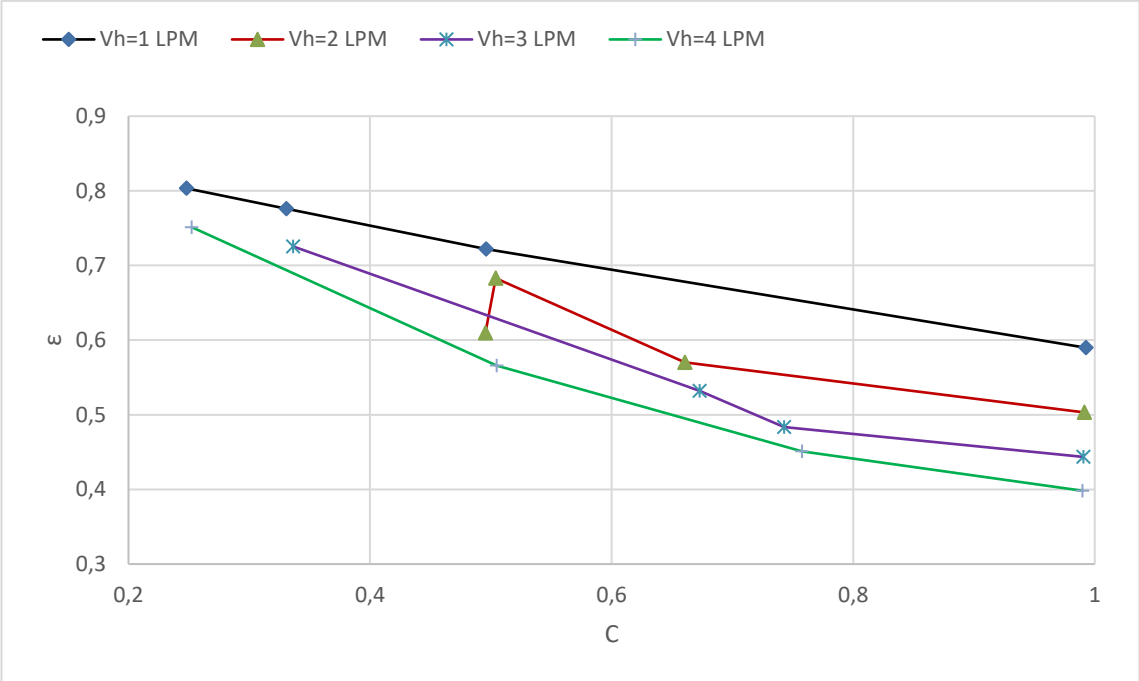

Figure 5.20. Variations of ε and C vary with cold water flow rate from 1 to 4 LPM at each hot water flow rate from 1 to 4 LPM in a helical annular finned pipe

5.1.6. Relation Between NTU and C

Figures 5.21 to 5.24 illustrate the relationship between C and NTU for pipes with different types of surfaces, including smooth, annular finned, half-annular finned, and helical annular finned surfaces. The hot water flow rates range from 1 to 4 LPM. In Fig. 5.21, it was observed that NTU's behavior at the flow rate of 1 LPM of hot water differed from the other flow rates. NTU increased with the increasing C values, when C was around 1. The values ranged from 0.216 to 0.337, whereas at the hot water flow rate of 4 LPM, the values changed from 0.45 to 0.26. It was noted that adding an extended surface to the outer surface of the inner pipe reduces NTU values in finned pipe heat exchangers compared to smooth pipes. In all types of finned pipe heat exchangers, the NTU value was found to be inversely proportional to the value of C. The helical-annular finned pipe exhibited the highest values of NTU, ranging from 1.86 to 1.43. The maximum NTU values for smooth, annular, and half-annular finned pipes were 0.45, 1.35, and 1, respectively, compared to helical annular pipes.

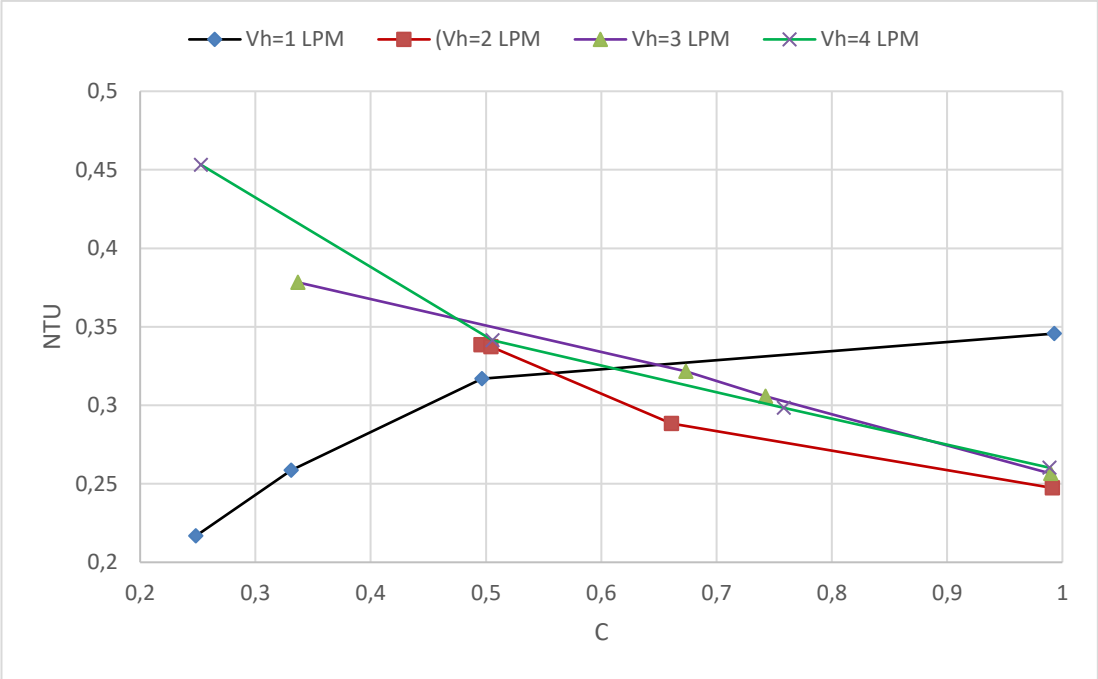

Figure 5.21. Variations of NTU and C vary with cold water flow rate from 1 to 4 LPM at each hot water flow rate from 1 to 4 LPM in a smooth pipe

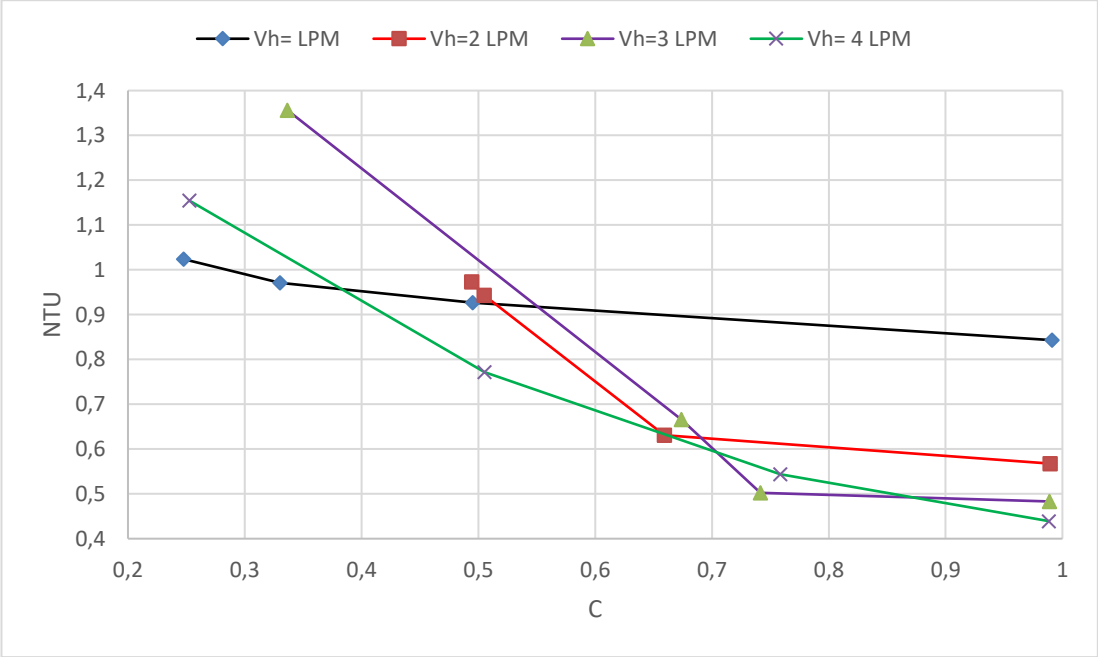

Figure 5.22. Variations of NTU and C vary with cold water flow rate from 1 to 4 LPM at each hot water flow rate from 1 to 4 LPM in an annular finned pipe

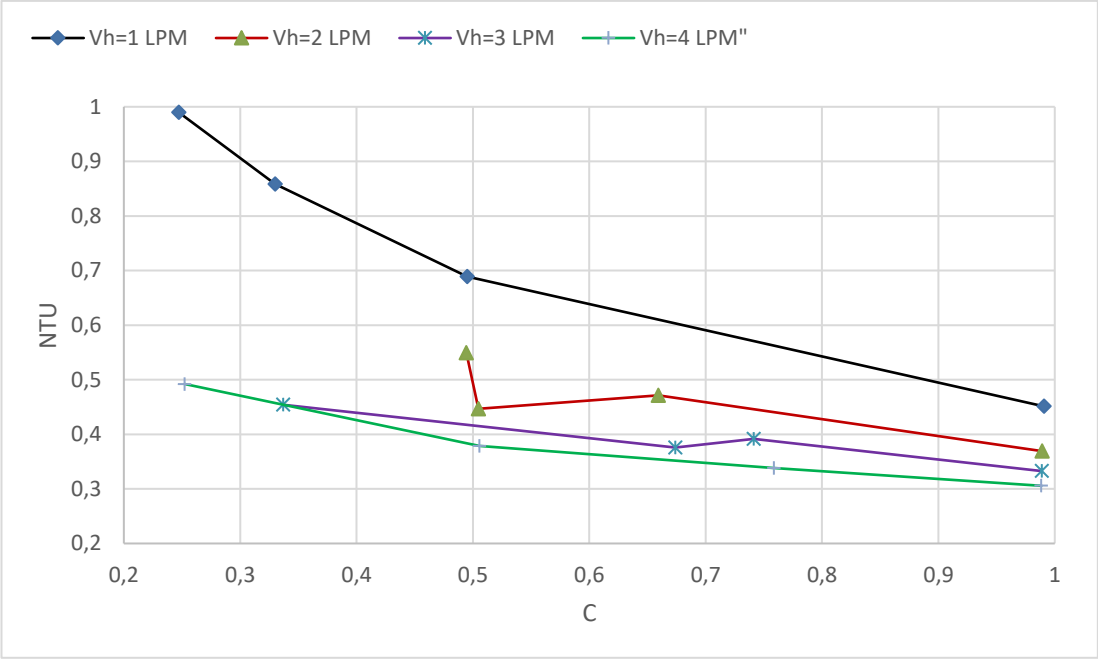

Figure 5.23. Variations of NTU and C vary with cold water flow rate from 1 to 4 LPM at each hot water flow rate from 1 to 4 LPM in a half-annular finned pipe

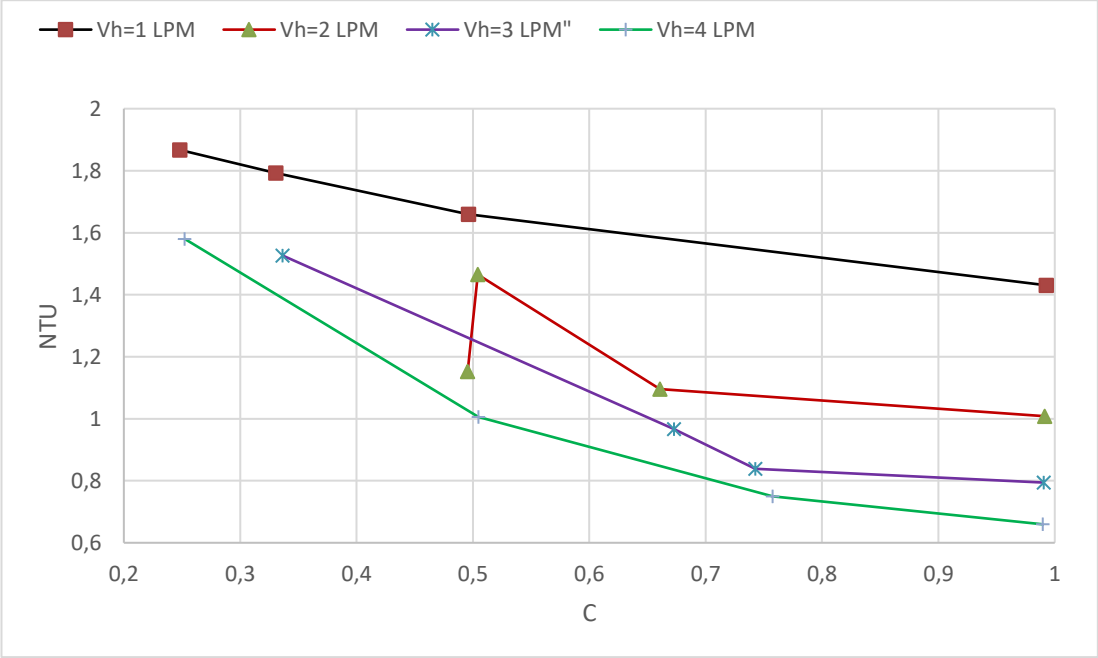

Figure 5.24. Variations of NTU and C vary with cold water flow rate from 1 to 4 LPM at each hot water flow rate from 1 to 4 LPM in a helical annular pipe

5.1.7. Comparison of Heat Exchanger Cases Based on Some Design Parameters

A comparative analysis was carried out on four heat exchangers operating at a flow rate of 4 LPM for hot water. This flow rate was chosen because it has the highest hydrothermal characteristics, identified in the previous discussions. The comparison includes the attributes of Nusselt number (Nuc), friction factor (FC), and heat exchanger effectiveness (Ɛ). Fig. 5.25 illustrates the variation between the Nusselt and Reynolds numbers (Re_c) in all heat exchangers. It has been found that adding fins to the heat exchange surface makes Nu_c numbers much better than with a smooth pipe heat exchanger. The improvement rates are about 21.48%, 37.97%, and 69.82%, respectively, for annular, half-annular, and helical-annular pipe heat exchangers compared to the smooth pipe heat exchanger. On the other hand, the f_C factor on the cold side, as shown in Fig. 5.26, was noted to be inversely linearly related to the Re_C number in all heat exchanger types. It was pointed out that the smooth pipe has the lowest friction factor where its average fc factor is the lowest by 8.66%, 18.58%, and 29.04% lower than compared to annular, half-annular, and helical-annular finned pipes, respectively.

Fig. 5.27 shows the effectiveness variation vs. C for four heat exchanger types operating at 4 LPM. It was discovered that the smooth pipe had the lowest efficiency across the cold-water flow rate. When the effectiveness of various heat exchangers was compared, only the smooth pipe's effectiveness increased as C increased, while the others' effectiveness decreased. It was observed that at C of 0.253, both half-annular and helical-annular finned pipes had the same effectiveness, which was about 0.75. Still, when C was increased, the effectiveness of the half-annular finned pipe was lower than that of the helical annular finned pipe heat exchanger. The helical annular finned pipe heat exchanger exhibited an effectiveness range of 0.75 to 0.4. In comparison, the effectiveness ranges for half-annular, annular, and smooth pipes were 0.75 to 0.3, 0.65 to 0.3, and 0.22 to 0.4, respectively, and it agrees well with obtained results by Abbas et al. [39] .

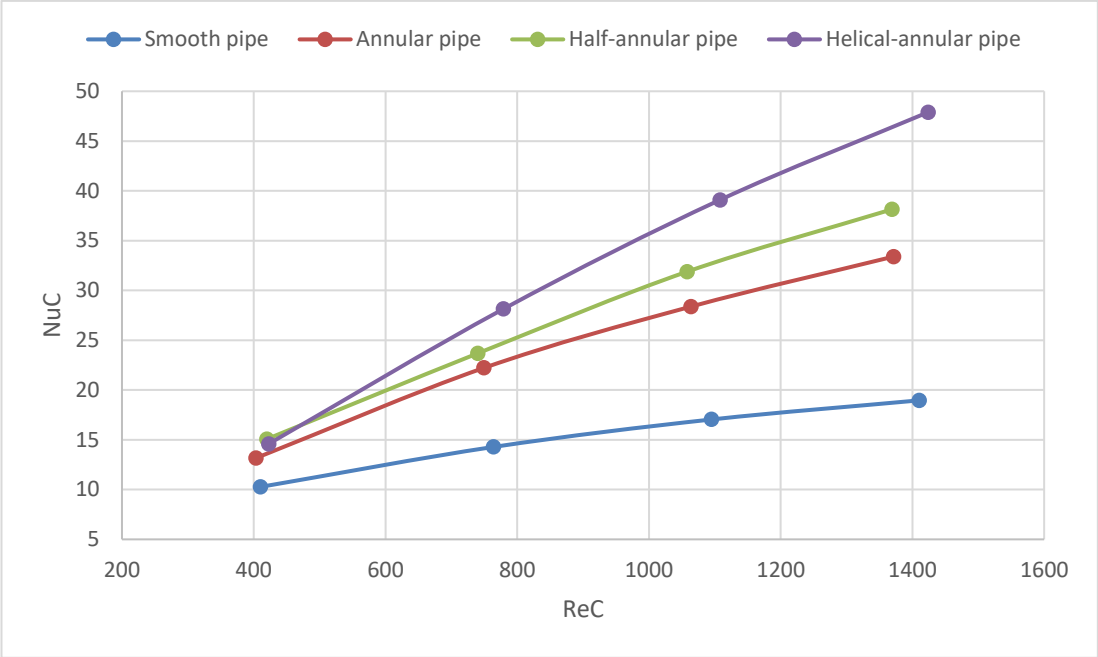

Figure 5.25. The relationship between Nu_c number versus and Re_C for four heat exchanger cases operating at a 4 LPM hot water flow rate

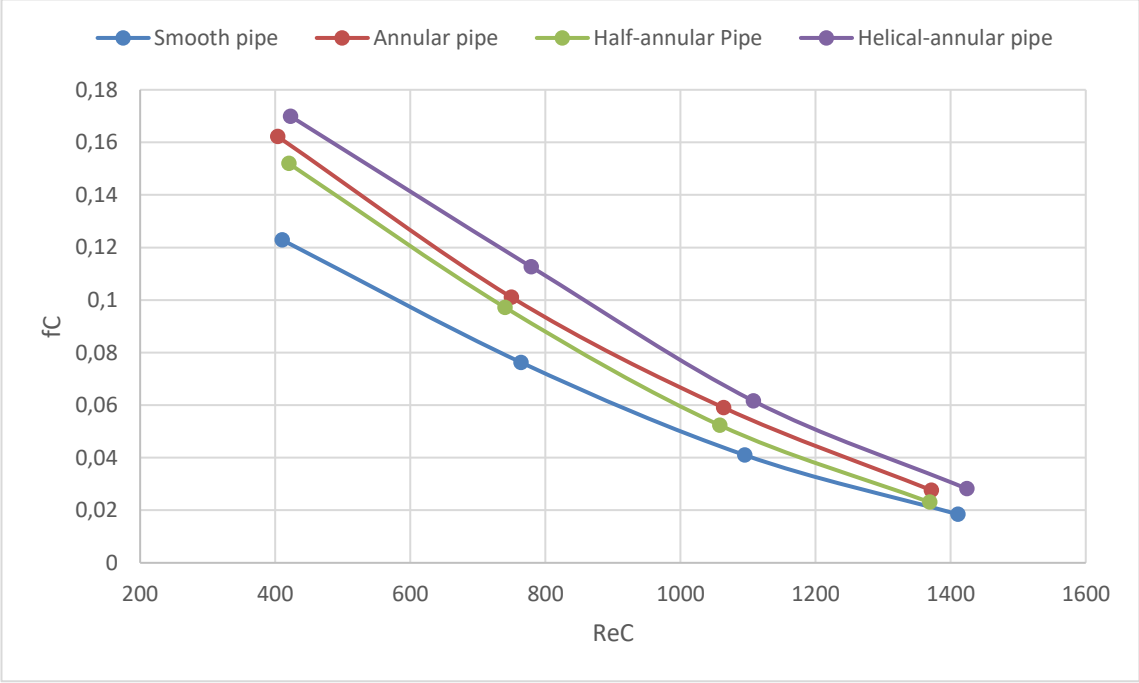

Figure 5.26. The relationship between the f_C factor versus and Re_C for four heat exchanger cases operating at 4 LPM of hot water flow rate

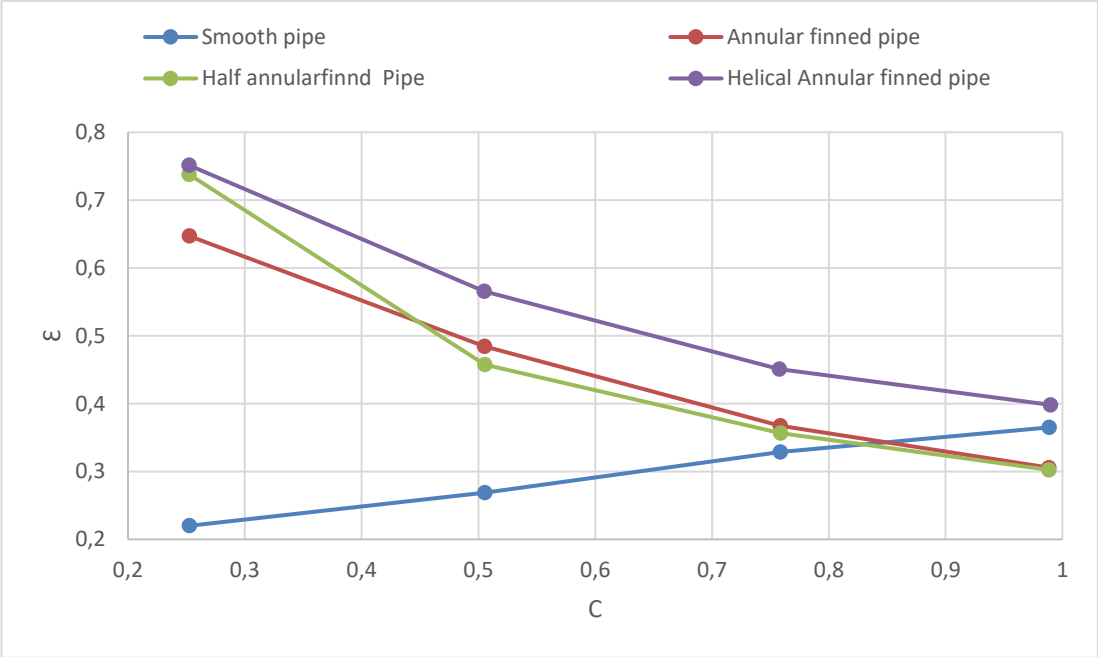

Figure 5.27. The relationship between Ɛ and C for four heat exchanger cases operating at 4 LPM of hot water flow rate

5.2 CONTOURS OF TEMPERATURE, VELOCITY, AND PRESSURE

The temperature distribution for different types of heat exchangers - smooth, helical-annular finned tube, half-annular finned tube and annular finned tube heat exchangers is shown in Figure 5.28. The measurements were taken at a Re_c of 1400, with a flow rate of 4 LPM for the hot water. It is indicated that the temperature ranges of different heat exchangers vary. The temperature ranges from 293 to 303 K in a smooth tube heat exchanger. However, the temperature ranges from 293.1 to 307 K in an annular finned tube heat exchanger. In a half-annular finned tube heat exchanger, the temperature ranges from 293 to 308 K. Finally, a helical-annular finned tube heat exchanger can have a temperature range from 293.1 to 309.55 K. Among various heat exchangers, the helical-annular finned tube demonstrated the most efficient heat exchange between hot and cold water.

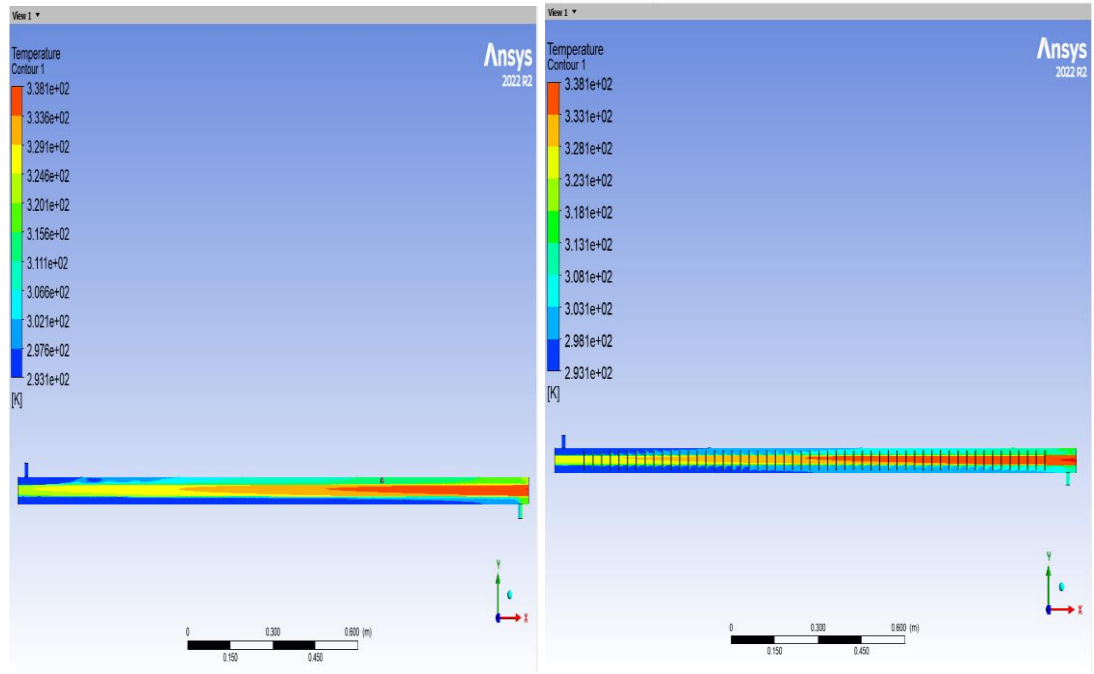

Smooth Annular

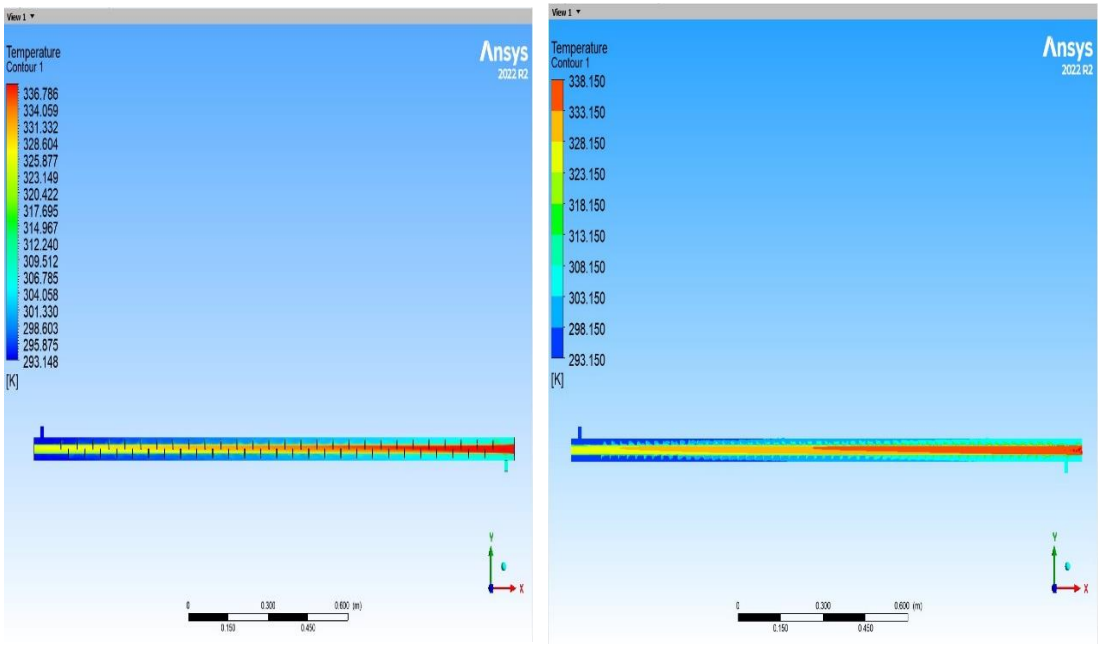

Half- Annular Helical- Annular

Figure 5.28. Temperature contours of different types of heat exchangers at Re_c=1410

Figure 5.29 illustrates the velocity contour in all four heat exchangers at a Re_c=1400. In a smooth tube heat exchange, the steady flow along the heat exchanger in cold water

is about 0.07 m/s, except the inlet and exit ports exhibit little change in velocity. However, the installed annular fins increased cold water velocity to about 0.08 m/s in an annual finned tube and 0.075 m/s in a half-annular finned tube. In contrast, due to the narrow fin gap and vortex water across the fin, the velocity of cold water increased significantly more than other fluids, reaching 0.116 m/s in a helical-annular tube.

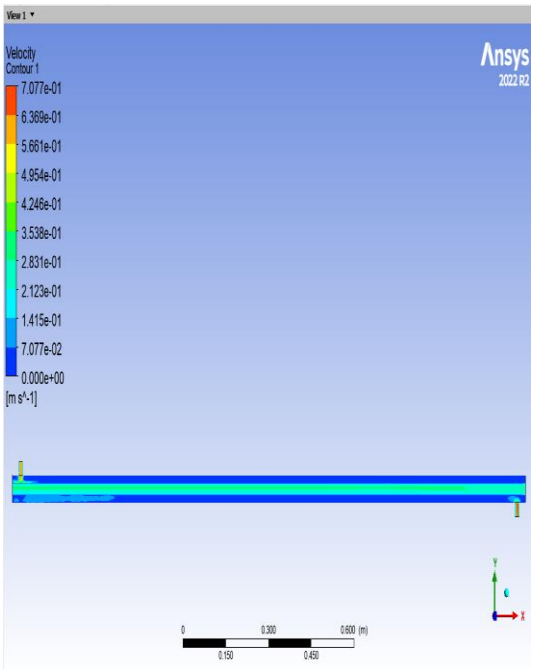

Smooth

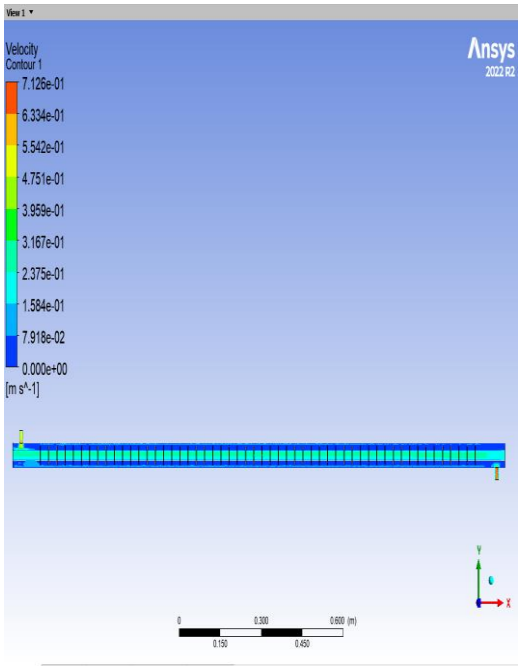

Annular

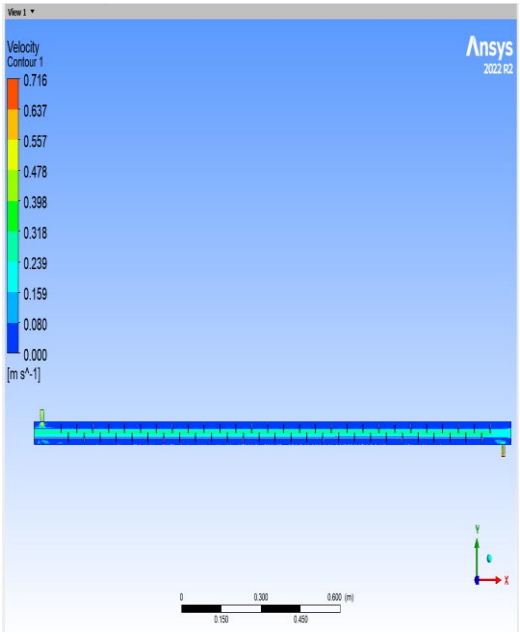

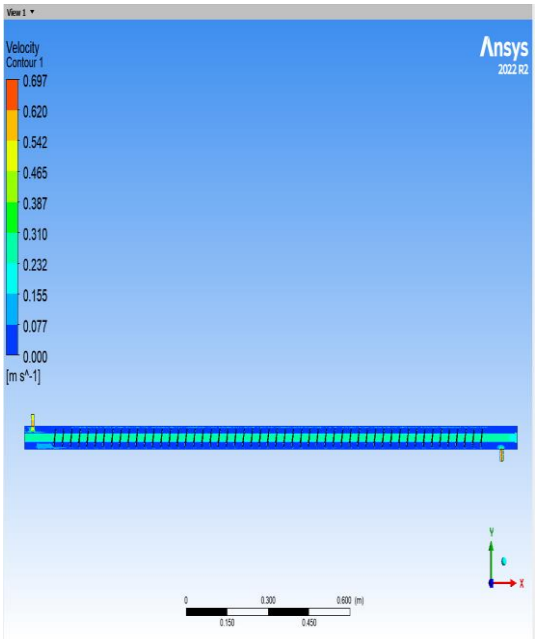

Half-Annular Helical- Annular

Figure 5.29. Velocity contours of different types of heat exchangeres at Re_c=1410

Figure 5.30 shows the pressure drops across the inlet and outlet of two types of heat exchangers: a smooth tube heat exchanger and two finned tube heat exchangers. The pressure drop is steady in a smooth tube heat exchanger and approximately 264 Pa. However, adding fins to the tubes in a finned tube heat exchanger causes a non-uniform pressure drop.

In an annular finned tube, the pressure drop across the first half of the tube is higher than the other half, ranging from 379.4 Pa to 208.5 Pa. Meanwhile, in a half-annular finned tube, the length of the higher pressure drop zone increases to about 60% of the tube length due to less narrowing in the annular area compared to the annular finned tube. In a helical-annular finned tube, the size of higher-pressure drop is less than in both finned tubes, but with higher levels than those, it ranges from 352 to 218 Pa.

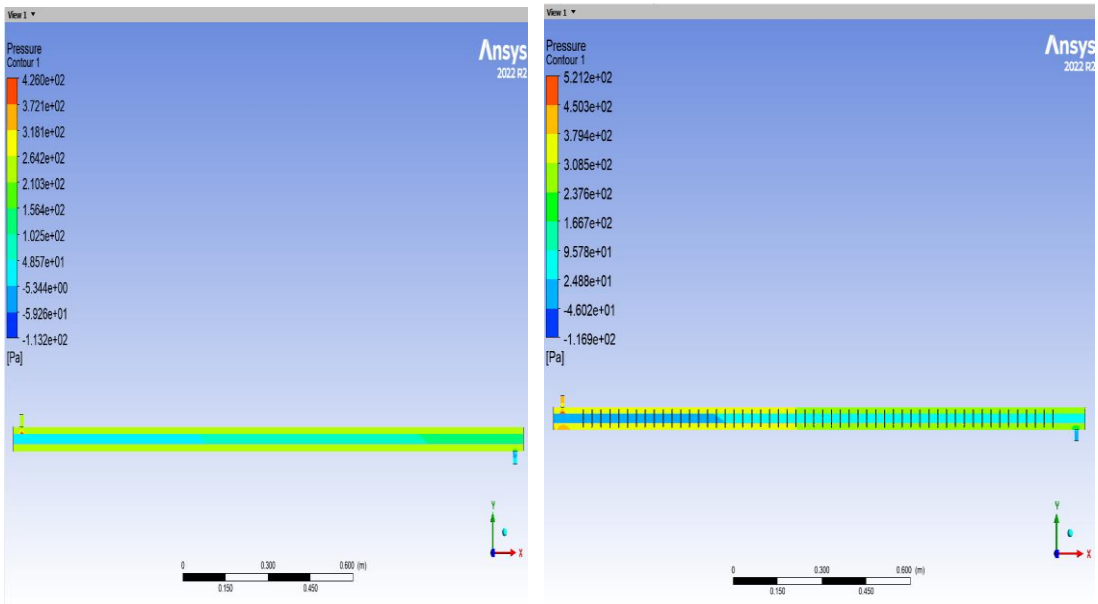

Smooth Annular

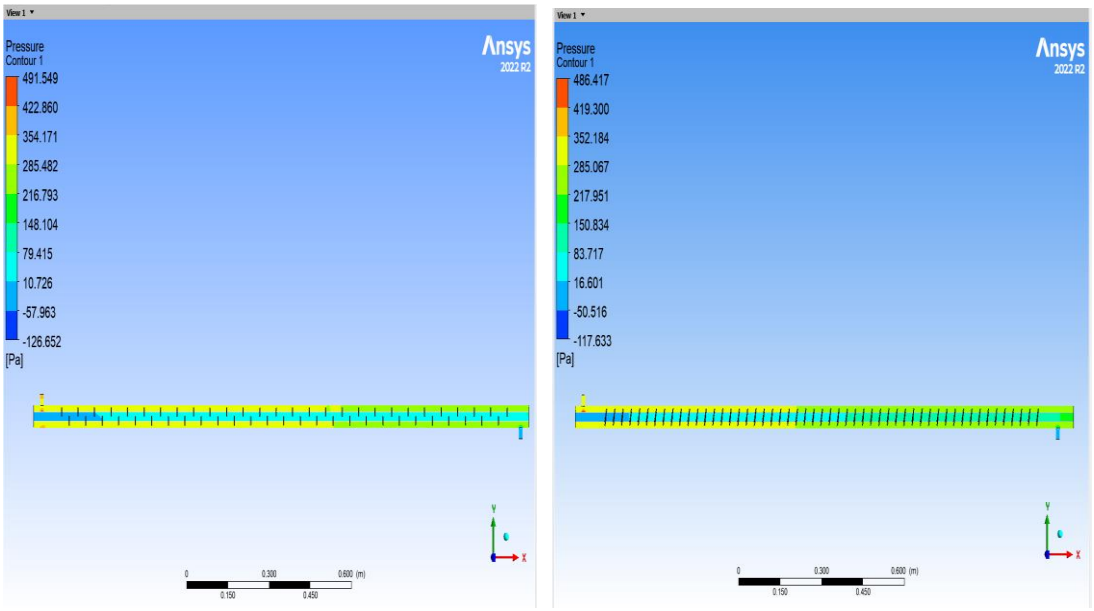

Half- Annular Helical- Annular

Figure 5.30. Pressure contours of different type of heat exchanger at Re_c=1410

The temperature, velocity, and pressure drop behavior in a helical-annular finned tube heat exchanger was investigated at three Rec numbers (400, 1000, and 1400) as shown in Figures 5.31 to 5.33. In a recording with a value of 400, it was noticed that the exit port of the cold water was overheating. This was due to the low flow rate of cold water in comparison to the flow rate of hot water. The Vc of the system is 1, 3, and 4 LPM, and the temperature difference is approximately 40°C at Rec=400, as shown in Fig. 5.31. The temperature difference decreases as the flow rate of cold water is increased. At a recording of 1000, the temperature difference is 30°C, and at 1400, it becomes 10°C. According to the continuity equation, cold-water velocity increases when the cold-water flow rate increases. In Fig. 5.32, it changed velocity from 0.034 to 0.077 m/s. The pressure drop in a system tends to increase with an increase in the flow rate, as depicted in Fig. 5.33. At a Rec of 400, the pressure drop is uniform, while it becomes non-uniform for values above it. Specifically, at Rec of 400, the pressure drop is approximately 31.6 Pa. However, when the cold-water flow increases to achieve Rec values of 1000 and 1400, the pressure drop is altered significantly, changing from 206 to 167 Pa, and from 352 to 218 Pa, respectively.

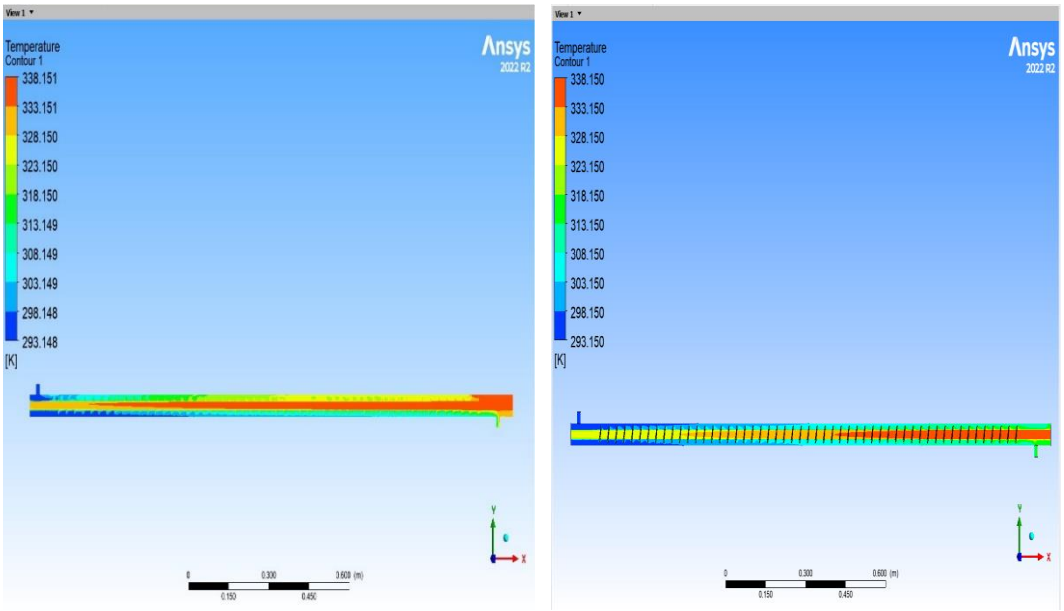

Re_c=400 Re_c=1000

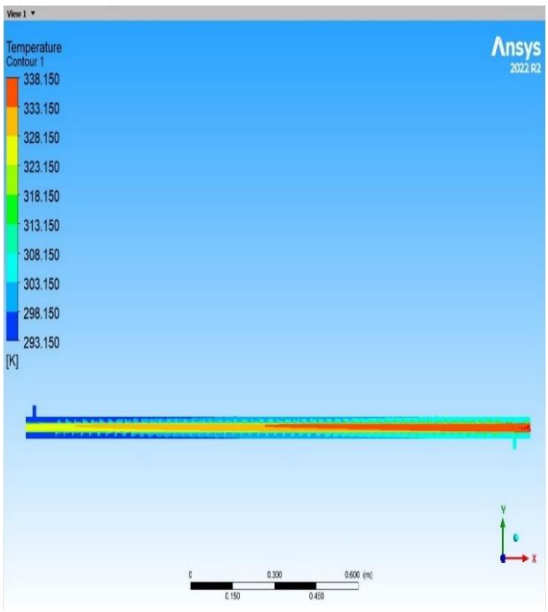

Re_c=1400

Figure 5.31. Temperature contours in a helical-annular-finned heat exchangers at different Re_c

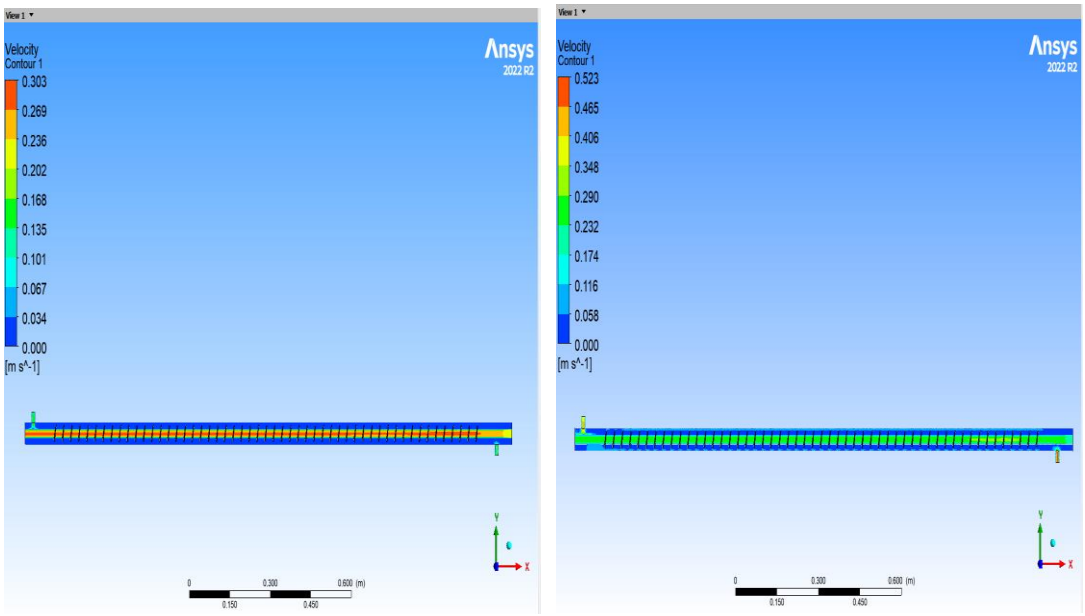

Re_c=400 Re_c=1000

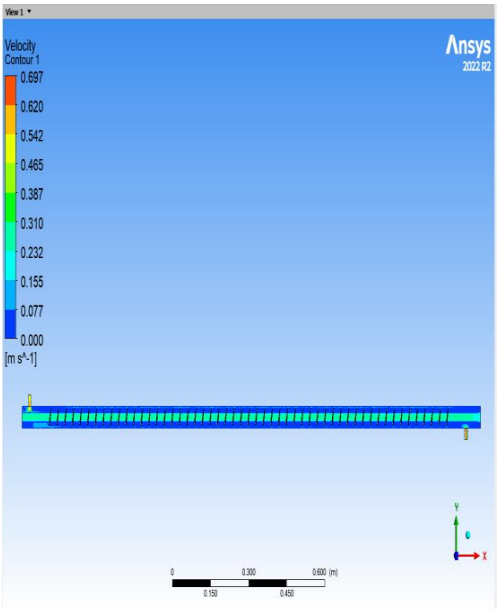

Re_c=1400

Figure 5.32. Velocity contours in helical-annular-finned heat exchangers at different Re_c

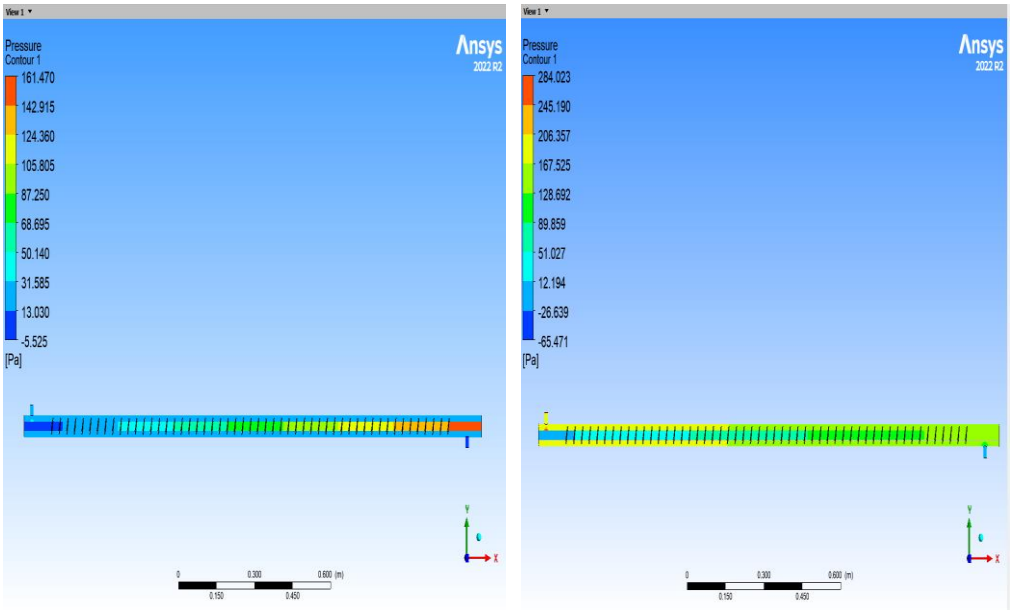

Re_c=400 Re_c=1000

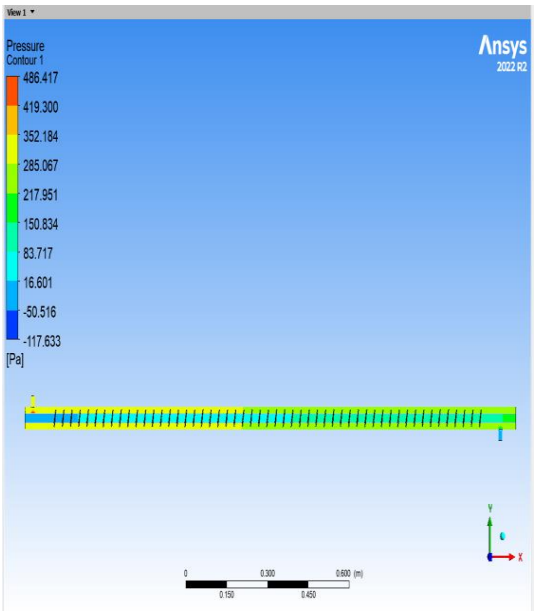

Re_c=1400

Figure 5.33. Pressure contours in a helical-annular-finned heat exchanger at different Re_c

PART 6

CONCLUSION

6.1. BACKGROUND

Chapter 6 displays the results obtained from the numerical simulation method of four heat exchangers with different outer surfaces of the inner pipe. Various types of pipes were used, including smooth, annular-finned, half-annular-finned, and helical annular-finned pipes. Two methods were performed: cold water flowing in the annular space while hot water flowing in the pipe. Both methods had four steps, ranging from one to four. The results of the double-pipe heat exchangers, including fins, were compared with those of a primary double-pipe heat exchanger containing a smooth pipe. Comparative analysis focused on Nu number and f factor vs. Re number, Ɛ, and NTU vs. C. The obtained results can be summarized below:

1. Fins increased the Nu_c number by a high level compared to smooth pipes. Annular, half-annular, and helical-annular pipe heat improved by 21.48%, 37.97%, and 69.82%, respectively, compared to smooth pipe.
2. Compared to annular and half-annular finned pipes, the helical-annular finned pipe achieved the highest Nu_c number, with an improvement rate of 39.93% and 23.1%, respectively.
3. The smooth pipe heat exchanger has the lowest friction factor compared to annular, half-annular, and helical pipe heat exchangers. The friction factor of the smooth pipe heat exchanger is 1**8.**58%, 8.**66**%, and 29.04% lower than that of annular, half-annular, and helical pipe heat exchangers, respectively.
4. Smooth pipe heat exchangers are less effective against C when compared to finned pipe heat exchangers. The effectiveness of smooth pipe heat exchangers decreases as the value of C increases, while other heat exchangers are unaffected similarly. Among all the heat exchanger types, the smooth pipe

5. heat exchanger has the lowest effectiveness except when C equals 0.99, where its efficacy becomes higher than that of annular and half-annular finned pipe heat exchangers.
6. The helical annular finned pipe heat exchanger is considered the most efficient because it provides the highest effectiveness across the range of C values. Compared to smooth, annular-finned, and half-annular-finned pipe heat exchangers, it offers a significantly higher effectiveness rate of 49.9%, 20.3%, and 21.8%, respectively.

6.2. FUTURE WORK

Experimental work might be proposed and designed according to this investigation's technological specifications. To emphasize the results, conducting experiments using the identical boundary conditions specified in this paper is advisable. If the experimental results align with the present study, both publications can be regarded as informative resources for designers in developing heat exchangers.

REFERENCES

1. R. K. Shah and D. P. Sekuli, *Fundamentals of Heat Exchanger Design*. John Wiley & Sons, Inc., 2003. doi: 10.1002/9780470172605.

2. J. P. Holman, *Heat transfer, 10th editi. ed*. 2010.

3. Y. Cengel, "Heat Transfer: A Practical Approach," *J Chem Inf Model*, vol. 53, no. 9, 2013.

4. K. Simhadri, G. V. D. Mohan, and P. Sai Chaitanya, "Comparison of the overall heat transfer coefficient value of double pipe heat exchanger without and with various twisted inserts of different twist ratios," *IOSR Journal of Mechanical and Civil Engineering*, vol. 12, no. 2, 2015.

5. T. L. Bergman, A. S. Lavine, F. P. Incropera, and D. P. DeWitt, "Fundamentals of heat and mass transfer, 2011," *USA: John Wiley & Sons. ISBN*, vol. 13, 2015.

6. C. Maradiya, J. Vadher, and R. Agarwal, "The heat transfer enhancement techniques and their Thermal Performance Factor," *Beni Suef Univ J Basic Appl Sci*, vol. 7, no. 1, pp. 1–21, Mar. 2018, doi: 10.1016/J.BJBAS.2017.10.001.

7. S. Rashidian and M. R. Tavakoli, "Using Porous Media to Enhancement of Heat Transfer in Heat Exchangers," *International Journal of Advanced Engineering, Management and Science*, vol. 3, no. 11, 2017, doi: 10.24001/ijaems.3.11.5.

8. E. Guen, P. O. Chapuis, N. J. Kaur, P. Klapetek, and S. Gomés, "Impact of roughness on heat conduction involving nanocontacts," *Appl Phys Lett*, vol. 119, no. 16, 2021, doi: 10.1063/5.0064244.

9. A.Hashim Yousif and M. Rehaif Khudhair, "Enhancement Heat Transfer in a Tube Fitted with Passive Technique as Twisted Tape Insert-A CompRehensive Review," *American Journal of Mechanical Engineering*, vol. 7, no. 1, 2019.

10. A.D. Kraus, A. Aziz, and J. Welty, *Extended Surface Heat Transfer*. A Wiley-Interscience Publication JOHN WILEY & SONS, INC., 2001. doi: 10.1002/9780470172582.

11. W. Chamsa-ard, S. Brundavanam, C. C. Fung, D. Fawcett, and G. Poinern, "Nanofluid types, their synthesis, properties and incorporation in direct solar thermal collectors: A review," *Nanomaterials*, vol. 7, no. 6. 2017. doi: 10.3390/nano7060131.

12. M. Medraj, E. Baril, V. Loya, and L. P. Lefebvre, “The effect of microstructure on the permeability of metallic foams,” *J Mater Sci*, vol. 42, no. 12, 2007, doi: 10.1007/s10853-006-0602-x.

13. P. Kumar and F. Topin, “State-of-the-Art of Pressure Drop in Open-Cell Porous Foams: Review of Experiments and Correlations,” *Journal of Fluids Engineering, Transactions of the ASME*, vol. 139, no. 11. 2017. doi: 10.1115/1.4037034.

14. S. Eiamsa-ard, S. Pethkool, C. Thianpong, and P. Promvonge, “Turbulent flow heat transfer and pressure loss in a double pipe heat exchanger with louvered strip inserts,” *International Communications in Heat and Mass Transfer*, vol. 35, no. 2, 2008, doi: 10.1016/j.icheatmasstransfer.2007.07.003.

15. N. Sahiti, F. Bunjaku, and D. Krasniqi, “ASSESSMENT OF SINGLE PHASE CONVECTION HEAT TRANSFER ENHANCEMENT,” 2013. [Online]. Available: https://api.semanticscholar.org/CorpusID:18558983

16. D. Wang, Y. Dong, S. Xiang, C. Xia, Y. Wang, and G. Zhang, “Performance of double-pipe heat exchanger enhanced by helical fins,” *Huagong Xuebao/CIESC Journal*, vol. 65, no. 4, pp. 1208–1214, 2014, doi: 10.3969/j.issn.0438-1157.2014.04.008.

17. P. S. Rao and K. K. Kumar, “Numerical and Experimental Investigation of Heat Transfer Augmentation in Double Pipe Heat Exchanger with Helical and Twisted Tape Inserts,” 2014. [Online]. Available: https://api.semanticscholar.org/CorpusID:2904189

18. O. P. Kailash, C. Bishwajeet Nk, G. Umang B, P. Sumit B, and K. Gopal, “Design and experimental analysis of pipe in pipe heat exchanger,” 2015. [Online]. Available: www.ijmer.com

19. Y. S. Dong, D. B. Wang, S. Xiang, and C. J. Xia, “Numerical simulation of double-pipe heat exchanger enhanced by oblique helical fins,” *Zhejiang Daxue Xuebao (Gongxue Ban)/Journal of Zhejiang University (Engineering Science)*, vol. 49, no. 2, 2015, doi: 10.3785/j.issn.1008-973X.2015.02.017.

20. M. Hatami, D. D. Ganji, and M. Gorji-Bandpy, “Investigations of fin geometry on heat exchanger performance by simulation and optimization methods for diesel exhaust application,” *Neural Comput Appl*, vol. 27, no. 6, pp. 1731–1747, Aug. 2016, doi: 10.1007/s00521-015-1973-1.

21. L. Zhang *et al.*, “Effects of the arrangement of triangle-winglet-pair vortex generators on heat transfer performance of the shell side of a double-pipe heat exchanger enhanced by helical fins,” *Heat and Mass Transfer/Waerme- und Stoffuebertragung*, vol. 53, no. 1, pp. 127–139, Jan. 2017, doi: 10.1007/s00231-016-1804-7.

22. M. R. Salem, M. K. Althafeeri, K. M. Elshazly, M. G. Higazy, and M. F. Abdrabbo, “Experimental investigation on the thermal performance of a double pipe heat exchanger with segmental perforated baffles,” *International Journal of Thermal Sciences*, vol. 122, 2017, doi: 10.1016/j.ijthermalsci.2017.08.008.

23. A.V. Rao, “Numerical Analysis of Double Pipe Heat Exchanger with and without Strip,” *Int J Res Appl Sci Eng Technol*, vol. 6, no. 6, 2018, doi: 10.22214/ijraset.2018.6130.

24. S. Sivalakshmi, M. Raja, and G. Gowtham, “Effect of helical fins on the performance of a double pipe heat exchanger,” in *Materials Today: Proceedings*, 2020. doi: 10.1016/j.matpr.2020.08.563.

25. A.Shahsavar, A. Goodarzi, H. I. Mohammed, A. Shirneshan, and P. Talebizadehsardari, “Thermal performance evaluation of non-uniform fin array in a finned double-pipe latent heat storage system,” *Energy*, vol. 193, 2020, doi: 10.1016/j.energy.2019.116800.

26. M. A. W. A. Sattar, K. A. Jehhef, and N. J. Yasin, “Thermal performance enhancement in double pipe heat exchanger by using inward and outward dimple and corrugated tape,” *Journal of Mechanical Engineering Research and Developments*, vol. 44, no. 1, 2020.

27. T. H. Farhan, O. T. Fadhil, and H. E. Ahmed, “Performance of a double-pipe heat exchanger with different met-al foam arrangements,” *Anbar Journal for Engineering Sciences*, vol. 12, no. 2, pp. 100–112, Aug. 2021, doi: 10.37649/aengs.2021.171162.

28. M. F. Al. , Rafeq A. Khalefa, “The Performance of the hairpin type U Shape Double pipe heat exchanger type under effect of using Passive and Active Techniques.,” *Design Engineering*, 2021, doi: 10.17762/de.vi.3595.

29. M. Ishaq, A. Ali, M. Amjad, K. S. Syed, and Z. Iqbal, “Diamond-shaped extended fins for heat transfer enhancement in a double-pipe heat exchanger: An innovative design,” *Applied Sciences (Switzerland)*, vol. 11, no. 13, 2021, doi: 10.3390/app11135954.

30. M. A. Hussein and V. M. Hameed, “Experimental Investigation on the Effect of Semi-circular Perforated Baffles with Semi-circular Fins on Air–Water Double Pipe Heat Exchanger,” *Arab J Sci Eng*, vol. 47, no. 5, 2022, doi: 10.1007/s13369-021-05869-0.

31. M. F. Albayati and R. A. Khalefa, “The Performance of the U Shape Double pipe heat exchanger under effect of using Active Techniques.,” *NTU Journal of Engineering and Technology*, vol. 1, no. 3, 2022, doi: 10.56286/ntujet.v1i3.61.

32. M. F. Hasan, M. Danışmaz, and B. M. Majel, “Thermal performance investigation of double pipe heat exchanger embedded with extended surfaces using

nanofluid technique as enhancement," *Case Studies in Thermal Engineering*, vol. 43, 2023, doi: 10.1016/j.csite.2023.102774.

33. H. D. Lafta and D. O. Mohammed, "Experimental Investigation of Heat Transfer Enhancement in a Double Pipe Heat Exchanger Using Compound Technique of Transverse Vibration and Inclination Angle," *Journal of Engineering*, vol. 29, no. 5, 2023, doi: 10.31026/j.eng.2023.05.07.

34. T. Hayat and S. Nadeem, "An improvement in heat transfer for rotating flow of hybrid nanofluid: a numerical study," *Can J Phys*, vol. 96, no. 12, pp. 1420–1430, Nov. 2018, doi: 10.1139/cjp-2017-0801.

35. H. Hussein and B. Freegah, "Numerical and experimental investigation of the thermal performance of the double pipe-heat exchanger," *Heat and Mass Transfer*, Aug. 2023, doi: 10.1007/s00231-023-03414-3.

36. A.Tongkratoke, A. Pramuanjaroenkij, S. Phankhoksoong, and S. Kakac, "The Experimental Investigation of Double Pipe Heat Exchangers Prepared from Two Techniques," in *IOP Conference Series: Materials Science and Engineering*, 2019. doi: 10.1088/1757-899X/501/1/012064.

37. Bejan, *Convection Heat Transfer: Fourth Edition*. 2013. doi: 10.1002/9781118671627.

38. L. M. (Latif M. Jiji, *Heat convection*. Springer, 2006.

39. E. F. Abbas, S. R. Aslan, and T. A. Ridha, "Experimental Investigation of Heat Transfer Enhancement Methods on the Thermal Performance of Double Pipe Heat Exchanger." [Online]. Available: www.ijert.org

40. T. Stolarski, Y. Nakasone, and S. Yoshimoto, *Engineering Analysis with ANSYS Software: Second Edition*. 2018. doi: 10.1016/C2016-0-01966-6.

41. [S. S. Godara, V. Brenia, A. K. Soni, R. Singh Shekhawat, and K. K. Saxena, "Design & analysis of connecting rod using ANSYS software," *Mater Today Proc*, vol. 56, 2022, doi: 10.1016/j.matpr.2021.11.166.

42. M. A. Ali and S. N. Shehab, "Numerical analysis of heat convection through a double-pipe heat exchanger: Dimpled influence," *Journal of Engineering Research*, vol. 11, no. 1, 2023, doi: 10.1016/j.jer.2023.100016.

43. P. C. Barman, "Introduction to Computational Fluid Dynamics," *International Journal of Information Science and Computing*, vol. 3, no. 2, 2016, doi: 10.5958/2454-9533.2016.00014.4.

44. ANSYS FLUENT Theory Guide

RESUME

Ali Mahmood Mohamed MOHAMED completed his bachelor's degree at the Technical College of Kirkuk, Department of Refrigeration and Air Conditioning Engineering in 2004–2005. Then, in 2022, he started studying at Karabük University in the Mechanical Engineering Department to complete his M.Sc. education.